



NTNU – Trondheim
Norwegian University of
Science and Technology

A Sedimentological and Petrographical Investigation of the Todalen Member and the Boundary Beds of the Endalen Member.

Within the Firkanten Formation (Paleocene)
in the Central Basin of Spitsbergen, Svalbard.

Ane Andrea Gjesdal Svinth

Geology

Submission date: June 2013

Supervisor: Atle Mørk, IGB

Co-supervisor: Mai Britt Mørk, IGB

Snorre Olausen, UNIS

Malte Jochmann, Store Norske Spitsbergen Kullkompani AS

Norwegian University of Science and Technology

Department of Geology and Mineral Resources Engineering

Abstract

The Todalen and Endalen members (Firkanten Formation, Paleocene) comprise the earliest clastic sedimentary fill of the Central Basin on Spitsbergen, Svalbard. These two members represent delta plain- and delta front deposits respectively. Coal seams are abundant in the Todalen Member, and these are being mined on Svalbard today.

The aim of this study was to carry out a sedimentological and petrographical investigation of the Todalen Member and the boundary beds of Endalen Member to interpret the deltaic environment in which they were deposited. Furthermore, it was also a goal to establish a provenance area for the sandstones and to point out the prevalent diagenetic processes taking place during the subsequent burial.

Sedimentological logs and samples were obtained from two cores and two outcrops on the northeaster flank of the Central Basin during two field periods.

Seven facies associations have been interpreted from the logged cores and outcrops. Facies association 1 - 6 are interpreted to represent a delta plain environment due to the presence of coal seams (mire deposits), tidal indicators, conglomerates and *in-situ* rootlets. Facies association 7 is interpreted to represent delta front (shoreface) deposits due alternating beds of *Ophiomorpha* burrowed- and hummocky cross-stratified sandstones.

It is found that the delta plain deposits of the Todalen Member were under significant tidal influence, and becoming more distal towards the west. The upper half of the Todalen Member is found to have been under a larger fluvial influence than the lower half.

The delta front (shoreface) deposits in the lower part of the Endalen Member also display more distal facies towards the west.

Modal analysis was performed on the sampled sandstones, and the results from this revealed that all of the Todalen and Endalen member sandstones are similar in composition, typically constituted by subarkoses and quartz arenites, and sourced from areas north and northeast of the Central Basin.

Only a small change in the detrital grain fraction is detected across the boundary to the Endalen Member. This is seen as an absence of spicular chert grains which represents a source rock fingerprint of the Tempelfjorden Group. This finding may indicate a small alteration of the source rock assembly across the Todalen - Endalen member boundary. Ferroan dolomite/ ankerite cement, as well as calcite cement, post-dated the quartz cement formation. The volume of carbonate cement is seen to decrease upwards in Todalen Member, which supports the interpretation of the upper half of the Todalen Member being more fluvial, as carbonate cement is a more common feature in sandstones deposited in an environment under marine influence.

Sammendrag

Todalsleddet og Endalsleddet (Firkantformasjonen, paleocen) utgjør det tidligste sedimentære fyllet av Sentralbassenget på Spitsbergen, Svalbard. De to leddene representerer deltaslette og deltafront (shoreface) avsetninger. Todalsleddet inneholder rikelig med kull, dette kullet blir utvunnet på Svalbard også i dag

Målet med denne studien var å gjennomføre en sedimentologisk og petrografisk undersøkelse av Todalsleddet, samt de nedre lagene av Endalsleddet, for å tolke det deltaiske miljøet som de ble avsatt i. Videre var det også et mål å etablere et provenansområde for disse sandsteinene samt å påpeke de diagenetiske prosessene som fant sted under den påfølgende begravningen.

Sedimentologiske logger og prøver ble tatt fra to kjerner og to blotninger på den nördøstre flanken av Sentralbassenget i løpet av to feltperioder

Syv facies assosiasjoner har blitt tolket utfra de to kjernene og blotningene. Facies assosiasjonene 1-6 er tolket til å representere et deltaslette miljø ut fra en tilstedeværelse av kullsummer (myravsetninger), tidevannsindikatorer, konglomerater og *in-situ* røtter. Facies assosiasjon 7 er tolket til å representere deltafront (shoreface) avsetning grunnet vekslende sandsteinslag som inneholdt *Ophiomorpha* gravespor og haugkrysslagning.

Deltaslette miljøet i Todalsleddet var under stor påvirkning av tidevannsprosesser, og dette leddet viser mer distale facies mot vest. Den øvre halvdel av Todalsleddet var betydelig mer påvirket av fluviale prosesser enn den nedre halvdel. Deltafront avsetningene i det nedre Endalsledd viste den samme trenden med mer distale facies mot vest.

Modal analyse ble utført på de prøvetatte sandsteinene, og resultatene viste at både Todals- og Endalsleddet var av en lik sammensetning hvor særlig subarkoser og kvartsarenitter var vanlig.

Sedimentene ble funnet til å være transportert fra områder nord og nordøst for Sentralbassenget. En liten endring i den detritale kornfraksjonen er registrert over grensen til Endalsleddet. Denne endringen består av en mangel på spikulære flintkorn, kornene som er å regne som et fingeravtrykk av Tempelfjordgruppen. Dette funnet kan indikere en liten endring i sammensetningen av kildebergarter over grensen fra Todalsleddet til Endalsleddet. Dolomitt-/ankeritt-sement, samt kalsittsement, ble utfelt i porerommet etter kvartssement var dannet. Volumet av disse karbonatholdige sementene avtar oppover i Todalsleddet, noe som støtter tolkningen om at den øvre halvdel av Todalsleddet er mer fluvial, siden karbonat er en sementtype som er mer vanlig i sandsteiner som er avsatt i ett miljø under marin påvirkning.

Acknowledgements

Field work in Svalbard is amazing! Nevertheless, arctic conditions are challenging, and the field work would not have been possible without the bigheartedness of a lot of people, companies and universities.

First off, I would like to thank my main supervisor, Professor Atle Mørk at NTNU/ SINTEF Petroleum Research, for his support, interesting discussions, motivation and humor.

Next, I would like to thank Store Norske Spitsbergen Kullkompani (SNSK) for their generous financial support. Especially a big thanks to SNSK geologist Malte Jochmann, who among many other things organized helicopter transport to the most remote field locations.

I would also like to thank Professor Mai Britt Mørk at NTNU for her inputs on my work, and my contact person at the University Center in Svalbard (UNIS), Professor Snorre Olaussen.

A thanks is also extended towards UNIS which provided the necessary camping- and safety equipment for field work, which among other things included a rifle in case of polar bears.

I further wish to thank Amanda Goss for her assistance during fieldwork, her glacial- and river crossing skills came in handy more than once. I also wish to thank SNSK geologist Bjarki Friis for his assistance during core sampling. Furthermore, a thanks goes out to Professor William Helland-Hansen for great discussions.

I am grateful to SINTEF Petroleum Forskning for the providing me with an office space, fruit and coffee.

To my friends and "non-Tertiary" geologists, Garreth Lord and Kristoffer Solvi; thank you for your support.

To my family, thank you for the endless encouragements.

Table of Contents

Abstract	1
Sammendrag.....	2
Acknowledgements	3
1. Preface.....	6
2. Geological Setting	8
2.1 Tectonic History of Svalbard	8
2.2 Tectonic Evolution of the Central Basin	12
2.3 The Central Basin Fill: The Van Mijenfjorden Group	16
3. Analytical Approach	24
3.1 Field Work Locations.....	24
3.2 Methodology	31
4. Sedimentological Results	37
4.1 Facies.....	37
4.2 Facies Associations	51
5. Petrographical Results.....	73
5.1 Petrographic Composition of Core 18-2009	73
5.2 Petrographic Composition of Core 15-2010	84
5.3 Petrographic Composition of the Endalen Outcrop	95
5.4 Petrographic Composition of the Grumantbyen Outcrop	106
6. Discussion	119
6.1 Sedimentology of Todalen Member and the Endalen Member Boundary Beds.....	119
6.2 The Depositional Environment	129
6.3 Petrographic Composition and Provenance	135
6.4 Diagenesis	144
7. Conclusion.....	148

References149
Appendix.....156-163

1. Preface

During the summer of 2011, I got a summer job with SNSK. A big part of the job involved logging cores from the Lunckefjellet and Operafjellet, which were two of the prospects at this time. During the end of this summer, I was offered to write a thesis for SNSK. SNSK and I agreed that the Todalen Member would make for a suitable topic, as it holds the coal seams which are being mined.

I returned to Svalbard later that year to log and sample two cores, one from Lunckefjellet and the other from Operafjellet. Then, after spending some time studying at the University of California in Santa Barbara (and attending some adventurous geological field trips in the Mohave Desert) I returned to the arctic in the summer and fall of 2012 to do some field work and to attend two courses at the University Center in Svalbard (UNIS).

Even though this was more than a sufficient workload, I decided to take a job as a logging geologist at Baker Hughes this same fall. Over Christmas, reality set in, and my employer at Baker Hughes (also a geologist by profession) was understanding, and let me take some time off to finish my thesis.

2. Geological Setting

2.1 Tectonic History of Svalbard

Svalbard is situated on the northwestern uplifted corner of the Barents Sea shelf. It is bordering to the Norwegian-Greenland Sea in the west and the Arctic Ocean in the north. The present plate configuration involves an ongoing separation between Greenland and Svalbard, bounded by the North-Atlantic spreading ridge (Ritzmann 2003). The tectonic history of Svalbard is long and complicated; it has traveled slowly towards its present arctic latitude from the southern hemisphere. This northward voyage is also reflected in the sedimentary successions, which bear the signs of the different climatic conditions and sea-level changes that Svalbard has succumbed to during its journey (Elvevold et al. 2007). In the Mid Paleozoic, Svalbard was a part of the Old Red Continent which was a minor super continent. It was formed after the break-up of the super continent Rodinia on the southern hemisphere, followed by a subsequent northward drift and collision of Baltican Continent and Laurentian Continent. The Old Red was later merged into the super continent of Pangea, which came to exist around the Late Paleozoic- Early Mesozoic. Pangea started to rift in the Early Mesozoic-Mid Mesozoic, and the plate configuration of today started to take form as the opening of the Atlantic Ocean was initiated, with Svalbard and Greenland drifting northwards (Martinsen and Nøttvedt 2008).

In the Late Cretaceous, Svalbard had more or less reached its current latitude. The position of Svalbard was on the northern edge of Greenland (Figure 1), and the movement of Greenland was towards Svalbard. As sea-floor spreading was initiated between Greenland and Norway in the early Eocene, Greenland started to slide northwestwards to accommodate the new sea-floor. This was however not the only new sea-floor that had to be accommodated at this time as sea-floor spreading also was taking place in the Arctic Ocean as well as in Baffin Bay. These three spreading-ridges were connected by a transfer zone north of Greenland, namely the De Geer Zone, which accommodated the dextral strike-slip movement between Greenland and Svalbard (Figure 1) (Bergh et al. 1997; Bruhn and Steel 2003; Von Gosen 2003; Lawver 2009).

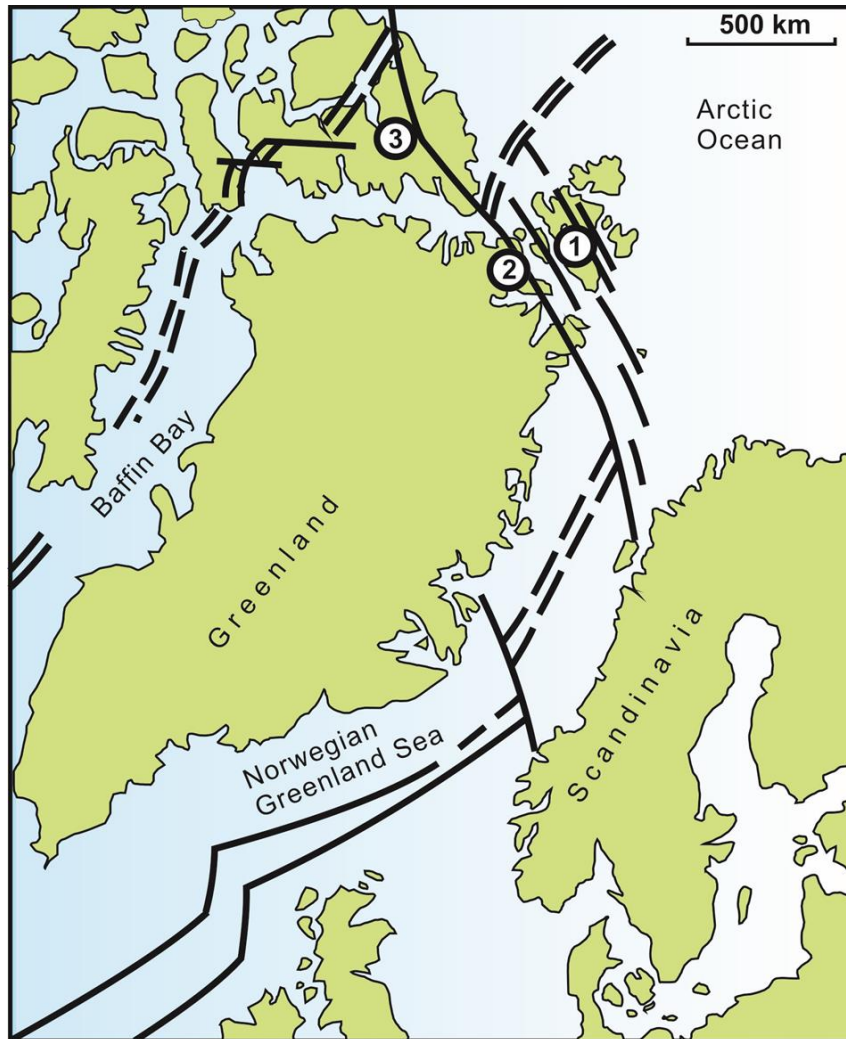


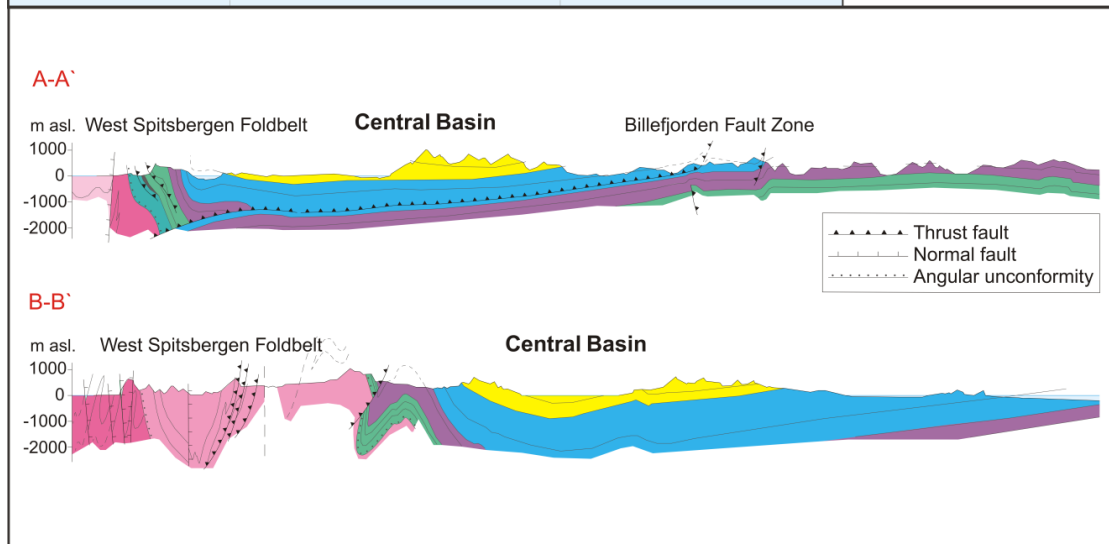
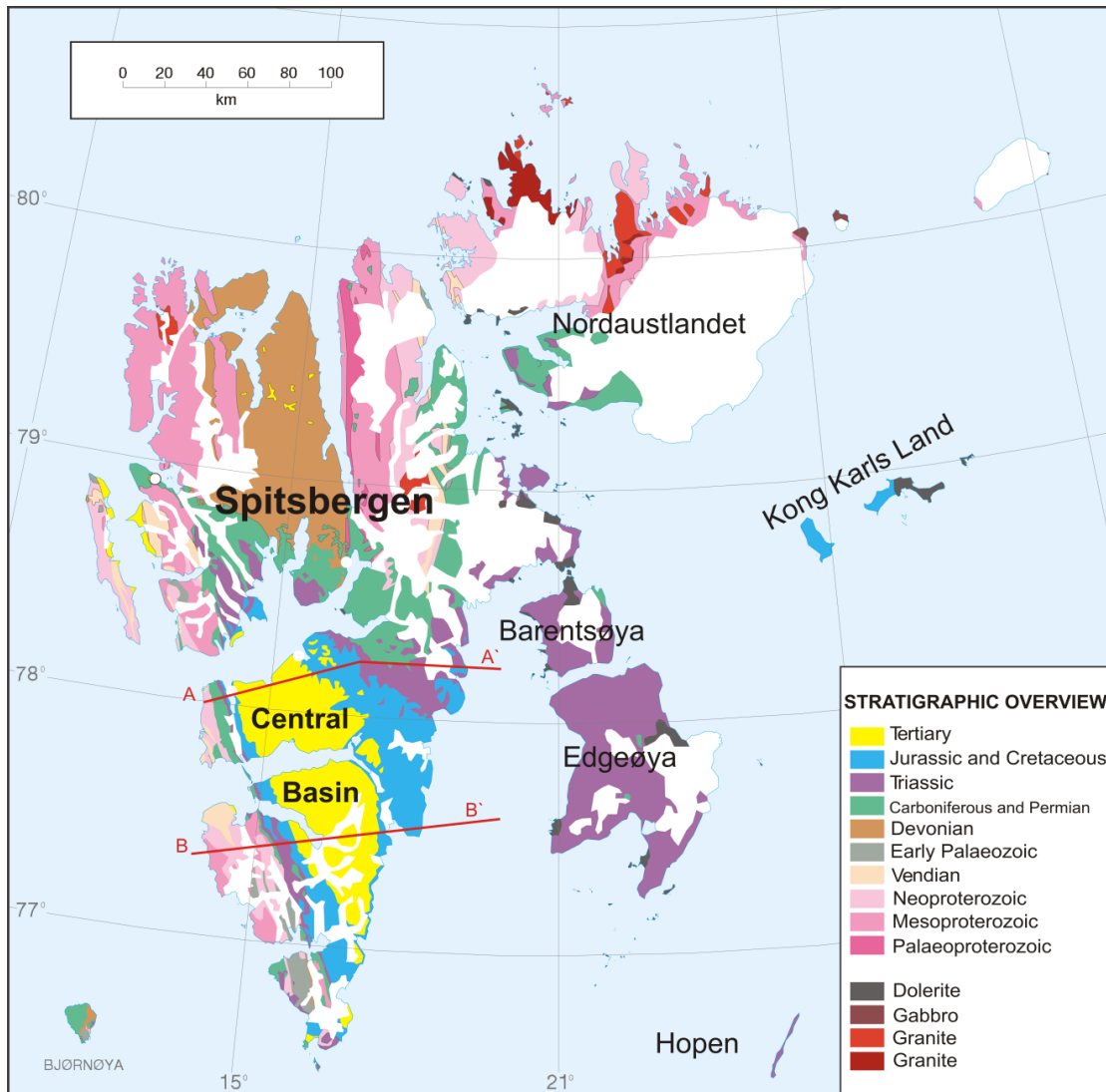
Figure 1: Paleographic reconstruction of the Arctic in the Late Cretaceous- Early Paleocene time. Spreading ridges are marked in dotted lines. 1. Svalbard. 2. Wandel Sea Strike-Slip Mobile Belt. 3. Ellesmere Island. The De Geer Zone is the zone of strike-slip faults between Spitsbergen and Greenland. Color modified illustration from Bruhn and Steel (2003).

An orogenic belt formed at this dextral transfer zone's margin, onshore on Spitsbergen, during the opening of the Norwegian-Greenland Sea. This transpressive orogen is referred to as the West Spitsbergen Fold and Thrust Belt (WSFTB) due to its distinct structural style. The WSFTB is 100-200 km wide and 500 km long, with its length axis running parallel to the west coast of Spitsbergen (Bergh et al. 1997). The crustal shortening which took place perpendicular to the length axis is estimated to have been around 20-40 km (Bergh et al. 1997; Leever et al. 2009). This orogen-induced crustal shortening led to the creation of the Central Basin, which is a north

northwest- south southeast trending, asymmetric syncline structure. A stratigraphic overview map of Svalbard and two cross-sections of the Central Basin are presented in Figure 2. The asymmetric nature of the Central Basin is due to the western flank's close location to the orogen and thus the main zone of deformation. It therefore displays a deeper and steeper dip than the eastern flank (Müller and Spielhagen 1990; Bergh et al. 1997).

Two different models attempt to explain the tectonic evolution of the Central Basin, these are presented in the next chapter.

Figure 2: Stratigraphic overview map of Svalbard today. The vertical scale is exaggerated 3 times in the two cross-sections of the Central Basin. Map from Dallmann et al. (2002).



2.2 Tectonic Evolution of the Central Basin

The original model of the Central Basins involved a two-stage tectonic evolution where the basin was proposed to have formed through a series of strike-slip sub-basins in the Paleocene, which during the Eocene developed into one compressional or transpressional basin (Figure 3). This model was based on three observations; (1) the contrast between the eastern derived Paleocene basin fill and the western derived Eocene basin fill, (2) offshore sea-floor spreading data which appeared to limit compression around the Paleocene-Eocene transition, (3) E-W striking faults suggesting an extensional setting for the early Central Basin (Steel et al. 1981; 1985; Mueller and Spielhagen 1990; Bruhn and Steel 2003).

The new, and more acknowledged model (Bruhn and Steel 2003) is for the Central Basin to have been developed as an eastward migrating foreland basin in response to flexural loading of the crust induced by the West Spitsbergen Orogen. In this foreland basin model the Paleocene succession represents the peripheral bulge derived basin fill sourced from the east and northeast. Whereas the overlying Eocene sedimentary succession represents orogen derived basin fill sourced from the west (Figure 4).

Figure 3: Illustration and explanation of the Spitsbergen Tertiary Basin (the Central Basin) evolution after Steel et al. (1985). The figure is redrawn in colors. Note the large vertical exaggeration.

I: Initial transtension: The early to mid-Paleocene Central Basin possibly evolved into a single basin from a series of partially connected basins in an extensional, possibly transtensional regime east of the De Geer Line.

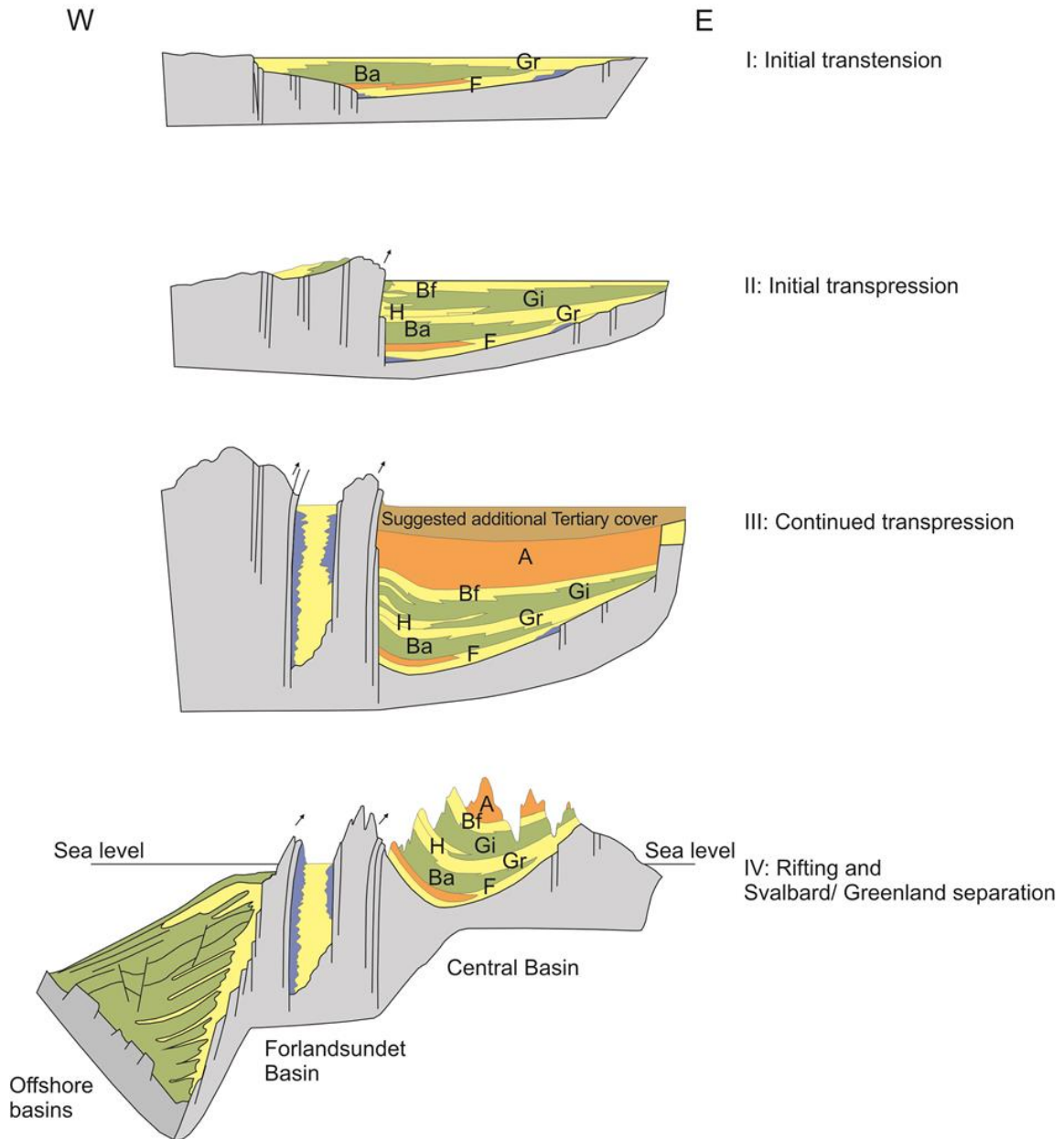
II: Initial transpression: The late Paleocene-Eocene development of the Central Basin. The region west of the basin became uplifted and served as the main source of sediments to the Central Basin.

III: Continued transpression: Suggested development of the Forlandsundet Graben as the transpression continued. Suggested additional sediment cover up to estimated sea level.

IV: Rifting and Svalbard/ Greenland separation: The Svalbard margin became rifted, and deep, offshore basins evolved west of Spitsbergen.

Central Basin Evolution and Depositional Architecture

Modified from Steel et al. (1985)



Legend		
	Mainly conglomerates	A - Aspelintoppen Fm.
	Mainly sandstones	Bf - Battfjellet Fm.
	Sandstones and siltstones	Gi - Gilsonryggen Mb
	Mainly mudstones	H - Hollenderdalen Mb
	Pre-Tertiary basement	Gr - Grumanbyen Fm.
	Oceanic basement	Ba - Basilika Fm.
		F - Firkanten Fm.

Although the idea of the Central Basin as a foreland basin to the West Spitsbergen Orogen is mentioned in the articles of the original model, the second and more “simplistic” approach to the Central Basin’s tectonic evolution is based on more recent ocean-floor spreading models as well as tectonic evidence from the West Spitsbergen Orogen and work on the Paleocene-Eocene sedimentary succession (Bruhn and Steel 2003).

The surface of the Central Basin on which the sedimentary infill rests represents a regional unconformity. This unconformity is attributed to a northward increasing hiatus spanning through most of the Late Cretaceous across the Northwestern Barents Shelf and thus Svalbard. Several suggestions attempt to explain this. One suggestion is that thermal doming north of Svalbard caused uplift and erosion. Another suggestion is that the uplift and erosion was due to initial transpression along the northern edge of the Barents Shelf (Steel and Worsley 1984; Maher et al. 1995; Braathen et al. 1999). However, the initial peripheral-bulge formation east of the West Spitsbergen Orogen may have played an important part in the regional uplift as well (Bruhn and Steel 2003).

Figure 4: Evolution of the Central Basin including development of depositional architecture and stacking patterns of small-scale sequences in the Firkanten, Basilika, Grumantbyen and post-Grumantbyen formations. For overview of the basin fill, see next subchapter. The figure is redrawn in colors from Bruhn and Steel (2003), figure text adapted from Bruhn and Steel (2003).

A, B, C and D represents the Early to Late Paleocene successions with sediments derived from the peripheral bulge side of the basin. E represents the shift to Eocene time and a drainage reversal with sediments derived from the thrust-belt side of the basin.

A: Todalen and lower Endalen members; after passage and relaxation of the initial peripheral bulge, small scale sequences on-lap the basal unconformity on the eastern basin margin.

B: Upper Endalen Member; uplift and basinward (eastward) migration of the peripheral bulge. Small-scale, basinward stepping sequences develop in response to this.

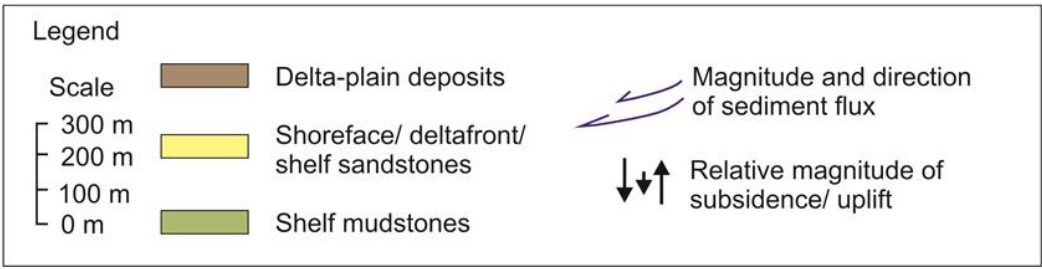
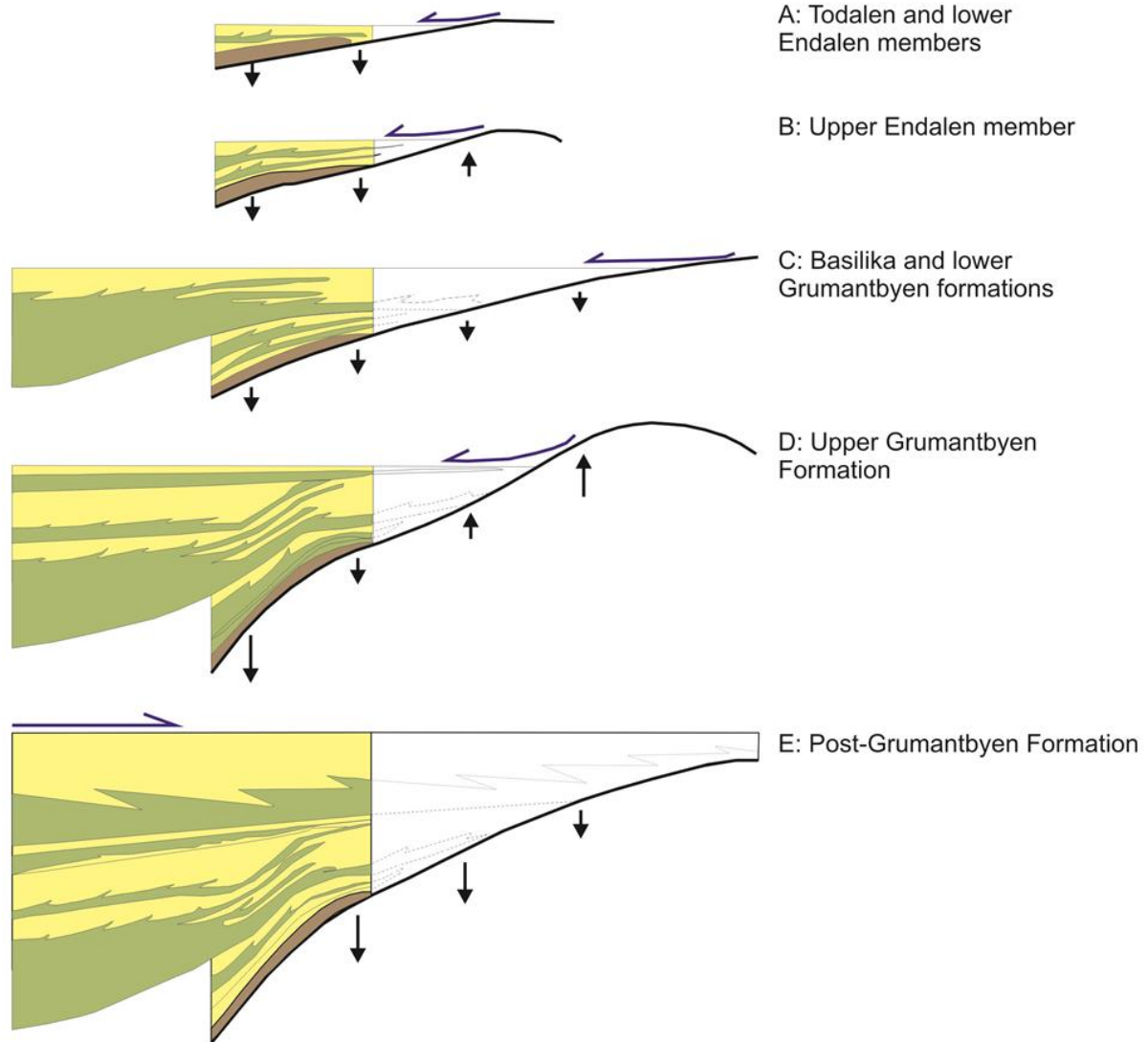
C, D: Upper Grumantbyen Formation; repetition of pattern A-B with strongly basinward stepping sand sheets in the upper part of the Grumantbyen Formation.

E: Post-Grumantbyen Formation; Eocene time, passage of the foredeep progradation of shelf clinoforms from the thrust-belt side of the basin, and thus a change in direction of sediment flux to towards the east.

Central Basin Evolution and Depositional Architecture

Modified from Bruhn & Steel (2003)

← Present exposure →



2.3 The Central Basin Fill: The Van Mijenfjorden Group

The Van Mijenfjorden Group makes up the sedimentary basin fill of the Central Basin (Figure 5) (Dallmann et al. 1999). The clastic succession is 2100 m thick, and consists of Paleocene to Early Eocene deposits, representing the landward-stepping and basinward-stepping parts of the basin fill respectively. However, the original thickness of the Van Mijenfjorden Group was larger and younger (Eocene to Oligocene), as an additional 1500-1700 meter of the succession is suggested to have been eroded during the Miocene uplift (Manum and Thronsen 1986; Bruhn and Steel 2003; Worsley 2008).

The Paleocene succession is up to 700 m thick and compromised by the Firkanten Formation (Grønfjorden Bed, Todalen Member and Endalen Member), the Basilika Formation and the Grumantbyen Formation. This succession represents a gradual transgression on the eastern part of the Central Basin, with the sediments derived from the peripheral bulge east of the basin (Bruhn and Steel 2003).

The Eocene succession is >1400 m thick and is compromised by the Frysjaodden Formation, the Hollendardalen Formation, the Battfjellet Formation and the Aspelintoppen Formation (Dallmann et al. 1999). In contrast to the underlying Paleocene succession, the Eocene succession is interpreted to be a large regressive unit derived from the West Spitsbergen Orogen, and thus west of the basin (Steel et al. 1985; Helland-Hansen 1990; Bruhn and Steel 2003). The lowermost part of the Frysjaodden Formation represents the latest Paleocene sediments and the zone of maximum flooding (Bruhn and Steel 2003). The two remaining formations of the Van Mijenfjorden Group belong to the Ny-Ålesund Subgroup (Figure 5). These are deposited in a separate basin north of the Central Basin and are probably related to the lower part of the Van Mijenfjorden Group (Dallmann et al. 1999).

A northward-increasing hiatus, spanning through most of the late Cretaceous, is extending through the northwestern Barents Sea Shelf and Svalbard. The Van Mijenfjorden Group rests on this hiatus, and thus on the Lower Cretaceous Carolinefjellet Formation (Bruhn and Steel 2003). This is marked by a slight discordance between the Carolinefjellet Formation and the Firkanten Formation (Paech 2001). A description of the formations, members and beds of the Van Mijenfjorden Group follows.

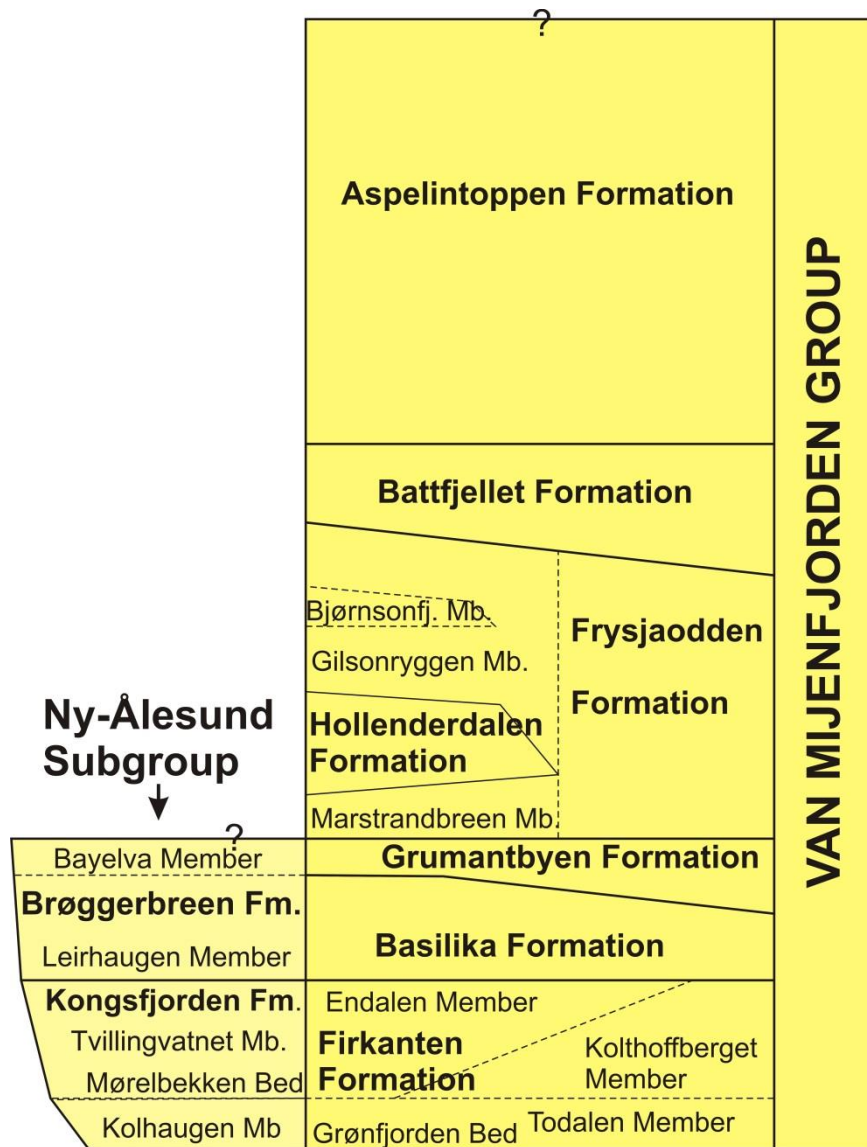


Figure 5: Lithostratigraphic scheme of the Van Mijenfjorden Group. The figure is modified in different colors after Dallmann et al. 1999).

Firkanten Formation

The Firkanten Formation makes up the lowermost infill of the Van Mijenfjorden Group (Figure 6). It was deposited during the Early Paleocene (Blythe and Kleinspehn 1998; Nagy et al. 2000; Cepek 2001; Spielhagen and Tripathi 2009). The Firkanten Formation thickens westwards in the basin from 80 m to 200 m (Kellogg 1975; Bruhn and Steel 2003) and consists of three members in addition to one distinctive bed (Steel et al. 1981; Dallmann et al. 1999). The overall trend of

the Firkanten Formation is suggested to be transgressive with several smaller regressive segments (Steel et al. 1981; Müller and Spielhagen 1990; Dallmann et al. 1999; Bruhn and Steel 2003).

The transgressive nature of the formation is based on the lower part being interpreted to be delta-plain deposits, in parts under tidal influence, whereas the upper part is interpreted to be delta-front deposits, which together with the pro-delta interpretation of the overlying Grumantbyen, fits nicely into a transgressive system tract interpretation (Steel et al. 1981).

The lower part of the formation may be recognized by its characteristic coal seams, typically interbedded by sandstones, siltstones and shales of marine- and non-marine origin. The upper part of the formation is in the north and northeastern region of the Central Basin characterized by bioturbated/ laminated marine sandstones as well as minor beds of clay ironstones, conglomerates and siltstones. In contrast, the upper part is in the western and southern regions made up of southwesterly thickening wedges of shales and siltstones (Dallmann et al. 1999).

The Firkanten Formation is situated immediately above the Early Cretaceous Carolinefjellet Formation, separated by a regional unconformity corresponding to a northward increasing hiatus that spans most of the late Cretaceous. The unconformity displays distinctive features which are helpful in detecting the base of Firkanten Formation (Examples after Dallmann et al. 1999);

- 1) A low-angle unconformity between the Firkanten Formation and the Carolinefjellet Formation.
- 2) A conglomerate in the base of the Firkanten Formation.
- 3) A well-developed paleo-weathering surface at the base of Firkanten Formation.

At locations where these classic boundary-identifiers are absent, the boundary may still be established by observing subtle differences between the two formations. The Firkanten Formation will commonly appear to be of a softer or more massive nature than the underlying, platy and well-laminated sandstones of the Carolinefjellet Formation (Dallmann et al. 1999).

Grønfjorden Bed

The Grønfjorden Bed is an irregular developed basal conglomerate with its base resting on the regional unconformity to the Carolinefjellet Formation (Figure 6). The thickness of the bed is recorded to be up to 2 m in the northeastern part of the basin, and 4.5 m in the northwestern part,

but it may also be completely absent at some locations (Dallmann et al. 1999). The conglomerate is both clast- and matrix-supported with well-rounded chert and quartzite pebbles. The nature of the Grønfjorden Bed is suggested to be of a braided river system, or an incised valley fill, sourced from areas east of the Central Basin (Vonderbank 1970; Kalgraff 1978; Ytreland 1980; Bruhn and Steel 2003; Nagy 2005).

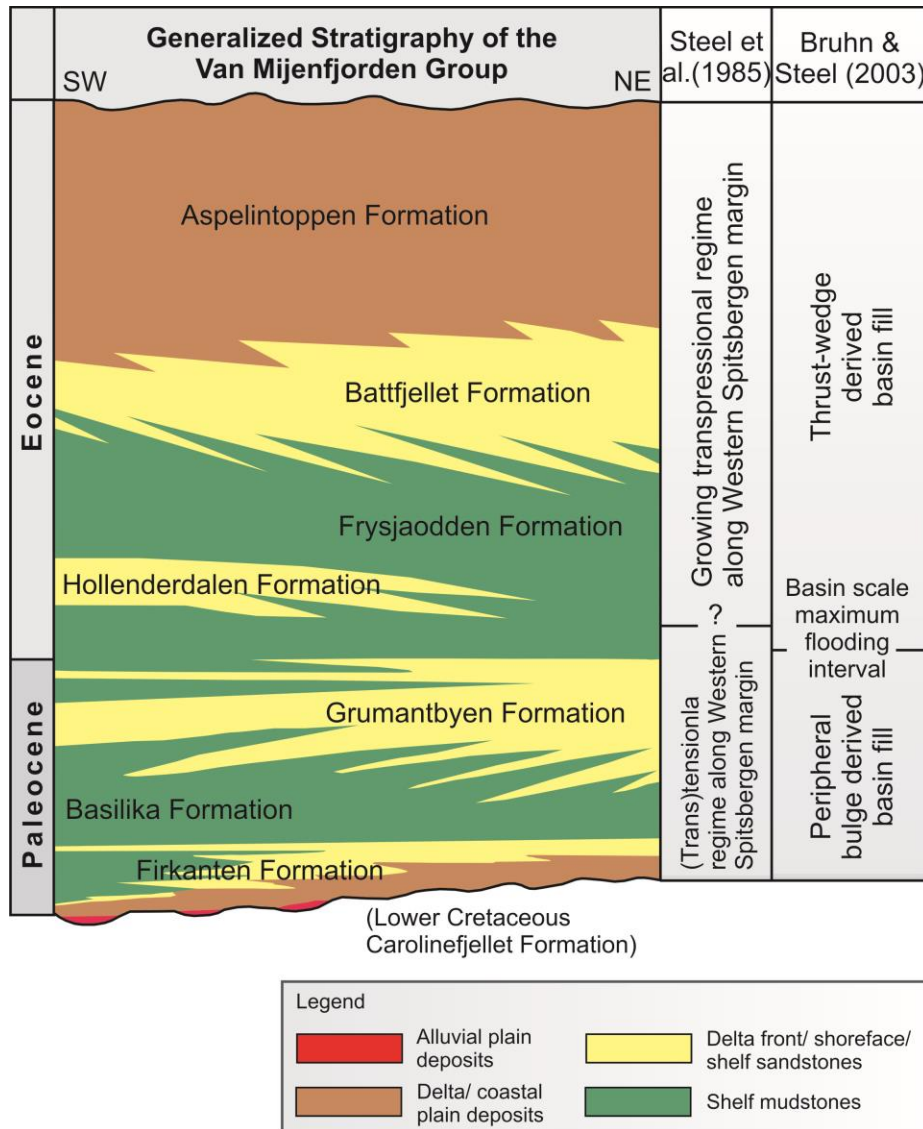


Figure 6: Generalized stratigraphy of the Van Mijenfjorden Group with a comparison of the interpretations by Steel et al. (1985) and Bruhn and Steel (2003) on the right-hand side. Modified in colors after Bruhn and Steel (2003).

Todalen Member

The Todalen Member (Figure 5) is commonly less than 60 m thick and made up by rhythmic, coarsening upwards successions, capped by either coal or clay ironstone (Dallmann et al. 1999). These successions are in large interpreted to represent delta-plain deposits with tidal influences at various levels (Steel et al. 1981; Bruhn and Steel 2003).

The delta itself is suggested to have been sourced from a number of distributary systems east and north of the present day Central Basins margins, building out towards the west, southwest and south (Steel et al. 1981; Bruhn and Steel 2003). The direction of the delta outbuilding is in concordance with fluvial paleotransport-data and thickness-trends of the interpreted shoreface facies of Bruhn and Steel (2003).

From evidence like bioturbation together with wave-and tidal generated structures, it is suggested that tidal processes were common on the delta plain, and that waves were probably reworking abandoned lobes. Therefore, the shape of the delta is suggested to have been lobate. Due to the different processes affecting the delta plain, stratigraphic variations occurs within the Todalen Member depending on whether it is the proximal or distal part of the deltaic system that is investigated. For instance, the characteristic coarsening upward sequence consisting of shale-siltstone-sandstone is in the proximal part capped by coal, whereas in the distal part, capped by shale. Other proximal-distal variation that occurs are; purely shale-coal sequences in the proximal part and, shallow marine sandstone dominance in the distal part (Steel et al. 1981).

Endalen Member

The Endalen Member (Figure 5) varies in thickness from 40 m in the northeast to 100 m in the south and southwest where it interfingers with its deep water equivalent; the Kolthoffberget Member (Figure 5) (Bruhn and Steel 2003). Generally, the Endalen Member consists of stacked series of sandstones, typically well bioturbated or cross-stratified, together with thin beds of conglomerates, clay ironstones and minor shales. It displays a deepening of facies to the western and southern reaches of the basin (Steel et al. 1981; Dallmann et al. 1999). Along the eastern basin margin the Todalen Member consists of shoreface to offshore sandstones and mudstones,

and in the western and deeper part of the basin; incised shoreface sandstone and sediment-gravity flow deposits (Bruhn and Steel 2003).

Kolthoffberget Member

The Kolthoffberget Member is the deep-water equivalent to the Endalen Member, and is only developed in the western and southern reaches of the basin with a maximum recorded thickness at the southwesterly-most edge of 100 m (Figure 5) (Steel et al. 1981; Bruhn and Steel 2003). It consists of several gradual, upward-coarsening sequences of dark, silty shales-poorly sorted, organic rich, very fine, sandstones (Steel et al. 1981). Each sequence is reported to be less than 10 m thick, with extreme bioturbation in the uppermost part. The sequences are interpreted to represent shoaling-upward conditions in a pro-deltaic setting. The base of the member may be recognized as a shale succession overlying Todalen Members upper sandstones (Dallmann et al. 1999).

Basilika Formation

The black shales of the Basilika Formation vary in thickness from 20 m in the northeast to 300 m in the south-and southwesterly reach of the basin (Figure 6). Its base is easily recognized as thick shales overlying the upper sandstone beds of the Endalen Member (Dallmann et al. 1999). The Basilika Formation is interpreted to represent an outer-shelf mud complex (Steel et al. 1985; Müller and Spielhagen 1990). The lowermost part of the Basilika Formation shows a deepening-upwards, and thus fining-upwards trend. This zone of deep-water mudstone at the base of the Basilika Formation is interpreted to represent the maximum flooding surface within both the Basilika- and the overlying Grumantbyen Formations (Bruhn and Steel 2003).

Grumantbyen Formation

The Grumantbyen Formation consists of well bioturbated, glauconitic marine sandstone with some siltstone, and is thus regarded to be entirely marine in origin (Steel et al. 1985; Bruhn and

Steel 2003). In contrast to the underlying formations, the overall thickness trend of the Grumantbyen Formation is thinning to the west and southwest from 450 m in the northeast and east, to less than 200 m (Figure 6) (Steel et al. 1985; Dallmann et al. 1999; Bruhn and Steel 2003). But it is suggested to be sourced from the east (Bruhn and Steel 2003). The base of the Grumantbyen Formation to the Basilika Formation is gradational, and is best recognized by incoming greenish, bioturbated, in parts silty, sandstone.

Frysjaodden Formation

The Frysjaodden Formation consists mainly of deep marine shales with some sand-rich, turbidite intervals (Bruhn and Steel 2003). The formation thickens from 200 m in the north and northeastern part of the basin, to more than 400 m towards the south- and southwestern parts (Figure 6). In terms of provenance, the Frysjaodden Formation represents a turnaround in sediment supply, as it is proposed to be sourced from the West Spitsbergen Orogen, situated along the western margin of the basin, as opposed to the underlying formations, sourced from the east (Dallmann et al. 1999; Bruhn and Steel 2003). The base of the Frysjaodden Formation is sharp to the sandstones of the Grumantbyen Formation underneath, and lenses of conglomerates are in parts developed at this boundary. The Frysjaodden Formation consists of three members; Marstrandbreen Member, Gilsonryggen Member and Bjørnsonfjellet Member. Respectively, the two first members represent deep water deposits (shales) adjacent to the growing West Spitsbergen Fold-thrust Belt, which is also true for the third member, but with additions of thin sandstone wedges as a result of high density turbidites and slump deposits.

Hollendardalen Formation

The Hollendardalen Formation is made up by several sandstone wedges, thinning out to the east, terminating in the center of the basin into the shales of the Frysjaodden Formation (Figure 6) (Steel et al. 1981; Dallmann et al. 1999). The maximum thickness of Hollendardalen Formation is in the west approximately 150 m. The formation is characterized by its well laminated, and in parts, cross stratified sandstones, together with plant fragments, rootlets and ripples. The formation is suggested to be of a tidal-dominated, deltaic sand-wedge nature, building out

towards the northeast. Provenance studies on metamorphic rock fragments in the formation, verifies the source to be from the West Spitsbergen Fold and Thrust Belt (Müller and Spielhagen 1990; Dallmann et al. 1999).

Battfjellet Formation

The Battfjellet Formation is constituted by up to seven, coarsening-upwards shoreline sequences (very fine to medium sandstones). Each sequence is ranging in thickness from 10 to 30 m (Helland-Hansen 1990). Overall, the thickness of the formation gradually changes from less than 60 m in the northeaster reaches of the basin, to more than 300 m in the south (Figure 6) (Dallmann et al. 1999). The sandstone wedges of the Battfjellet Formation are pinching out towards northeast, dipping down into the Frysjaodden Formation (Kellogg 1975; Steel et al. 1985; Helland-Hansen 1990). Generally, the westernmost sandstone wedges display sedimentary structures characteristic for those of sandstones deposited below storm-wave base, whereas the easternmost situated wedges display features associated with deposition above storm-wave base (Helland-Hansen 1990). The base of the Battfjellet Formation may be recognized as the first sandstone bed above the Frysjaodden Formation shales.

Aspelintoppen Formation

The Aspelintoppen Formation represents the final preserved infill of the Central Basin, and is only occasionally overlain by Quaternary deposits (Müller and Spielhagen 1990; Dallmann et al. 1999). It consists of alternating sand- and siltstone intervals, as well as intervals of mudstones and thin coals. The Aspelintoppen Formation covers the whole basin with a thickness of >1000 m (Figure 6), with one of its most characteristic features being, besides the thickness, a terrestrial influence which today may be observed as neatly preserved fossil leaves in the field. The majority of the sediment infill is interpreted to be different types of shallow-water deposits like distributary channels, crevasse splays and swamp deposits (Dallmann et al. 1999).

3. Analytical Approach

3.1 Field Work Locations

The field work was carried out along the north eastern flank of the Central Basin on Spitsbergen, Svalbard during one period of core logging and one field work season. During the core logging period, 1.th - 12.th of December 2011, two cores were logged and sampled in SNSG core storage in Endalen, close to Longyearbyen. These are listed from east to west (Figure 7, location 1 and 4):

- Core 18-2009, Lunckefjellet.
- Core 15-2010, Bassen on Operafjellet.

For the period of the field season, 16.th July - 15.th of September 2012, the following five field locations, listed from east to west, were investigate (Figure 7, locations 2, 3, 5-7):

- Stempelen.
- Boret.
- Endalen (Bayfjellnosa mountain).
- Grumantbyen.
- Bjørndalen.

Excellent exposures of the Todalen Member and lower Endalen Member strata were logged and sampled in Grumantbyen and Endalen.

The Stempelen and Boret exposures were of mixed quality as they held major scree covered sections. The Bjørndalen cliff was inaccessible.

The field locations were selected from geological maps (Steel et al. 1989; Dallmann et al. 2002), unpublished LIDAR-photos provided by SNSK and previous work on the Firkanten Formation (Steel et al. 1981, 1985; Nøttvedt 1985; Dallmann et al. 1999; Bruhn and Steel 2003).

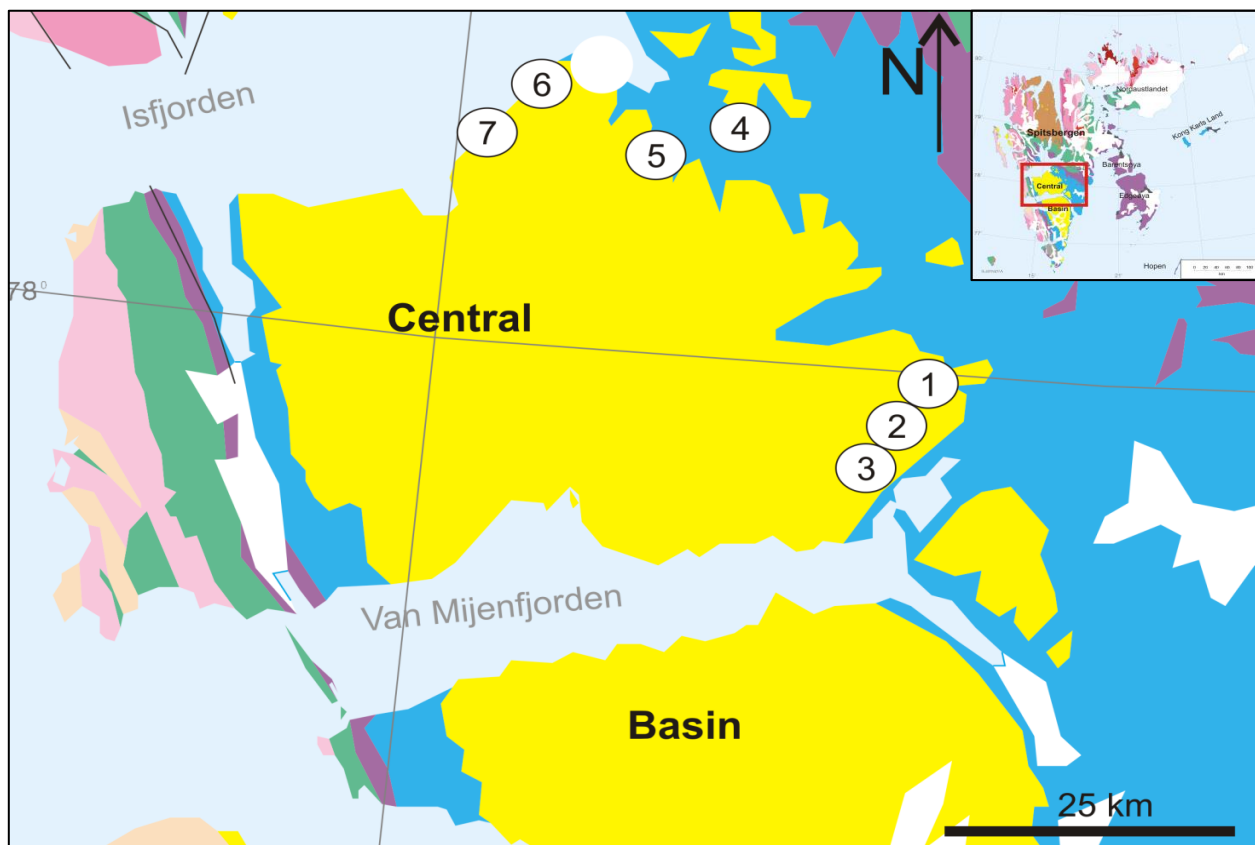


Figure 7: Bedrock map of southern Spitsbergen, Svalbard (see Figure 2 for legend). The Central Basin fill is in yellow color. The seven investigated location are numbered from east to west (1-7):
 1) Lunckefjellet (Core 18-2009). 2) Stempelen. 3) Boret. 4) Bassen (Core 15-2010).
 5) Endalen (Bayfjellnosa). 6) Bjørndalen. 7) Grumantbyen. Map after Dallmann et al. (2002).

Loc. 1 Core 18-2009

The 18-2009 core was drilled as a part of SNSG`s Lunckefjell-project, located on the eastern side of the Marthabreen glacier, 11.9 km north of Braganzavågen (Figure 7, loc.1). The core was selected by its abundance of coal seams, in addition to an ash layer (bentonite). See Appendix 2.1 for log. Lunckefjellet will host the next main mine when the Svea North mine is depleted in 2015 (M. Often, pers. comm., 2013).

Loc. 2 Stempelen

The Stempelen mountainside is situated on the northeastern flank of the Central Basin, between the Gruvfonna and Helsingborgreen glaciers, north of Van Mijenfjorden (Figure 8). It was discovered by visual inspection of the area by helicopter. The horizontal L-shape of the crag allowed the excellent exposure to be inspected along both the south facing, east-west striking arm and the east facing, north-south striking arm. Due to the peculiar geometry of Stempelen, sedimentological features may also be observed in three dimensions where the north-south and east-west striking arms intersect.

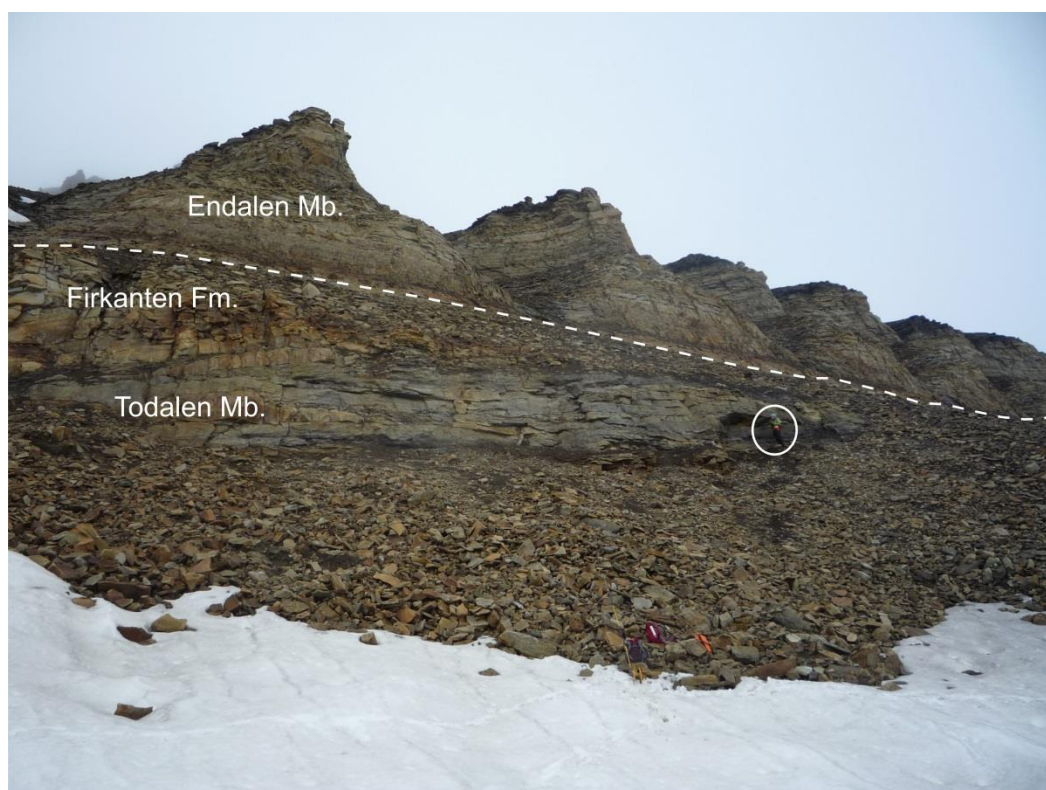


Figure 8: Overview photo of the Stempelen outcrop along the south-facing exposure. Person to scale in the white circle.

Loc. 3 Boret

The Boret mountain is situated 3.4 km south-southwest of the Stempelen crag and is host to the mine entrance of Svea North. The mine entrance is located on Boret's southernmost edge at an elevation slightly above the Høgenesbreen glacier. The Svea North Mine is exploiting the coal found in the Todalen Member. In the very steep, east-facing hillside of Boret, the upper part of the Endalen Member is nicely exposed (Figure 9) and may be logged all the way to across the upper boundary of the Basilika Formation. The Todalen Member is completely covered by scree/glacial ice at this location, and only the Endalen Member and its upper boundary can be logged at this location.



Figure 9: Overview photo of the Endalen Member in the Boret Mountainside.

Loc. 4 Core 15-2010

The 15-2010 Core was drilled on Bassen on the Operafjellet mountain, situated east of Longyearbyen (Figure 7). The core was drilled as a part of SNSG mapping of coal in proximity to Longyearbyen. Core 15-2010 was selected from its abundance of coal seams (Appendix 2.4).

Loc. 5 Bayfjellnosa in the Endalen Valley

The Bayfjellnosa mountain makes up the northeastern side of the Endalen valley (Figure 10). The valley was appropriately named as “the No. 1 valley” to Longyeardalen by the American Company, Arctic Coal Co., which was taken over by SNSK in 1916 (NPI/stadnavn 2013). The boundary between the Carolinefjellet Formation and Firkanten Formation is cropping out nicely below the old mine entrance at 229 meter above sea level. The upper part of the Firkanten Formation (Endalen Member) forms prominent cliffs above the mine entrance. The Todalen Member and lower Endalen Member strata was logged and sampled in the Endalen outcrop (Appendix 2.5).



Figure 10: Overview photo of the logged Endalen outcrop, with the boundary between the Todalen Member and Endalen Member marked by a white, punctuated line. Note the whiteish appearance of the massive sandstone above the boundary. An old mine entrance can be seen to the left where wooden sticks are pointing out.

Loc. 6 Bjørndalen

The Bjørndalen outcrop is situated in the cliffside west of the Bjørndalen river-outlet to Isfjorden (Figure 11). The exposure is clean, but the accessibility is limited by the steep nature of the cliff.

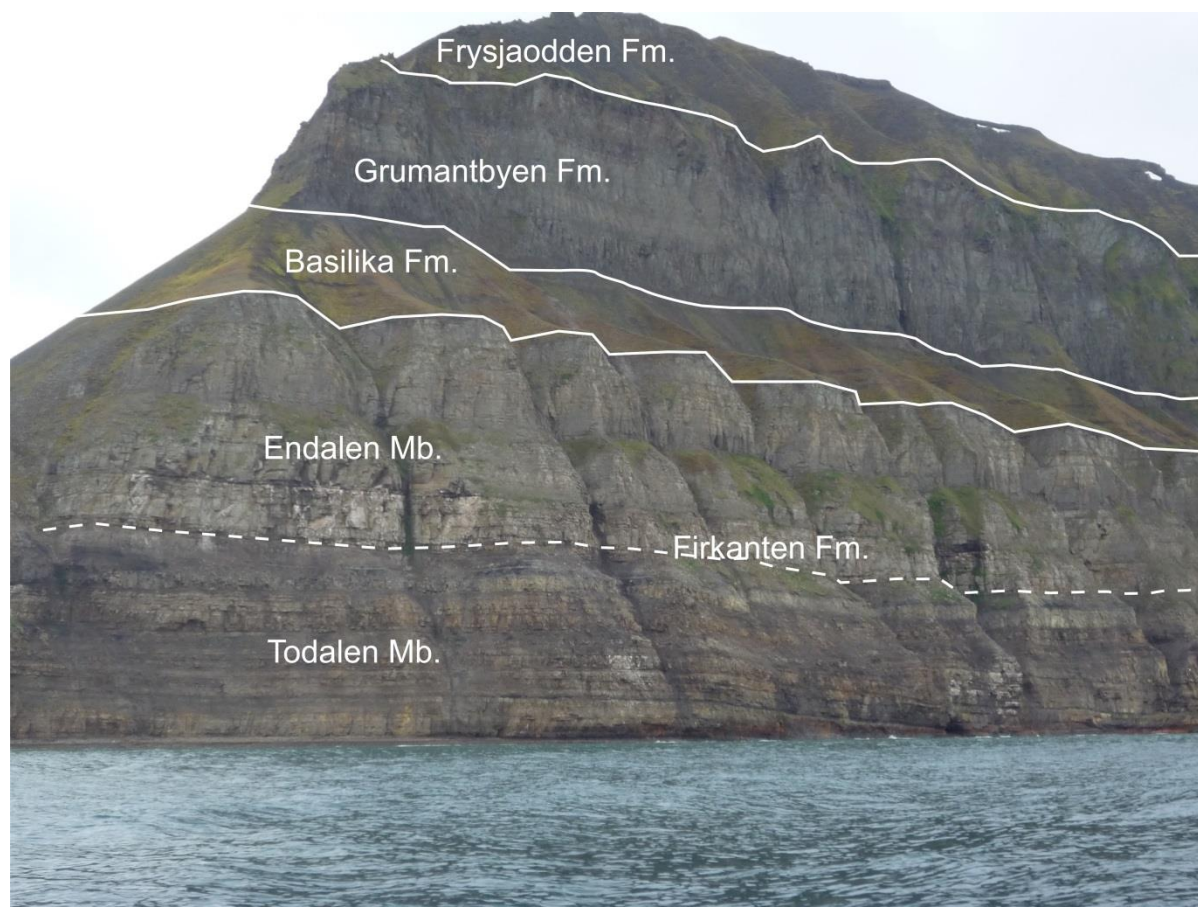


Figure 11: Overview photo of the Bjørndalen cliff, which was attempted logged on the left side of the photo. The Firkanten Formation is here comprised by the Todalen Member and Endalen Member. The Basilika Formation, Grumantbyen Formation and Frysjaodden Formation are outlined above.

Loc. 7 Grumantbyen

Grumantbyen is located 13.3 km south southwest of Longyearbyen. The Todalen Member exposure is situated directly in the cliff along the shoreline below the old, abandoned, Soviet settlement of Grumantbyen.

The slight, apparent southwest-ward dip of the Firkanten Formation allows the whole Todalen Member (and its lower boundary to Carolinefjellet Formation) together with the lower Endalen Member strata, to be accessed effortlessly by walking westwards along the shoreline at low tide (Appendix 2.6). The two lowermost coal seams of the Todalen Member is displayed in Figure 12.



Figure 12: Photo of the two lowermost coal seams in the Grumantbyen outcrop.

3.2 Methodology

Sedimentological Core Logging and Sampling

The aim of the core logging was to make a representation of the lithology and sedimentological structures encountered in the Todalen Member and the lower Endalen Member strata. Two sedimentological core logs were obtained: Core 18-2009 from the Lunckefjellet mountain and Core 15-2010 from Bassen on the Operafjellet mountain. Both cores were drilled vertically.

The cores were whole with a diameter of 5 cm. They were stored in boxes containing five one-meter-long core pieces per box. The sedimentological logs were made during hands-on investigation of the cores. Color and color changes of the core provided helpful clues to where the grain size should be investigated as both abrupt and gradual changes in grain size often is reflected in the color of the core. Darker color often indicates smaller grain size and vice versa. The grain size was established by the use of a hand lens and grain size chart on fresh surfaces.

First hand investigation of the coal beds of Todalen Member was not possible since they had been removed for mining related analyses by the SNSG. The coal beds were replaced in the core boxes by wooden sticks with the thickness of each respective coal bed written on. These thicknesses were double checked with pictures taken of the cores before the coal was removed. The core pictures were provided by SNSG.

The small diameter of a core provides limitations in regards to observation of horizontal features. Large-scale structures like the nature of cross-beds, presence of channels as well as other lateral variations within beds may not be established with great certainty. The advantage with core logging is the clean, smooth and most often unweathered surface which generally makes ripples easy to recognize, and also allows for mudrock to be properly investigated (Nichols et al. 2009).

Samples for petrographic thin sections were collected by the use of a stationary drill which extracted cylinder shaped plugs from the cores (Figure 13). The orientation of the plugs were perpendicular to the length axis of the core and measured ~1,5 cm x 3 cm (diameter x length). An arrow marking “way up” was drawn on every sample before it was drilled. This was done in case of any distinct grading should be seen in the thin sections.



Figure 13: Drilled core plug for petrographic thin section. The shiny material on the core is frozen water (core storage temperature in December 2011 was about -20°C).

Sedimentological Outcrop Logging and Sampling

Outcrop logging and sampling was carried out on several locations (see Chapter 3.1) on the northeastern flank of the Central Basin on Svalbard. When possible, a meter stick was used to measure the bed thicknesses. Samples for petrographic thin sections were marked with “way up” and then partitioned into fist-sized specimens with a hammer and put in marked plastic bags. Overview and close-up photos were taken on every location.

Graphic Illustrations of Logs

The technical drawing software *CorelDraw* was used to digitalize the hand drawn sedimentological logs. This was done by scanning the raw logs into the computer, and thereafter utilize the different drawing tools in *CorelDraw* to digitally trace the lines of the raw log. A legend for the logs are given in Appendix 2.1.

Facies and Facies Associations

The term “facies” stems from Latin and refers to an object’s external appearance (Walker 1994). It is used to categorize a rock unit by its objective properties like for instance sedimentological

structures, grain size distribution and presence of fossils. Whether a single facies also should include an interpretation of the environment in which it was deposited has been widely discussed (Walker 1994). A solution to this has been presented by Middleton (1978) which stated that facies are units which will be given an environmental interpretation later on. This is reasonable as a single facies may occur in a spectrum of environments. It is therefore key to study the surrounding facies before an interpretation of a depositional environment is made. Therefore, the majority of facies described in Chapter 4 will be purely descriptive. Nevertheless, each facies in Chapter 4 is presented together with a suggested depositional flow regime as this may be helpful when establishing facies association. The flow regimes of Boggs (2006) has been applied for this purpose. The facies are named after what dominates their appearance in the field and cores.

Interpretation of the facies was carried out as described by Reading and Levell (2006) “by investigation of a facies affiliation to neighboring facies and grouped into facies associations which are environmentally related”. Thus the facies associations in this work have been done from an environmental perspective and are based on observations of characteristic depositional features, the sequences in which they occur, and the nature of the bounding surfaces between them.

Petrographic Analysis

Thin Sections and the Microscope

Fifty-four standard polished thin sections with blue epoxy have been examined from the logged cores and outcrops. Thirty-five of these displayed sandstone lithologies, these were analyzed in a petrographic microscope. Photo micrographs were taken with a Nikon DS-Fil digital camera mounted on top of the microscope. It was in some cases necessary to further enhance the sharpness and contrast of the micrographs, this was done by using the gamma adjustment feature in the picture editing program *PhotoCorel*.

Modal Analysis

To establish the grade and content of minerals and porosity, three hundred points were counted in the thin sections displaying sandstone lithologies (Table 1). The step length (distance) between each point was 0.1 mm. The point counting results were recorded by the use of *PelCon* software.

Sorting of grain size was established using Harrell (1984) visual comparator for degrees of sorting. The grain size was determined by measuring the length axis of thirty grains in the dominant grain fraction and calculates the mean value. This mean value was classified using the Wentworth size class terminology.

Scanning Electron Microscope (SEM)

Four polished thin section were coated by carbon and analyzed in a Scanning Electron Microscope (Table 1) to determine the chemical composition of the clay matrix, cement, heavy minerals and detrital grains using a combination of backscattered light images and EDS analysis.

Sources of Error during Petrographic Analysis

Three hundred points in a representative area of each thin section were counted during the modal analysis. This leaves possibilities for statistical error as the whole sample is not counted.

Counting distance was set to 0.1 mm, this means that smaller sized components like cement, matrix, silt and in parts very fine grains, could be missed during counting, thus leaving the counted volumes somewhat smaller than they really are.

Quantification of quartz cement and rounding of grains was at times a challenging task as the quartz overgrowths occasionally had very poorly developed dust rims. This may have led to an underestimation of the quartz cement, and perhaps also to an overestimation of the angularity of quartz grains. Regarding grain size, it is suggested that the length axis of spherical and ellipsoid grains will be under-estimated by 10-15% during thin section measurements (Johnson 1994).

Detrital quartz and orthoclase grains could be delicate to differentiate in the thin sections as orthoclase may resemble quartz in both plane light and under crossed-nichols. The presence of

orthoclase was established by either observing one or two directional cleavage of the grain, or creating an interference figure in the microscope. Nevertheless, some orthoclase grains may have mistakenly been counted as quartz.

Table 1: Overview of thin sections and the respective analysis methods applied. For abbreviations, see Appendix 2.3

Core/ Outcrop	Thin Section #	Elevation a.C.Fm. (m)	Member	Lithology	Point Counted	Other Analysis
Core 18-2009, Lunckefjellet						
Core 18-2009	18-1	3,08	Todalen	Mudrock	No	SEM
Core 18-2009	18-3	11,00	Todalen	Sandstone	Yes	
Core 18-2009	18-4	14,60	Todalen	Siltstone	No	
Core 18-2009	18-5	14,95	Todalen	Siltstone	No	
Core 18-2009	18-6	15,60	Todalen	Sandstone	Yes	
Core 18-2009	18-7	20,05	Todalen	Sandstone	No	
Core 18-2009	18-8	22,20	Todalen	Sandstone	Yes	
Core 18-2009	18-9	30,90	Todalen	Siltstone	No	
Core 18-2009	18-10	33,80	Todalen	Sandstone	Yes	
Core 18-2009	18-11	39,00	Todalen	Siltstone	No	
Core 18-2009	18-12	42,55	Todalen	Siltstone	No	
Core 18-2009	18-13	43,73	Todalen	Sandstone	Yes	
Core 18-2009	18-14	44,80	Endalen	Sandstone	No	
Core 18-2009	18-15	45,70	Endalen	Siltstone	No	
Core 18-2009	18-16	47,10	Endalen	Conglomerate	Yes	
Core 18-2009	18-17	50,45	Endalen	Sandstone	Yes	
Core 15-2010, Bassen						
Core 15-2010	15-2	0,72	Todalen	Sandstone	Yes	SEM
Core 15-2010	15-5	7,30	Todalen	Sandstone	Yes	
Core 15-2010	15-6	14,29	Todalen	Sandstone	Yes	
Core 15-2010	15-8	21,05	Todalen	Sandstone	Yes	
Core 15-2010	15-9	33,50	Endalen	Sandstone	Yes	
Core 15-2010	15-10	37,75	Endalen	Sandstone	Yes	
Core 15-2010	15-11	38,92	Endalen	Sandstone	Yes	
Endalen Outcrop						
Endalen	EN 1-2	1,00	Todalen	Sandstone	Yes	
Endalen	EN 1-3	9,70	Todalen	Sandstone	Yes	
Endalen	EN 1-5	22,90	Todalen	Sandstone	Yes	
Endalen	EN 1-6	31,70	Todalen	Sandstone	Yes	
Endalen	EN 1-7	43,05	Endalen	Sandstone	Yes	
Grumantbyen Outcrop						
Grumantbyen	GR 1-2	1,80	Todalen	Sandstone	Yes	
Grumantbyen	GR 1-3	2,87	Todalen	Sandstone	Yes	SEM
Grumantbyen	GR 1-4	16,67	Todalen	Sandstone	Yes	
Grumantbyen	GR 1-7	23,13	Todalen	Sandstone	Yes	
Grumantbyen	GR 1-9A	27,87	Endalen	Conglomerate	Yes	SEM
Grumantbyen	GR 1-9	28,45	Endalen	Sandstone	Yes	
Grumantbyen	GR 1-10	32,42	Endalen	Sandstone	Yes	

4. Sedimentological Results

4.1 Facies

Eleven facies were identified in the Todalen Member and lower Endalen Member strata. The facies are attempted listed after apparent increasing energy level.

The eleven facies are listed below, an overview of these facies are also given in Appendix 1.1:

A – Coal

B – Mudrock

C – Rippled Mud Rich Sandstone

D – Planar Bedded Sandstone

E – Asymmetrically Rippled Sandstone

F – Symmetrically Rippled Sandstone

G – Tabular- and Trough Cross-Bedded Sandstone

H – Hummocky Cross-Stratified Sandstone

I – Burrowed Sandstone

J – Carbonate Cemented Sandstone

K – Rooted Sandstone

L – Conglomerate

A – Coal

Description

The coal is recognized by its black to almost bluish color, shiny appearance and brittle texture (Figure 14). Coal seams >30 cm display a banded textures in the outcrops, and occasionally pyrite lenses.

Flow Regime Interpretation

The flow regime in which the organic material (precursor of peat which is a precursor of coal) was deposited must have been very low for it to be preserved, and not transported away or oxidized by currents (Nichols 2008).

B – Mudrock

Description

This facies consist of mudrock. In outcrops, it can be recognized by its characteristic fissility and orange weathering surface (Figure 14). The fresh color of the mudrock facies is dark to black. In the cores, the mudrock is frequently seen to contain silty laminas (Figure 15).

Flow Regime Interpretation

Mudrocks may be deposited by clay settling out of suspension in a sufficiently low energy regime (Boggs 2006). The silt component may be due to periods of increased flow and sediment supply, and may display a record of cyclicity in the depositional environment (Longhitano et al. 2012).

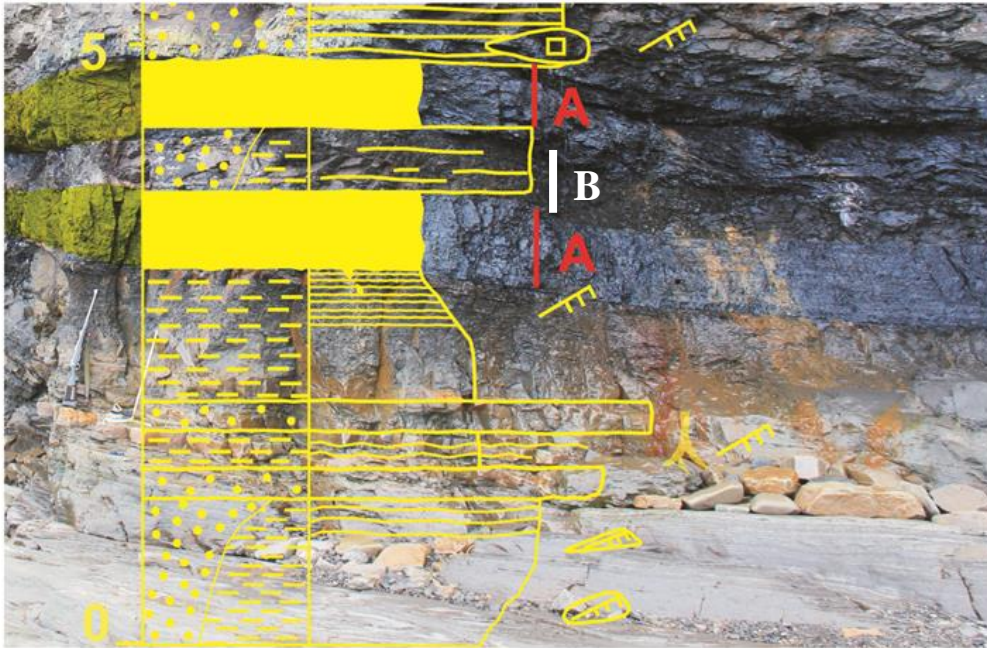


Figure 14: Red colored “A” marks the coal facies in the Grumantbyen outcrop. The coal beds are drawn in transparent yellow to the left of the log, and in solid yellow in the log itself. Note that the color of coal in the outcrop is almost bluish black. The log scale is in meters.

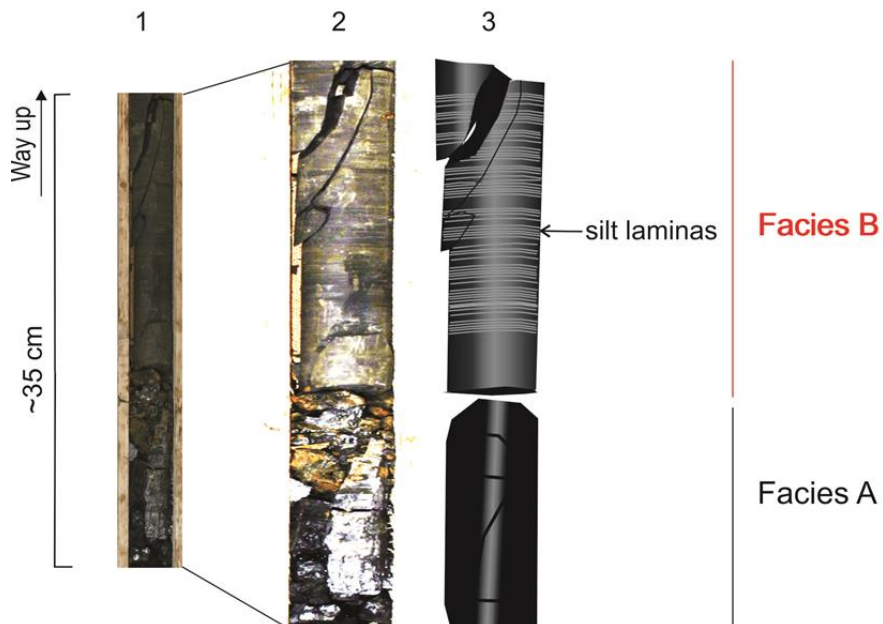


Figure 15: Facies B (mudrock) in Core 15-2010. The picture of the core is denoted 1, magnified and extremely contrast enhanced picture is denoted 2 and drawn illustration is denoted 3. The picture was contrast enhanced and horizontally exaggerated to bring out the thin and planar silt laminae. A coal bed (facies A) is situated beneath the mudrock (facies B).

C – Rippled Mud Rich Sandstone

Description

The facies consist of muddy sandstone unit with ripples of asymmetric geometries and unidirectional or bidirectional orientations (Figure 16 and 17). Bioturbation is rare to moderate. The ripples commonly display mud drapes on the ripple foresets and ripple crests. Frequently encountered bedding styles include lenticular bedding (isolated ripples of silty to fine grained sand surrounded by mud) and wavy bedding (sandy ripple beds interbedded by mud). One or several gradual transitions between the bedding styles are common within the facies.

Moderately bioturbated sections of the facies often appear together with thin coal laminas. The sand fraction in these cases is often pale with an almost white fresh color while the color of the mud fraction is dark.

The weathered surface of the facies in outcrops is multicolored reddish brown and dark grey. The fresh surface (when broken with a hammer and observed in cores) reveals the true color to be of pale- to medium grey nature.

Flow Regime Interpretation

Overall, the asymmetrical ripples indicate that it belongs to a subaqueous lower flow regime (Selley 2000). The flow was of multiple directions since the ripples are of at least two different orientations (Nichols 2009). The muddy beds and mud draping on ripples may be a result of a cyclicity in the depositional environment which allowed mud to settle out of suspension during periods of still waters. The occasional increase in the proportion of sand to mud may be interpreted as an increase in clastic input, stronger flow, or perhaps both. The dark appearance of the mud-fraction and the presence of brittle coal-laminas in the moderately bioturbated sections may indicate a significant content of organic material. Another feature of the moderately bioturbated sections is the “bleached” appearance of the sand fraction which is probably a secondary feature of leaching acidic waters from the organic rich mud into the sand.

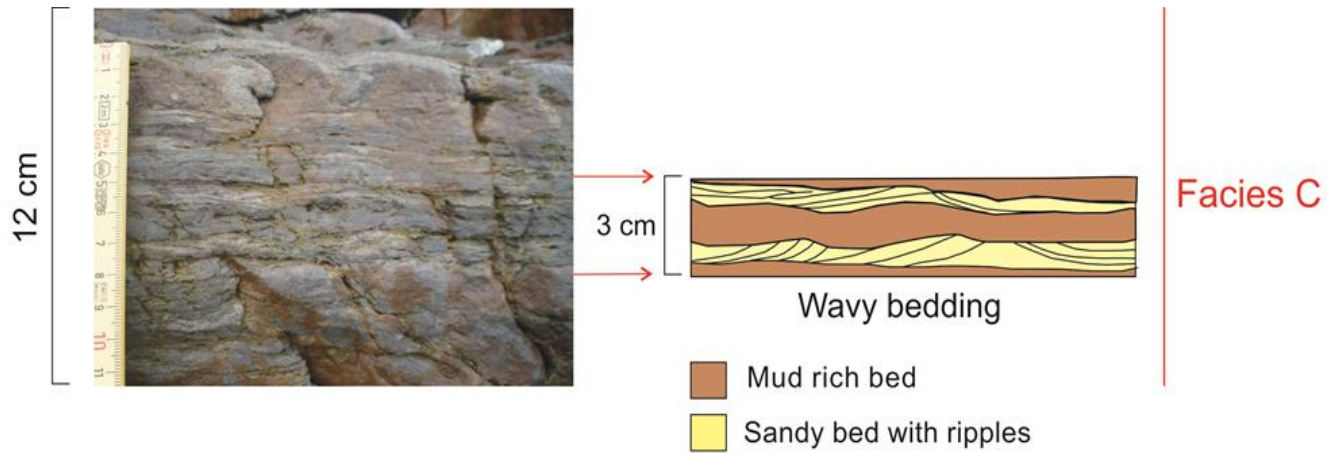


Figure 16: Facies C in the Grumantbyen outcrop. The illustration shows the sandy beds with asymmetric and bi-directional ripples. The wavy crests of the sand beds seem to have been erosionally induced as the ripple “topsets” are truncated. Note the reddish weathering surface of the outcrop in the picture.

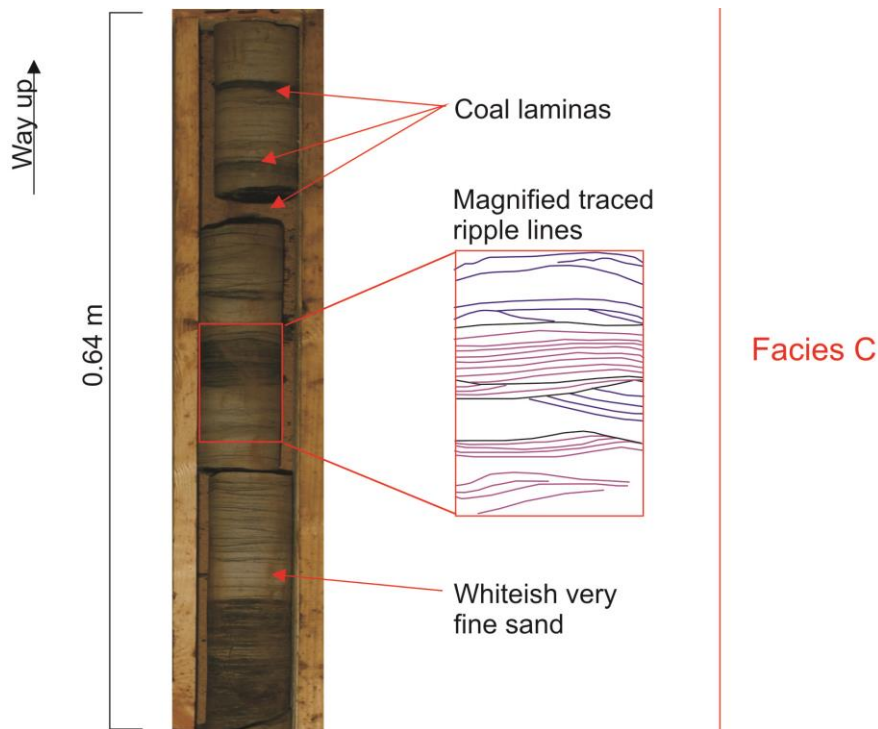


Figure 17: Facies C in Core 18-2009. Ripples of similar orientations are marked in similar colors (pink and blue), and illustrate multiple flow directions. Note the pale sand and dark clay laminas. The ripple foresets appear to have a curved asymptotic contact to the underlying ripple crests.

D – Planar Bedded Sandstone

Description

This facies consists of clean planar laminated sandstones of very fine-fine grain size. The thickness of the beds varies from about 5 mm (laminae) to 20 mm (thin beds) (Figure 18). It has no apparent grain size grading within or between laminae. The fresh color of the sandstone is light yellowish grey, and the weathered surface is light yellowish brown. This facies also includes siltstones which are interbedded by small scale planar beds of cross-laminated very fine to fine sand.

Flow Regime Interpretation

The thinly bedded sandstone may represent both the upper and lower flow regime (Nichols 2009). In theory, at water depths of 1 meter, planar beds of medium to very coarse sand is restricted to the upper flow regime (Nichols 2009). The planar bedded siltstones may be interpreted to represent a slightly lower flow regime due to its small scale planar cross-laminated sand (Tucker 2003).

E – Asymmetrically Rippled Sandstone

Description

The rippled sandstone facies consists of clean sandstone of very fine to medium grain size. The ripples are generally asymmetric and of a unidirectional nature (Figure 19). The facies display a fresh light yellowish grey color, while the weathered surface is often in the shades of light yellowish brown. Some bioturbation is occasionally present in this facies.

Flow Regime Interpretation

Ripples are a common indicator of a low flow energy regime (Nichols 2009). Uni-directional ripples may be interpreted as deposited in an environment with one dominant flow direction (Boggs 2006).

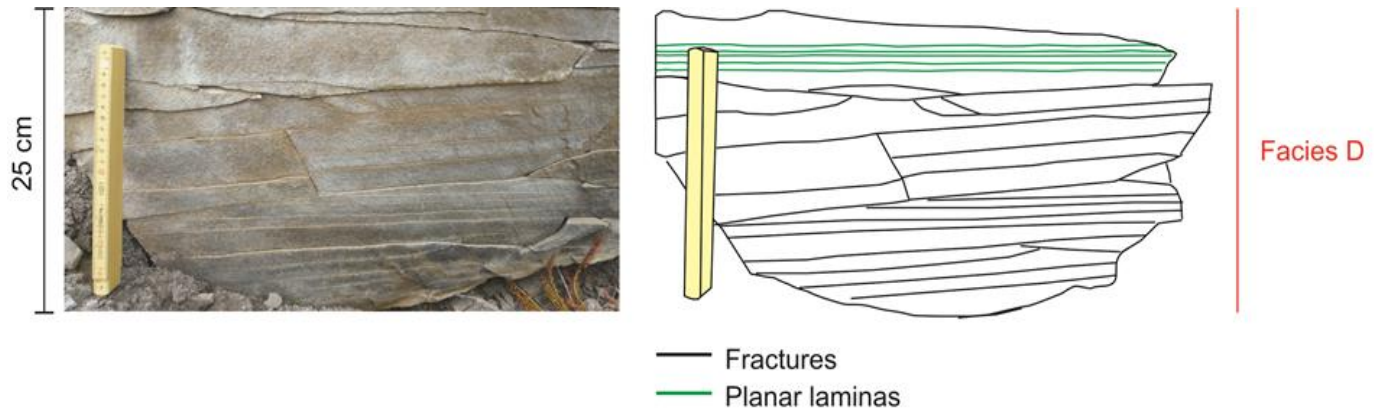


Figure 18: Planar laminated sandstone in the Endalen outcrop. The weathered surface of the outcrop disguises most of the bedding, but the horizontal fractures seems favor the bedding planes as they often will follow weaker zones in the rock.

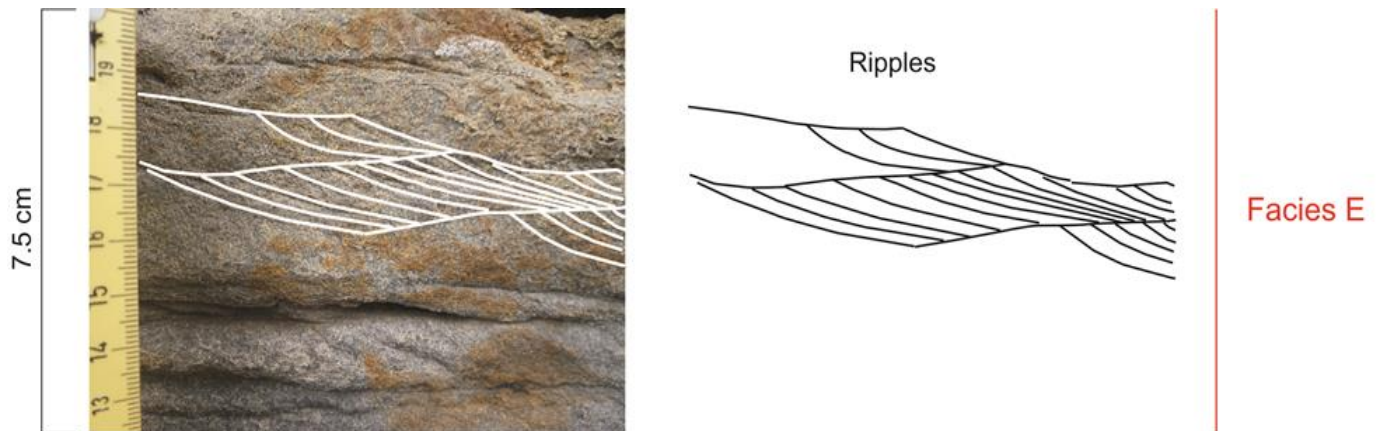


Figure 19: Facies 4 in the Endalen outcrop. The three most prominent ripple sets are illustrated by white lines in the picture.

F – Symmetrically Rippled Sandstone

Description

The symmetrically rippled sandstone facies is of a very fine to fine grain size. The ripples form thin horizontal beds with sinusoid crests which are stacked vertically. The ripple laminae are dipping gently down on both sides, which results in the symmetrical appearance.

Flow Regime Interpretation

Oscillatory motions within a standing body of water are known to produce symmetrical ripples. Such a motion is commonly encountered within the lower parts of a standing body of water within the lower flow regime (Nichols 2009).

G – Tabular- and Trough Cross-Bedded Sandstone

Description

The tabular cross-bedded sandstones consist of high angle cross-beds of very fine to fine sand which are either normally graded or non-graded. The upper- and lower bedding surface is either erosional or planar, and the foresets are apparently tabular to slightly tangential. The spacing between each foreset is >1 cm. The trough cross-bedded sandstones has a curved upper and lower bedding surface. The grain size may be uniform, or fining upwards. The foresets are slightly tangential towards the lower bedding surface. The apparent distance between the foresets varies between 1 and 5 cm. The weathered color of the facies is light yellowish orange, while the fresh color is light yellowish grey (Figure 20).

Flow Regime Interpretation

Tabular cross-beds are generally considered to be a two-dimensional bedform produced by migration of straight-crested dunes within a moderate flow regime (Tucker 2003; Nichols 2009). The trough cross-beds on the other hand are suggested to be produced by curve-crested dunes displaying a three-dimensional bedform (Tucker 2003). The latter may have been created under a slightly stronger flow regime than the tabular cross-beds (Nichols 2009).

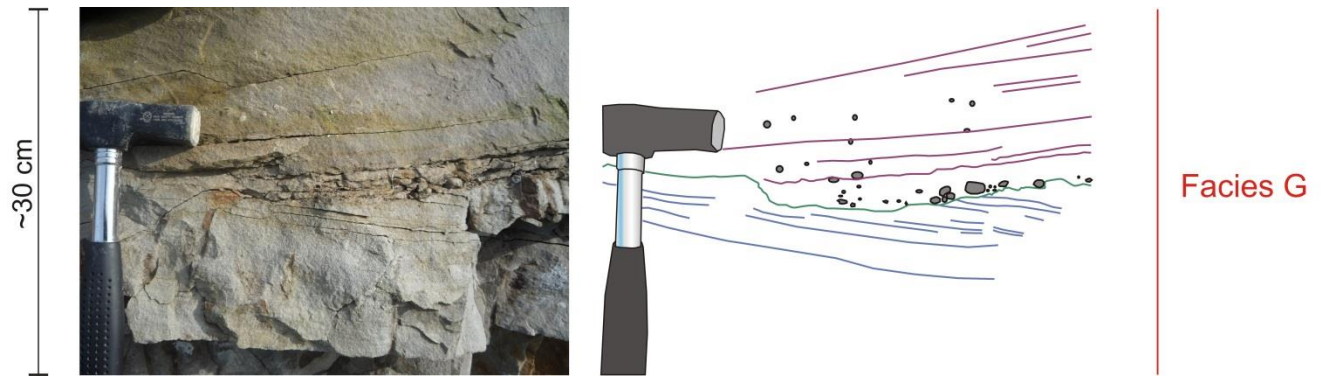


Figure 20: Tabular cross-bedded sandstone in the Grumantbyen outcrop. Note the direction change of the foresets across the green line which is an erosional surface. A paraconglomerate (See Facies L) (grey colored clasts in the illustration) is present at this boundary. The upper cross-bed (purple color) is fining upwards and has a few gravel sized clasts in the base of each cross-bed.

H – Hummocky Cross-Stratified Sandstone (HCS)

Description

This facies consists of undulating low angle cross-stratified beds of very fine to fine sand. The cross-beds are apparently of meter scale length with low angle truncations. This facies includes both the concave-up bedding style, so called swales and convex-up bedding style; hummocks (Figure 21) (Boggs 2006).

Flow Regime Interpretation

Hummocks and swales are generally considered diagnostic of re-worked and subsequently deposited sands between the fair-weather wave base and storm-wave base (Nichols 2009).

I – Burrowed Sandstone

Description

The burrowed sand is commonly poorly sorted and contains sand of very fine to medium grain size. The weathered color is light yellowish grey, whereas the fresh color is light grey.

Ophiomorpha-Type Burrows

The *Ophiomorpha*-type burrows are recognized by their vertically oriented tubes with a pellet-walled surface (Figure 21). The burrows typically occur in a large abundance. The diameter of one burrow is about 1 cm, and does not vary much from burrow to burrow. The apparent length of these burrows varies from a few cm up to 30 cm. The burrow fill is of equal color as the surrounding sand.

Skolithos-Type Burrows

The *Skolithos*-type burrows are also characterized by “vertical tubes”, but with a smooth-walled surface. The thickness of a burrow varies from a 2 mm to maximum 10 mm. The apparent frequency these burrows varies are also numerous. The burrow fill is generally darker than the surrounding sand.

Flow Regime Interpretation

The apparent lengths of the burrows are like every other sedimentary structure depending on how the inspected surface intersects the outcrop. The vertical orientation and high number of *Ophiomorpha*-type burrows indicates an environment where this burrowing organism thrived, thus indicating that the flow regime was not too powerful. *Ophiomorpha* are commonly encountered in the upper shoreface-, beach- and lagoonal environments (Gerard and Bromley 2008).

The dark fill of the smooth burrows of the *Skolithos*-type burrows may indicate these also were made for feeding purposes. *Skolithos* is common in all environments between the offshore basin- and lagoonal settings, but is regarded to be most common in a beach environment (Gerard and Bromley 2008).

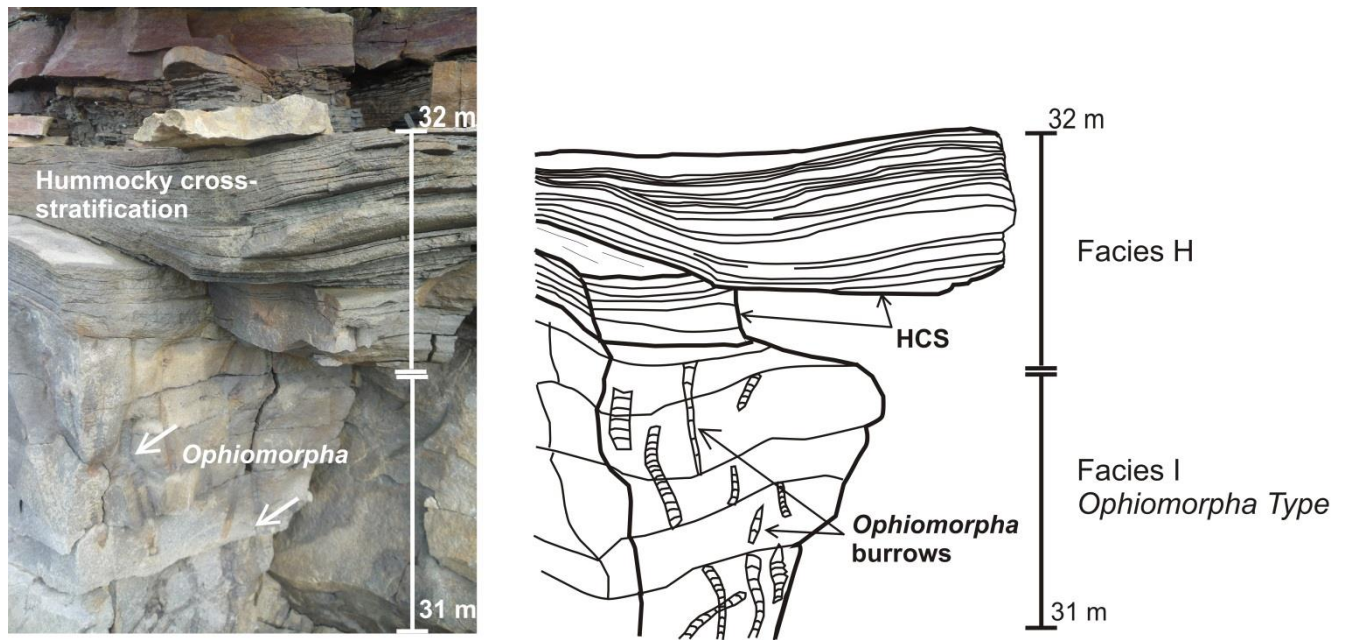


Figure 21: Facies H and I in the Grumantbyen outcrop. Facies I displays an abundance of *Ophiomorpha* burrows which are recognized by the distinct pellet-lined burrow-walls.

J – Carbonate Cemented Sandstones and Concretions

Description

This facies embraces two sorts of carbonate cemented sandstones. The first sort is massive carbonate cemented sandstones which lacks visible structures and grain size grading. The grain size can be fine, medium or coarse. The weathered color is light reddish brown, and the fresh color is pale yellowish grey. The second sort is cemented concretions (Figure 22). These are characterized by prominent brick-like structures coated by a reddish brown layer. The concretions occur in silty to very fine grained sandstones which tend to be finely laminated/ rippled above and below the concretions. The dimension of a concretion ranges between 4 cm x 3 cm x 2 cm and 12 cm x 8 cm x 5 (length x width x height).

Flow Regime Interpretation

The presence of carbonate cement is tested with hydrochloric acid. The facies alone provide limited information about the flow regime in which it was deposited. The massive carbonate cemented sandstones may however be a result of marine reworking of sediments (and thus indicative of a high energy environment) as it is both massive and carbonate cemented (Elliot

1974). Another suggestion for the massive carbonate cemented sandstones are that the depositional structures are in fact present, but not visible to the naked eye (Boggs 2006). Carbonate cemented concretions on the other hand are often considered to be a secondary diagenetic feature, but they can also indicate deposition in brackish waters (Boggs 2006). The dark red color of the concretions indicates an iron carbonate composition of siderite (Boggs 2006).

K – Rooted Sandstone

Description

This facies is recognized by dark, vertical thread-like streaks in silty to fine grained sandstone (Figure 23). The threads are apparently 2-15 cm long and often slightly thicker at the top (~3 mm in diameter) than in the lower part (~1 mm in diameter). The weathered color of the facies is light yellowish orange, the fresh color is light yellowish grey. Root-like structures may occasionally be a misinterpretation of burrows and vice versa. A combination of both interpretations can be even more correct as roots may grow into old burrows as they provide path of less resistance down in the sediments.

Flow Regime Interpretation

Within the lower flow regime as the roots were able to fasten in the sediments.

L – Conglomerate

Description

Two sorts of conglomerates have been identified; clast supported conglomerates (orthoconglomerates) and matrix supported conglomerates (paraconglomerates).

Orthoconglomerates

The orthoconglomerates are made up by conglomeratic sandstone units with a sharp, erosional bases. They are bimodal (granules-cobbles sized constituents), polymictic and predominantly clast supported with a matrix of fairly uniform grain size (very fine-fine sand). The clasts are generally sub- to well-rounded and of white, light grey, dark grey and black colors (Figure 24).

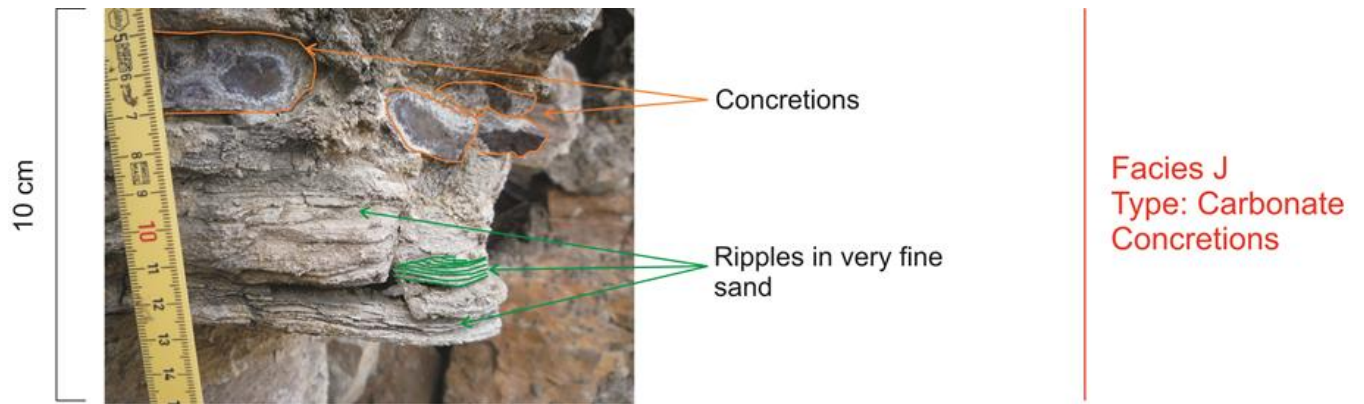


Figure 22: Concretions in Grumantbyen. The concretions are outlined in orange, ripples are marked in green.

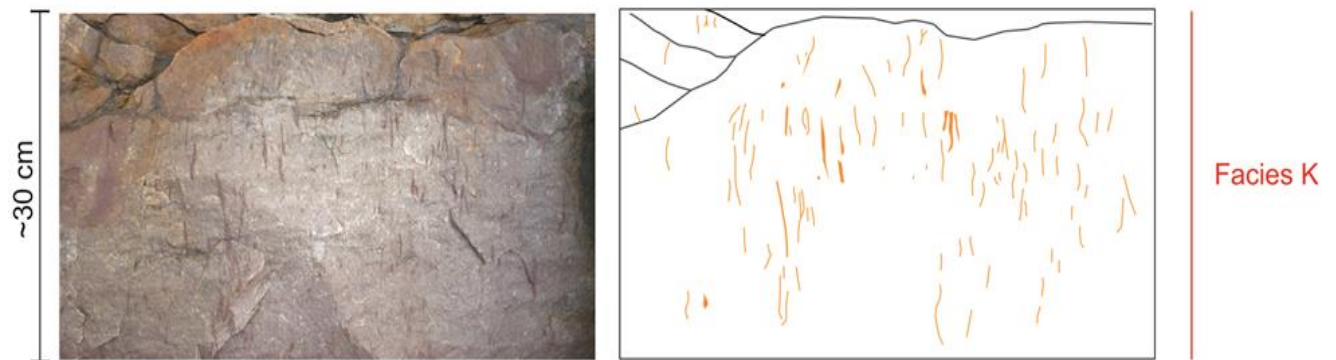


Figure 23: Rooted Sandstone in the Grumantbyen outcrop. The interpreted roots are drawn in orange in the illustration.

Paraconglomerates

The paraconglomerate consists of thin and discontinuous conglomeratic beds or lenses. The conglomerates clasts are made up by small, pale grey to white colored, rounded pebbles supported by a matrix of very fine-medium sand.

Flow Regime Interpretation

The described conglomerates are often associated with a high energy subaqueous environment (Nichols 2009). The orthoconglomerates may have been deposited under slightly more violent flows as they contain larger sized pebbles and less matrix. The lighter colored pebbles consist of

quartzite and the dark grey and black pebbles consist of sandstone and chert respectively. The chert pebbles had the distinct burnt smell when struck on with a hammer.

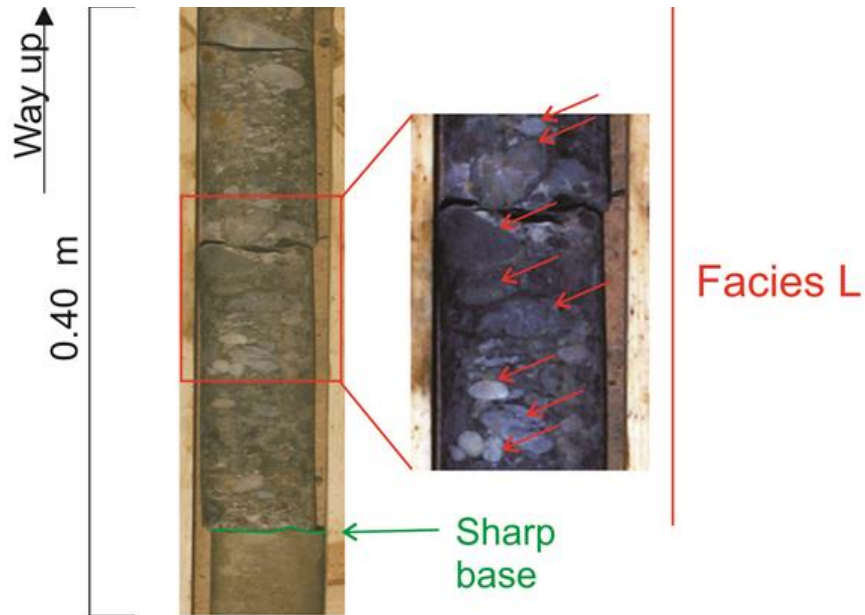


Figure 24: Orthoconglomerate in Core 18-2009. The area within the red rectangle has been magnified and contrast enhanced to better display the pebbles which are pointed out with red arrows.

4.2 Facies Associations

The aim of this chapter is to present an overview of the facies associations (FA) interpreted within Todalen Member and the lower Endalen Member strata. Each facies association is attributed to a depositional environment and named thereafter. One facies may be assigned to several depositional environments as a facies is purely descriptive of lithology and structures (Appendix 1.2).

Seven facies associations (FA 1-7) have been recognized from the logged cores and outcrops. These have been grouped into two main depositional settings. The delta plain due to the presence of distributary channels, mires and delta lobes. The delta front (shoreface) due to observations of *Ophimomorpha* trace fossils and hummocky cross-stratified sandstones. The depositional environments are ordered, based on their position within this overall depositional environment of a delta system, and attempted ranged from proximal settings to distal settings.

Delta Plain

FA 1: Distributary channels

FA 2: Crevasse splays

FA 3: Mires

FA 4: Intertidal- and supratidal flats

FA 5: Interdistributary bays/ marsh

FA 6: Abandoned delta lobe

Delta Front (Shoreface)

FA 7: Foreshore to basin

Facies Association 1: Distributary Channels

Description

This facies association defined as distributary channels consists of conglomerate (L), tabular- and trough cross-bedded sandstone (G), planar bedded sandstone (D), rippled mud rich sandstone (C), asymmetrically rippled sandstone (E) and carbonate cemented sandstone (J).

The associated facies are seen to occur together in three distinct sedimentary sequences which are suggested to represent distributary channel features:

Sequence 1: This sequence is characteristically made up by a conglomerate bed with a sharp base and gradual upward transition into an asymmetrically rippled- or massive carbonate cemented sandstone. It commonly occurs in close association to coal seams and rooted sandstone facies. The total thickness is between 0.5 and 5 meters. This sequence is present in the upper part of Todalen Member, and in the Endalen Member, in Core 18-2009 (Appendix 2.3). It is also seen at the base of the Todalen Member in Core 15-2010 (Appendix 2.4). In the Endalen outcrop, it is present about 1 meter above the second uppermost coal seam (Appendix 2.5). The Grumantbyen outcrop displays a unit resembling this sequence at the boundary between the Todalen and Endalen members (Appendix 2.6).

Sequence 2: This sequence is recognized by a conglomerate bed with a sharp base. The conglomerate bed gradually shifts upwards into a rippled mud rich sandstone with bidirectional ripples and mud drapes on ripple foresets and on the ripple crests (Figure 25). The thickness is commonly less than 1 meter. It is present above the thick coal seam at the 30 meter mark in the log from Core 18-2009 (Appendix 2.3).

Sequence 3: This sequence holds a cross-bedded sandstone in its lower part which grades upwards into an asymmetrically rippled- or planar bedded sandstone. The sequence is typically fining upwards in the cases where it is grading into an asymmetrically rippled sandstone, whereas it in the case of planar bedded sandstones are coarsening upwards. The total thickness is ranging from 2 to 4 meters. It is present in the lower Endalen Member strata in Core 15-2010, here, it also holds a matrix supported conglomerate in its base (Appendix 2.4). The Endalen outcrop display five segments of Sequence 3 which are located in-between very thin coal seams (Appendix 2.5).

The Grumantbyen outcrop display a characteristically fining upwards Sequence 3 at the 25 meters mark in the log (Appendix 2.6).

Interpretation

Sequence 1: The erosive base of the conglomerate and the gradual upwards transition from a conglomerate into lower density sediments, being either a rippled- or massive carbonate cemented sandstone, represent a distributary channel environment. The lower density sediments represent the channel fill; the asymmetrically rippled sandstone may represent a middle ground bar while the massive carbonate cemented sandstone may be indicative of marine reworking/ bioturbation (destroying primary bedding structures, Elliot (1974)). The distributary channel interpretation is supported by the sequence`s proximity to subaerial indicators like coal beds and rooted sandstones.

Sequence 2: Bidirectional ripples and mud drapes in the sandy fill overlaying a conglomerate with an erosive base suggest that this sequence represent a distributary channel environment which has been subjected to tidal influence (Reading and Collinson 2006a).

Sequence 3: Middle ground bars may be regarded as elongated, subaqueous dunes migrating up- or downstream in the middle of the channel (Reading and Collinson 2006a). The characteristics of middle ground bars has been further described by Selley (2000) to display cross-beds in its lower part, and rippled- or planar bedded sand in its upper part depending on whether the flow in the channel was decreasing or increasing respectively. Point bars may display similar characteristics to middle ground bars, but with epsilon-type stratification of the cross-beds (Tucker 2003). As epsilon-type stratification was not observed, the middle ground bar interpretation is a sensible suggestion since the observed sequence consists of a cross-bedded unit which is grading upwards into asymmetrically rippled- or planar bedded sandstone, thus matching the description of Selley (2000). Neither the Endalen nor Grumantbyen outcrop yielded any information on channel geometries due to in-parts scree-covered sections.

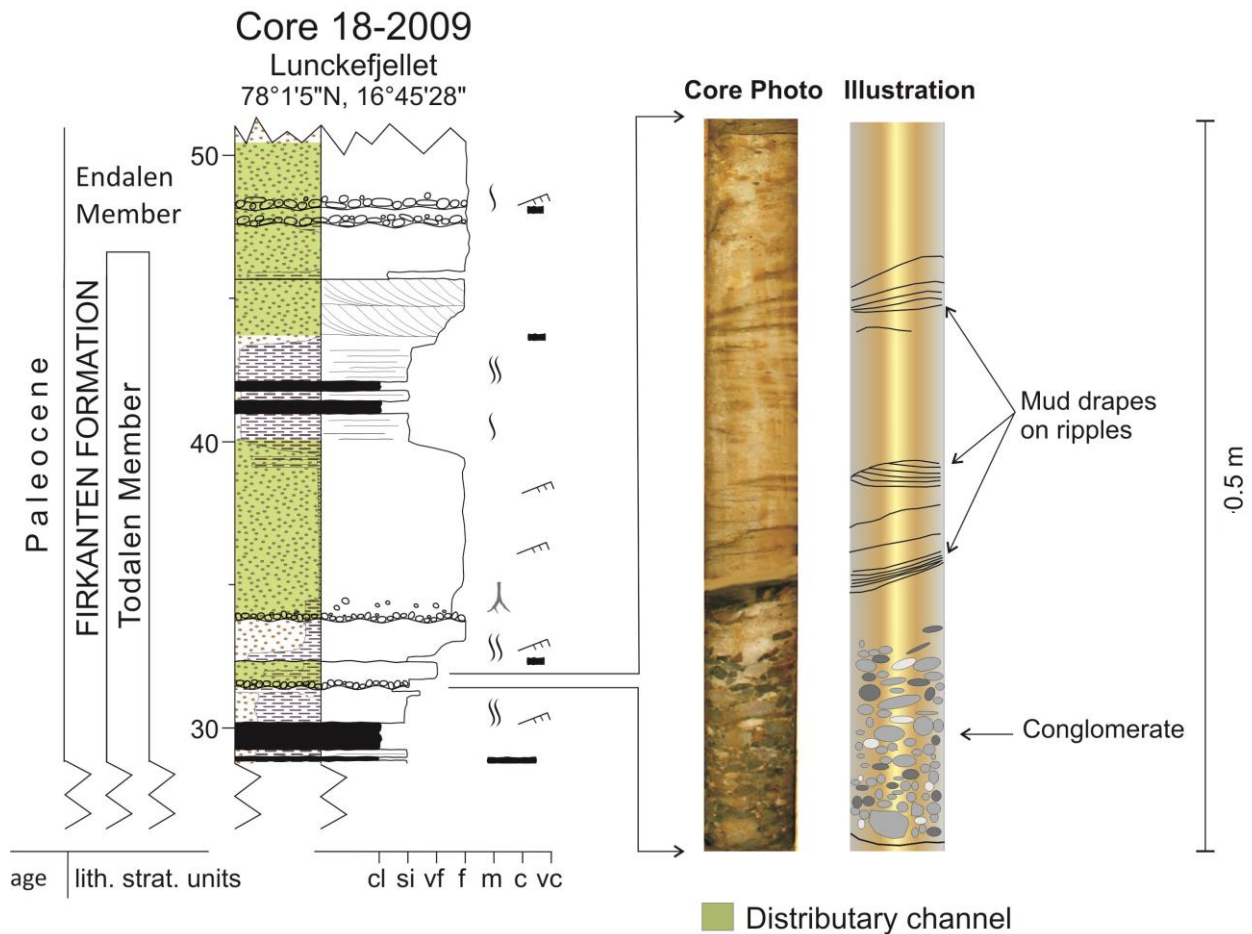


Figure 25: Core 18-2009 with distributary channel features marked in light green in the lithology column. A photo of Sequence 2 type sedimentation style is shown in the core photo to the right with an illustration of its structures next to it. Note the gradual transition from the conglomerate into the overlying, rippled sandstone unit with mud drapes on the ripple crests. The core is stained by an orange color medium, induced by dried drilling fluids.

Overview of Occurrence within the Investigated Area from East to West

In summary, the thickness of the facies association spans from 0.5-5 m. The described sedimentary sequences are most frequently encountered in the upper part of Todalen Member to across the lower Endalen Member strata in the logger cores and outcrops. This facies association is most frequently encountered in Core 18-2009 and in the logged section from the Endalen outcrop.

Facies Association 2: Crevasse Splays

Description

This facies association consists of mudrock (B), asymmetrically rippled sandstone (E), small scale tabular- and trough cross-bedded sandstones (G), carbonate cemented sandstone (J) and rooted sandstone (K). The crevasse splays are characterized by the following sequences:

Sequence 1: The crevasse splay environment of sequence 1 consists of 10-20 cm thick cross-bedded sandstones interbedded by 5-10 cm thick planar laminated mudrocks with a silt content of ~15%. It is present in the upper part of the Todalen Member in the Endalen outcrop (Appendix 2.5).

Sequence 2: This sequence is recognized by 10-30 cm thick massive carbonate cemented sandstones or rippled sandstones containing traces of *in-situ* rootlets (Figure 26). The thin sandstone beds are often seen to be interbedded by 5-10 cm thick planar laminated mudrocks with variable silt content of ~15%. It occurs in close stratigraphic proximities to coal seams. It is present on all stratigraphic levels within the Todalen Member in the Grumantbyen outcrop (Appendix 2.6).

Interpretation

Crevasse splays are associated with a break in the levee of a channel (Reading and Collinson 2006b). The sand may originate from the levee as well as the sediment loaded river, and the laminated mudrock may be caused by less violent overbank splays. The rhythmicity between the sand- and mudrock beds may have been induced by seasonal variations in the channel flow and suspended sediment load. The presence of *in-situ* rootlets and close affinities to coal seams confirms an overall subaerial setting.

Overview of Occurrence within the Investigated Area (from East to West)

No inferred crevasse splays are recognized in Core 18-2009 or in Core 15-2009.

In the Endalen outcrop, a suggested crevasse splay is present slightly below the uppermost coal seam (Appendix 2.5).

In the Grumantbyen outcrop, several thin and massive sandstone units containing *in-situ* rootlets were recognized together with thin planar laminated mudrocks, thus displaying the characteristics of a Sequence 2 type crevasse splays (Figure 26).

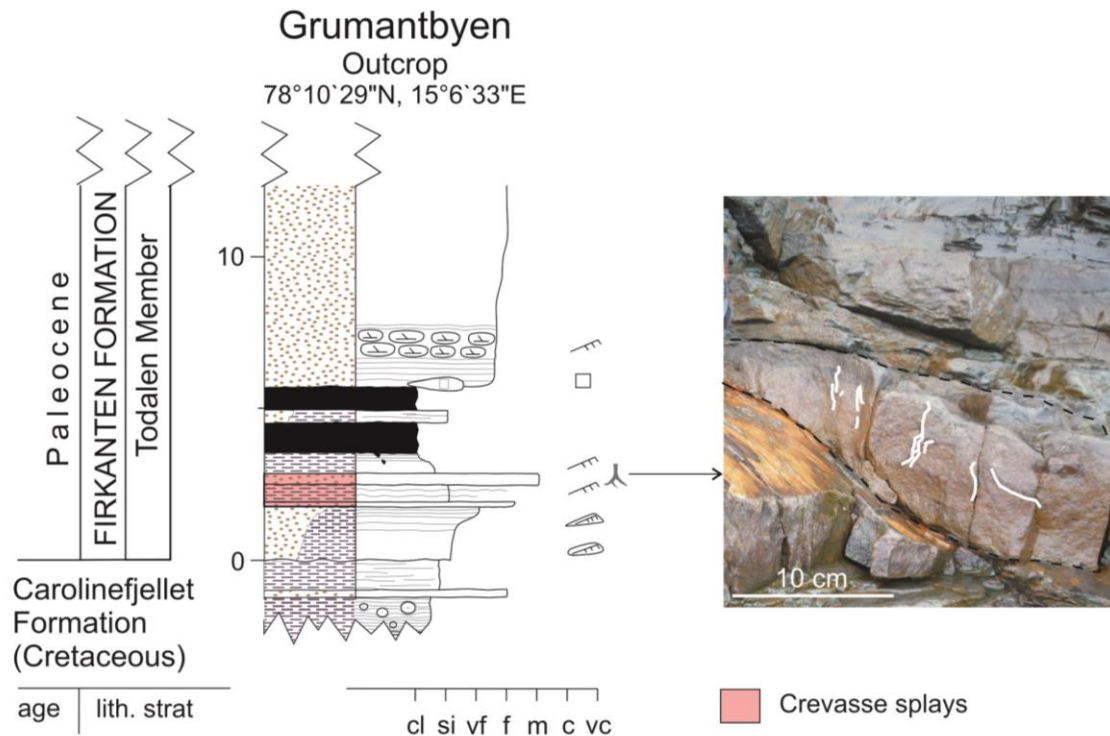


Figure 26: In-situ rootlets (white lines in the photo) in a thin sandstone beds (within the black dotted lines in the photo). A fault plane with an orange colored slickenside is intersecting the sandstone bed which is representing a sequence 2 type crevasse-splay.

Facies Association 3: Mires

Description

This facies association consists of coal (A). The presence of coal is limited to the Totalalen Member in all the logged sections.

Peat is the precursor of coal and must be buried for coal to form (Boggs 2006). The term “mire” is generally accepted for all types of peat-forming eco systems (Thomas 2002). Deeply buried coals are suggested to have a compaction of 30 to 1 (Ryer and Langer 1989; Boggs 2006).

The following conditions must be achieved for peat to accumulate in a mire:

- The input of water to the mire must balance the output (Thomas 2002).
- Organic material have to be preserved either by rapid burial or anoxic conditions (McCabe and Parrish 1992; Thomas 2002)

In addition to the biochemical properties of the mire, like for instance the type of peat-forming plant communities, nutrient supply, acidity, bacterial activity, temperature and redox potential, the final characteristic of the coal depends largely on geochemical alterations induced by burial/tectonic effects. The geochemical alteration (diagenesis) determines the rank of the coal. Low rank coals may in the most simplistic way be referred to as “brown coal”, while high rank coals are commonly referred to as “black coal”. Black coal forms by metamorphism of brown coal and has therefore a significantly lower content of volatiles as well as a higher calorific content than brown coal.

Coal has been defined by Thomas (2002) to be: “...essentially it is a sediment, organoclastic in nature, composed of lithified plant remains, which has the important distinction of being a combustible material...”.

Description of Coal Seams in Core 18-2009 and Core 15-2010

In Core 18-2009 and Core 15-2010, coal seams occur on all stratigraphic levels within the Todalen Member and are intimately coupled with the intertidal-and supratidal flat deposits of FA 4 (see FA 4). The intertidal- and supratidal flat deposits are fining upwards beneath the coal seam in the middle of Todalen Member in both cores, forming an upward sequence of facies C-B-A (Appendix 2.3 and 2.4). The remaining coal seam commonly makes up B-A sequences (see FA 4).

Occasionally, relatively thin (~2-40 cm), closely spaced coal seams are separated by either a very thin bed of mudrock or sandstone (Figure 27). A thin sandstone bed is separating the lowermost coal seams in both Core 18-2009 and Core 15-2010, while thin mudrock beds are separating several of the overlying coal seams in the mid- to uppermost part of the Todalen Member (Appendix 2.3 and 2.4).

A bentonite bed is observed above the second lowermost coal seam in Core 18-2009. Preservation of fine ash layers require a very low flow regime, and may thus possibly be inferred to represent a subaerial environment.

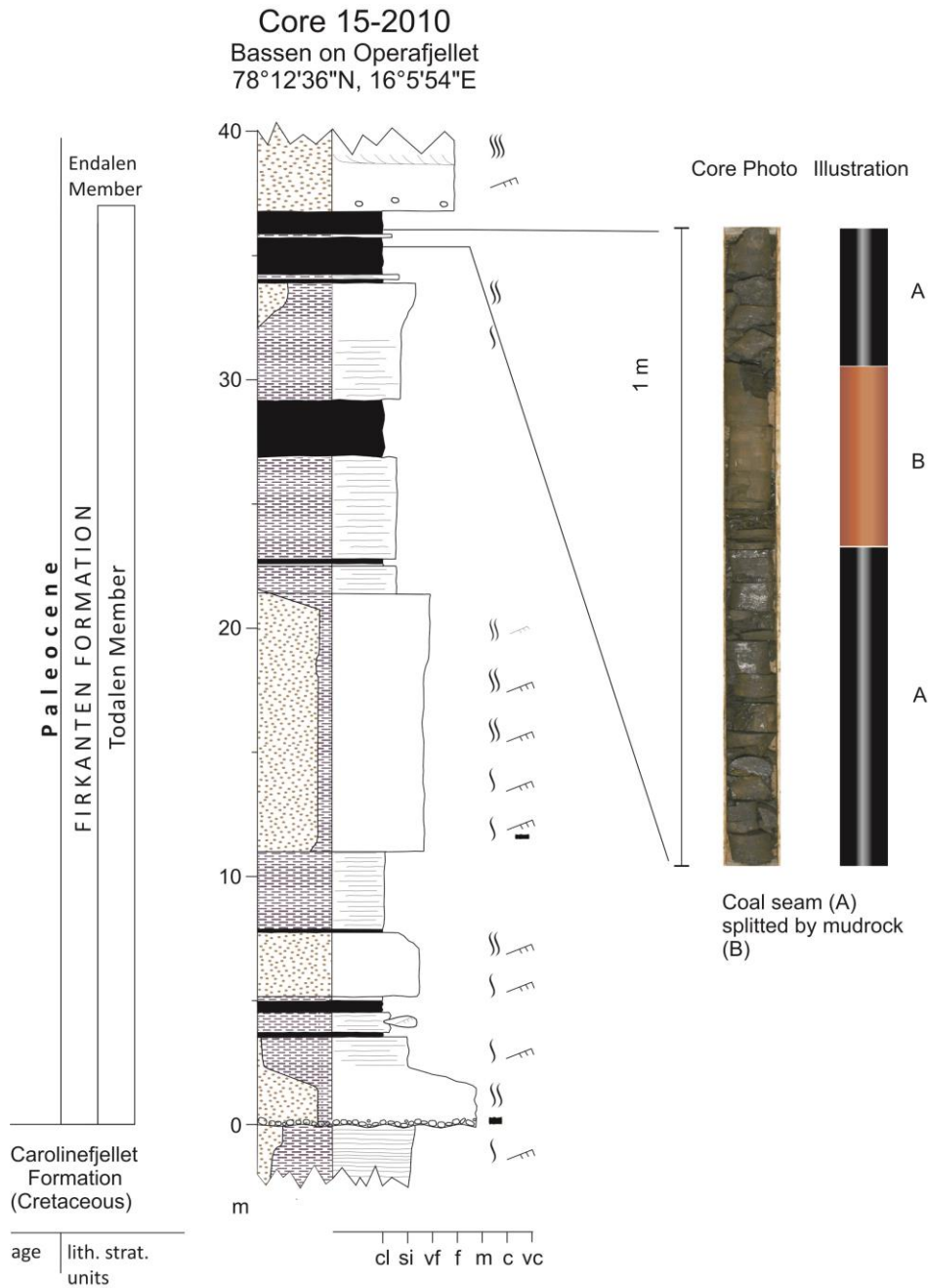


Figure 27: Coal seams in Core 15-2010. Photo and illustration to the left of a split coal seam.

Description of the Coal Seams in the Endalen Outcrop

The logged section from the Endalen outcrop lacks data from the lower part of the Todalen Member due to two scree covered areas. The logged section in Endalen shares few similarities to the logged cores both structure- and grain size wise, even though Core 15-2010 is situated only ~9 km northeast of the Endalen outcrop. The Grumantbyen outcrop on the other hand, situated ~14 km directly east of the Endalen outcrop, shares some similarities to the Endalen outcrop in both structures and grain size. As two thick coal seams are present in the base of the Grumantbyen outcrop, coal seams may perhaps also be present underneath the scree in the Endalen outcrop (Appendix 2.5 and 2.6).

The uppermost coal seam in the Endalen outcrop has a thickness of 60 cm, while the six coal seams situated further below this measures ~2-15 cm. The coal seams are almost exclusively over- and underlain by meter thick sandstones of different properties; the three lowermost coal seams are located between burrowed sandstones, carbonate cemented sandstones and concretions attributed to an interdistributary bay/ marsh environment of facies association 5 (see FA 5 sub-chapter). The four remaining coals seams above are largely situated between thick cross-bedded and rippled sandstones predominantly attributed as features of the distributary channel facies association (FA 1). The described coal seams are laterally extensive in the outcrop over 10s of meters.

Description of the Coal Seams in the Grumantbyen Outcrop

Three coal seams are present in the Grumantbyen outcrop (Appendix 2.6). All of which are laterally traceable over an area of about 40 + meters. The coal seam exposure is limited by a fault in the north and by the dip of the outcrop in the south (Figure 28). Every coal seam is black with a silky luster and banded texture (~2-10 centimeter thick bands). The thicknesses of the coal seams are fairly uniform, and the small observed thickness differences are due to tectonic influence as faults are intersecting the outcrop. The two lowermost coal seams are located close to the base of Todalen Member and are separated by ~40 cm thick mudrock. The coal seam below the mudrock is 0.85 meter thick, and the coal seam above is 0.65 meter thick. The latter coal seam contains several pyrite lenses (3 centimeters thick, and apparently up to 15 centimeters wide) in its upper part (Figure 29). The third and last coal seam is situated in the upper part of the

Todalen Member. This coal seam makes up a characteristic C-B-A sequence as described in FA 4, and has also pyrite lenses in similar dimensions as the coal seam below in its upper part.

More interestingly is perhaps the planar laminated mudrock above the middle coal seam (separated from the coal by a thin sandstone unit) which contains several black and well rounded, oval clasts about 10-20 cm long with a diameter of 6-8 cm (Figure 29).

A bentonite horizon is present immediately above the mudrock with oval clasts, it is seen in the outcrop as a laterally extensive (traceable over 20+ meters), ~1.5 cm thick bed with a yellowish grey color and plastic-like texture (Figure 29).

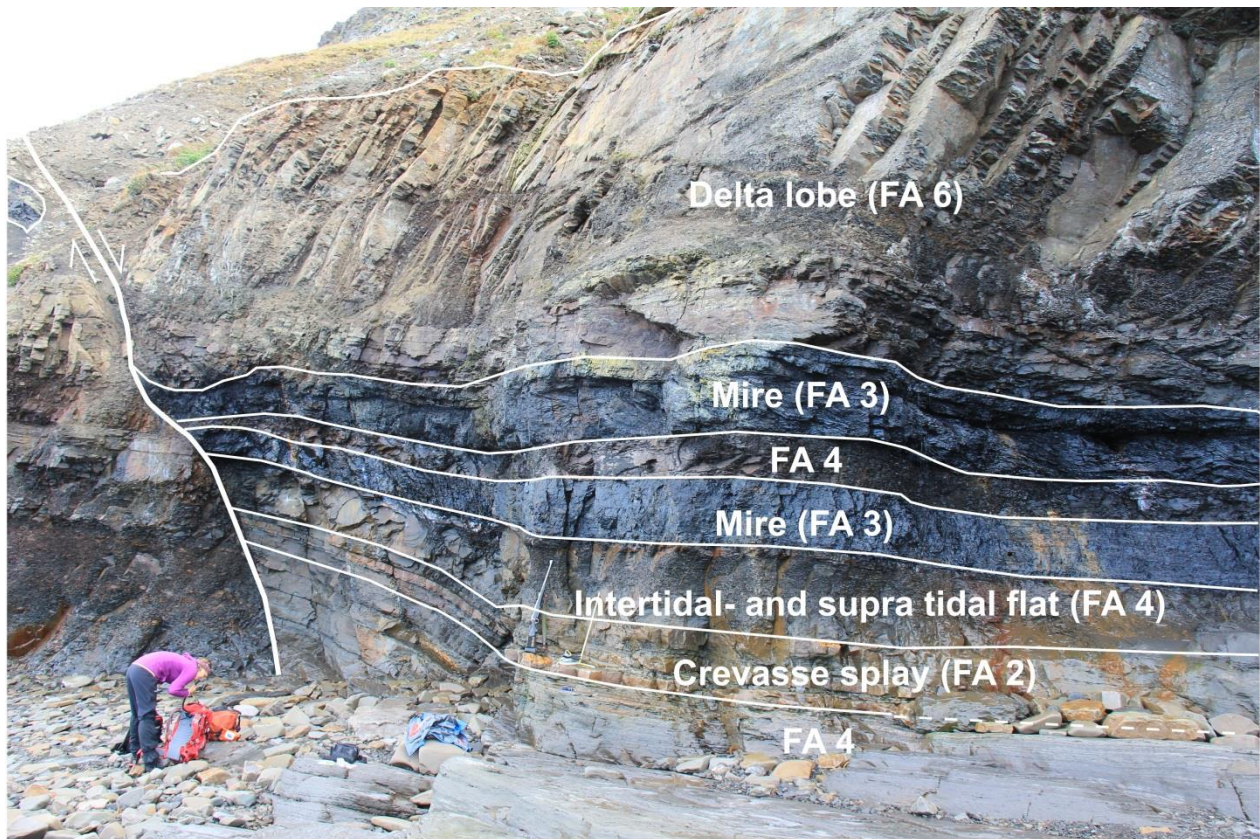


Figure 28: Normal fault in Grumantbyen (white vertical line to the left in the photo) and the recognized facies associations, several of which explained in the next sub-chapters, are drawn in white text with white lines marking their boundaries.

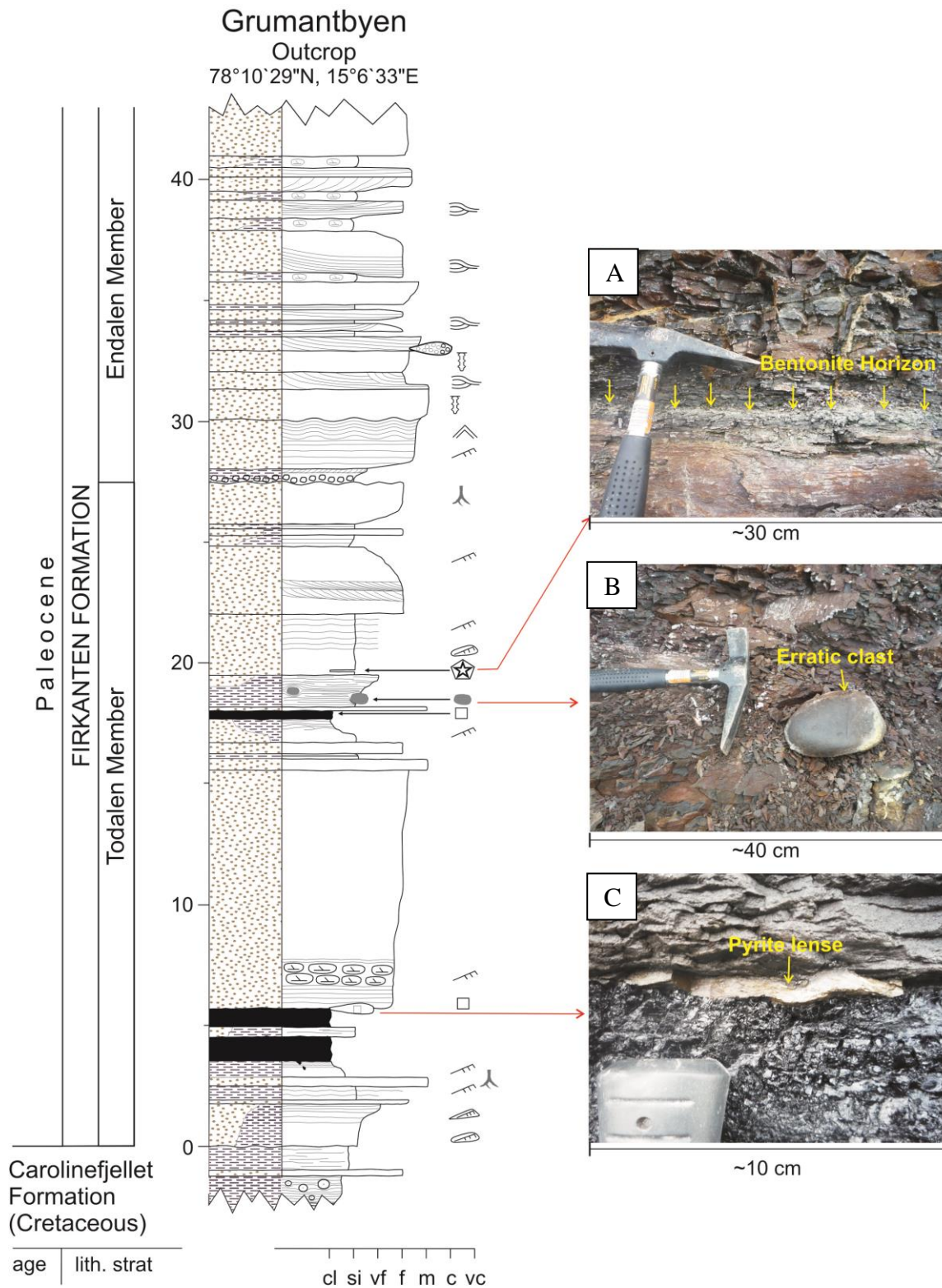


Figure 29: Log of the Grumantbyen outcrop. **A)** bentonite horizon with yellowish grey color and plastic texture. **B)** Erratic clast (drop stone) dug out of the mudrock. **C)** Pyrite lense in the upper part of the second lowermost coal bed.

Interpretation of the Coal Seams in Core 18-2009 and 15-2009

Closely spaced coal seams separated by a thin mud rock bed is a phenomena referred to as “splitting” and is attributed to flooding of the mire (Thomas 2002). Flooding may indeed provide a plausible explanation for these thin mudrock as they are interpreted to represent a supratidal part of the intertidal- and supratidal flat facies association (see FA 4).

The coal seams may also be splitted by, although less commonly, thin sandstone beds. These may be attributed to either a local crevasse splay, or, marine flooding producing laterally extensive sand sheet over the coal by reworking of delta front sands (Thomas 2002).

Interpretation of the Coal Seams in the Endalen Outcrop

The three lowermost coal seams may have been deposited on the lower delta plain due to their close relations to the burrowed- and carbonate cemented sandstones and concretions (see FA 5 on interdistributary bays/ marsh). These are all traceable over about 15 meters in the outcrop, which suggests that the bays/ marsh were of a minimum extent. The four coal seams stratigraphically above are all occurring in close proximities to distributary channel and crevasse splay deposits (FA 1 and 2) which suggest that these were deposited in a mire further up on the delta plain.

Interpretation of the Coal Seams in the Grumantbyen Outcrop

The pyrite lenses in the two uppermost coal seams may originally have been woody fragments, which in a marine environment with a low oxygen content (reducing conditions) became pyritized (Boggs 2006). This implies that the mires in which they were deposited were subjected to marine water incursions. Woody fragments, though not pyritized, have been reported in Todalen Member before (Jochmann 2004).

An explanation to the oval clasts in the mudrock unit above the uppermost coal seam can be that they are erratic clasts (dropstones) which were rafting on ice-sheets out to the basin. Erratic clasts in the Firkanten Formation have been reported before (Spielhagen and Tripiati 2009).

Nevertheless, it is quite odd to have a humid climate indicator like coal situated (almost) immediately below a cold climate indicator which the erratic clasts represent. There may be

several explanations to this like large seasonal temperature variations, perhaps like mid-Norway today, or a climatic shift. But as a rooted sandstone unit is present above the cold climate indicator, the first suggestion is most favorable.

Bentonite horizons in proximities to coal seams have been reported by Grenard (2002) and Jochmann (2004). The source area is suggested by Dypvik and Nagy (1979) to have been 100-200 km away, possibly from Tertiary volcanism on northern Spitsbergen (Woodfjorden) or Northern Greenland (Peary Land).

Overview of Occurrence within the Investigated Area from East to West

High rank coals, 2 centimeters to 2 meters thick, are present on all stratigraphic levels in the Todalen Member in all of the logged sections. No observations were made of low rank coal. The number of coal seams decreases from the east to west in the investigated area. The thickness of the coal seams generally increases upwards in all logged sections except for the Grumantbyen outcrop. The bentonite horizons in Core 18-2009 and the Grumantbyen outcrop occur on different stratigraphic levels, which suggest that they are not correlative.

Facies Association 4: Intertidal- and Supratidal Flat

Description

This facies association is made up by mudrocks (B) and rippled mud rich sandstones (C).

The mudrock and mud rich sandstones are best observed in the logged cores as they do not crop out nicely in the field. This facies association appears to be closely related to the coals seams of FA 3 as it is, with the exception of a few thin coal seams in the Endalen outcrop, always occurring above/ below coal seams in addition to in-between closely spaced coal seams.

The rippled mud rich sandstone holds structures like flaser and wavy bedding. The ripples are often of a bidirectional orientation. Mud drapes are common on the ripple crests and ripple foresets in cleaner segments of the facies. The mudrock has very thin, rhythmic silt laminas.

A gradual upwards transition from the rippled mud rich sandstone into a laminated mudrock is present in the middle of Todalen Member in Core 18-2009. This C-B facies sequence is ultimately capped by a coal seam, thus forming a ~10 m thick C-B-A facies sequence (Figure 30). This sequence is also recognized in Core 15-2010, but with a sharp bounding surface between the rippled mud rich sandstone and mudrock (Figure 30). Both of these C-B-A sequences contain a rippled mud rich sandstone with a significant content of organic material. The organic material is occurring as black, shiny pieces/ laminas in the mud and sand fraction.

More commonly are the pure, laminated mudrock-coal sequences (B-A sequences), which are present in all logged sections. These are seen to measure ~1-5 meters with a thickness decreasing from east to west within the investigated area.

In Core 18-2009, the thickest interval of the facies association, ~15 meter thick, is located in the middle part of the Todalen Member (Appendix 2.3). It shows a gradual transition from a rippled mud rich sandstone to a planar laminated mudrock which is ultimately capped by a coal bed (C-B-A facies sequence).

In Core 15-2010, eight intervals of the facies association are encountered (Appendix 2.4). The first interval is located at the base of the Todalen Member and display a gradual transition from a rippled mud rich sandstone into a planar laminated mudrock capped by a coal bed. The fourth interval measures about 10 meters and is located in the middle of Todalen Member, this interval displays a similar C-B-A facies sequence as encountered in Core 18-2009. Four subsequent intervals of planar laminated mudrocks are located below the coal seams above this, forming B-A facies sequences.

At the Endalen outcrop, two thin intervals of the facies association are observed in the upper part of the Todalen Member (Appendix 2.5). It may however also be present in the lower half as it has two scree covered areas.

Two relatively thin intervals of the facies association (<2.4 meters) are recorded in the Grumantbyen outcrop (Appendix 2.6). The first interval is located immediately above the unconformity to the Carolinefjellet Formation and displays a sharp boundary to the crevasse splay facies association (FA 2) above. The second interval is located beneath the uppermost coal seam, and displays the characteristic C-B facies sequence.

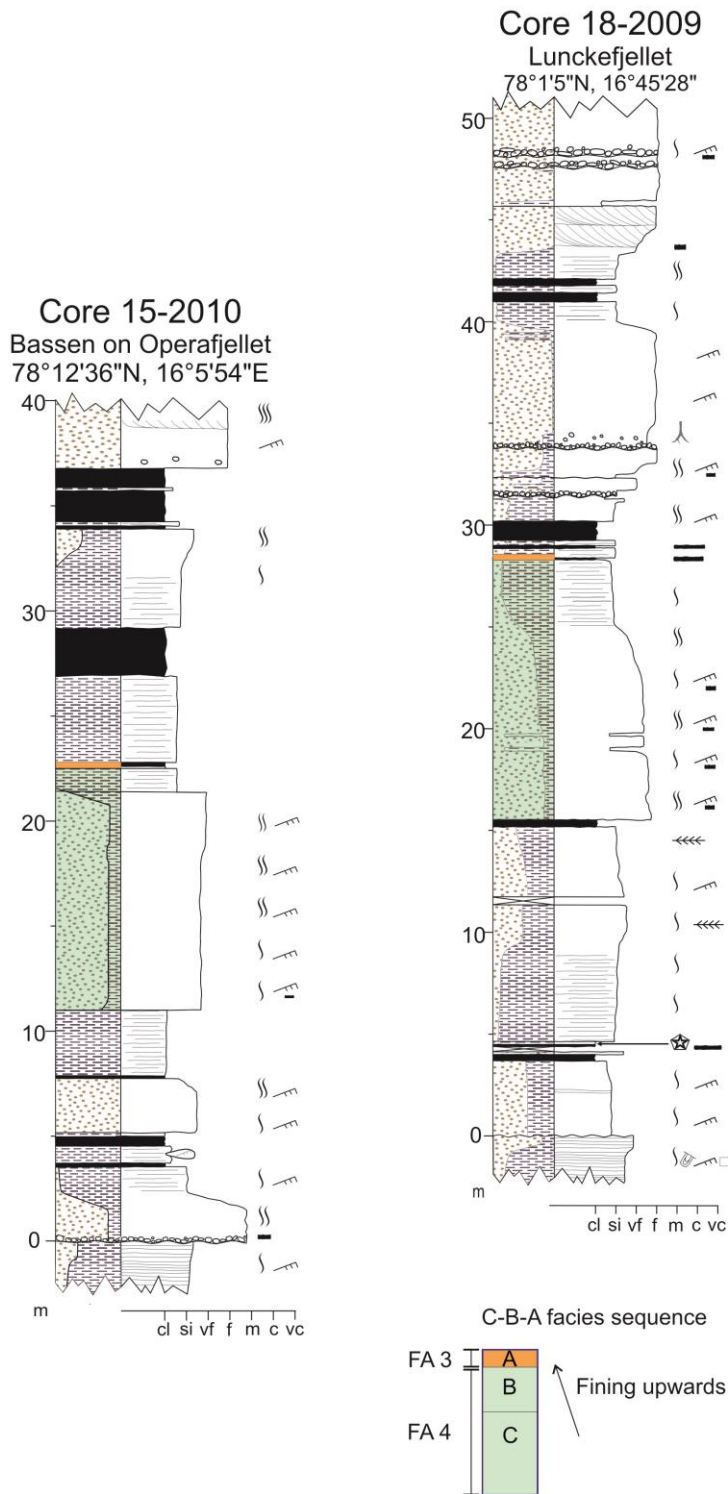


Figure 30: C-B-A facies sequences in Core 15-2010 and Core 18-2009 (also see Appendix 2.3 and 2.4) The log to the right is placed slightly higher up as this location was closer to the forebulge (Bruhn and Steel 2003).

Interpretation

Bidirectional ripples, mud drapes on ripple foresets as well as flaser- and wavy bedding are all common indicators of a tidally influenced environment (Bhattacharya 2006; Reading and Collinson 2006a; Nichols 2009). Ripples with mud drapes may form during periods of calm water at changing tides. The calm waters allow mud to settle out of suspension and accumulate on the ripple foresets. The preservation-potential of mud in such an environment may be low due to the force of the tidal currents, but possible due to the cohesiveness of the mud which prevents it from being transported away as the tidal current increases. Flaser- and wavy bedding may form by the same processes as mud drapes on ripples, but with a significant larger mud component. The flaser bedding may grade into wavy bedding as the proportion of mud decreases in the system and vice versa (Readings and Collinson 2006b). Mud drapes may form in other environments as for instance in rivers with seasonal flow (Nichols 2009). No compelling evidence is observed to suggest that this facies association is of a seasonal flooded river. Firstly, if it was in fact a seasonally flooded river, one would expect to observe channel incision and channel geometries as well as other fluvial signatures of the upper flow regime. And lastly, bidirectional ripples are generally not expected with unidirectional flow in such a river.

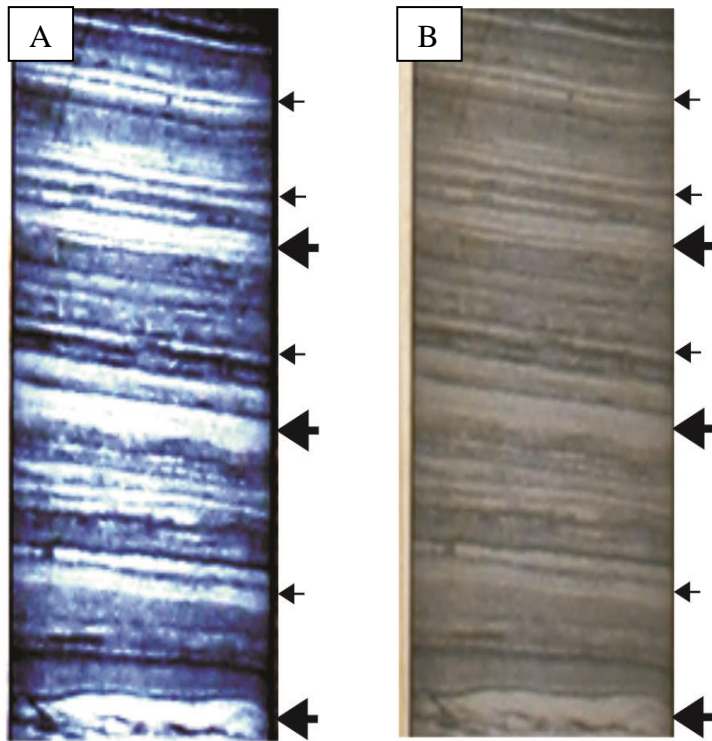


Figure 31: A) Color enhanced photo of B to better display the rhythmicity. **B)** Photo of Core 15-2010, length of core is 20 centimeters, way up is to the left. Note the rhythmicity between the thick and thin silt laminae (large and small arrows) as well as the mud drapes.

Walther Law can be applied on facies B and C since the rippled mud rich sandstones of facies C has a gradational boundary to the laminated mudrock of facies B. Facies B is again overlain by the “subaerial” facies A (coal). This suggests that the laminated mudrocks were deposited basinwards of facies A, and landwards of facies C. An environment which fits this setting is the higher parts of a tidal flat, which often is muddier than the lower lying tidal flat (Boggs 2006,). Thus the laminated mudrock may be interpreted to represent a supratidal flat, while the rippled mud rich sandstones may represent an intertidal flat. Rocks deposited in tidal flat environments may display rhythmic lamination as a result of the tidal variations (Longhitano et al. 2012). Such rhythmicity is observed in Core 18-2009 and Core 15-2010 (Figure 31).

Tides may influence a low gradient delta plain as far as 50 km inland (Allen 1965; Longhitano et al. 2012). This coincides well with the observed regional extent of the lower delta plain facies association within the investigated area. The Todalen Member has also previously been attributed to such a setting by various authors like Steel et al. (1981, 1985), Helland-Hansen (1990) and Bruhn and Steel (2003).

Overview of Occurrence within the Investigated Area from East to West

The frequency and thickness of the facies association is apparently decreasing from east to west within the investigated area. It occurs most frequently in Core 18-2009 (eastern most investigated location) where it is encountered seven times in ~0.2-15 m thick intervals. Whereas it in the westernmost investigated location of Grumantbyen is only observed five times in intervals less than ~2.5 m thick.

Facies Association 5: Interdistributary Bay/ Marsh

Description

The associated facies consists of carbonates cemented sandstone (J) with siderite concretions, burrowed sandstone (I), coal (A) and mudrock (B).

This facies association is only observed in the investigated outcrops. It is seen as carbonate cemented sandstone with siderite concretions/ burrowed sandstone with *Ophiomorpha* burrows, interbedded by thin coal and mudrock beds measuring a few centimeters in thickness (Figure 32). The thickness of this association is seen to be between 1-4 meters, but can possibly be thicker as the outcrop in Endalen was of mixed quality with two scree-covered areas.



Figure 32: Interdistributary bay/ marsh (FA 5) deposits in the Endalen outcrop.

Interpretation

Interdistributary bays are protected from wave- and storm action on the shallow water part of the delta plain by outbuilding delta lobes, thus representing areas of low energy sedimentation (Nichols 2009). The described combination of the facies above agrees with this interpretation as thin beds of mudrock and coal can be attributed to low energy sedimentation in shallow waters (Selley 2000). Siderite concretions are commonly associated with brackish conditions, which may occur in distributary bays with a sufficient fresh water influx from the channel (Boggs 2006, Nichols 2009).

Overview of Occurrence within the Investigated Area from East to West

No observations of this facies association were made in the investigated cores or in the Grumantbyen outcrop. In the Endalen outcrop however, two segments of interdistributary bay deposits are present in the lower half of the Todalen Member. These may represent one large segment of an interdistributary bay environment as they are separated by a scree-covered area covering ~6 meters of the outcrop.

Facies Association 6: Abandoned Delta Lobe

Description

This facies association consists of a massive carbonate cemented sandstone with and without concretions (J) and asymmetrically rippled sandstone (E). The association is present in Core 15-2010 and the Grumantbyen outcrop where it is seen to hold siderite concretions in its lower part. Sedimentary features include ripples and burrows in the core, whereas none of these features could be seen in the outcrop due to an extensive redish-brown weathering surface. The abandoned delta lobe facies association is present right above the second lowermost coal seam in the Grumantbyen outcrop and the core.

In the Grumantbyen outcrop the abandoned delta lobe facies association is seen to be of uniform thickness, about ~10 meter thick and laterally extensive over 40+ meters (Figure 28). It does not display any channel geometries, nor an irregular erosive base.

Interpretation

According to Elliot (1974), the destructive phase of sedimentation which follows the abandonment of a deltaic lobe, may produce a distinct marker horizon, seen as a laterally extensive sheet-like distribution of sand. One could argue that this sandstone body may represent a mouth bar or a channel, this does however not correspond to the field observation as the sandstone body does not display an erosive base, nor channel geometries. The base is indeed sharp, but not erosive, as the sandstone body rests directly on top of a coal seam which also is laterally extensive and of fairly uniform thickness in the Grumantbyen outcrop. The carbonate concretions (siderite) are only seen in the lower part of the abandoned delta lobe in Grumantbyen which suggests that the early stages of deposition took place in an interdistributary bay with brackish waters, the thickness suggests that a rapid increase in accommodation space followed, which enabled the sand to compact and subside.

Overview of Occurrence within the Investigated Area (from East to West)

The abandoned delta lobe facies association is encountered once within the lower strata of the Todalen Member in the Grumantbyen outcrop and Core 15-2010.

Facies Association 7: Foreshore to Basin

Description

This facies association consists of hummocky cross-stratified sandstone (H), burrowed sandstone (I), carbonates cemented sandstone (J), conglomerate (L), mudrock (B), mudrock (B) with large oval rock clasts (described and discussed in FA 3), asymmetrically rippled sandstones (E) and symmetrically rippled sandstone (F).

The following three sequences (S1-3) of the associated facies have been observed:

Sequence 1: Sequence 1 is characterized by a rippled sandstone unit. The appearance of the ripples in the lower part is asymmetric, whereas the ripples in the upper part are clearly symmetric. The transition between the two ripple types is gradational. The sequence is seen to be ~2 meter thick.

Sequence 2 (I, H/ L): This sequence consists of alternating beds of burrowed sandstone with an abundance of vertical *Ophiomorpha*-type burrows and hummocky cross-stratified sandstones with minor conglomerate lenses in the hummocks. The boundaries between the alternating beds are typically slightly curved and sharp. The thickness of this sequence is ~3.5 meters.

Sequence 3 (H, J/B): This sequence is made up by alternating beds of hummocky cross-stratified sandstones and mud rich carbonate cemented sandstones. The latter often bear sign of soft sediment deformation seen as undulating thickness of the beds. The maximum observed thickness of this sequence is approximately 10 meters.

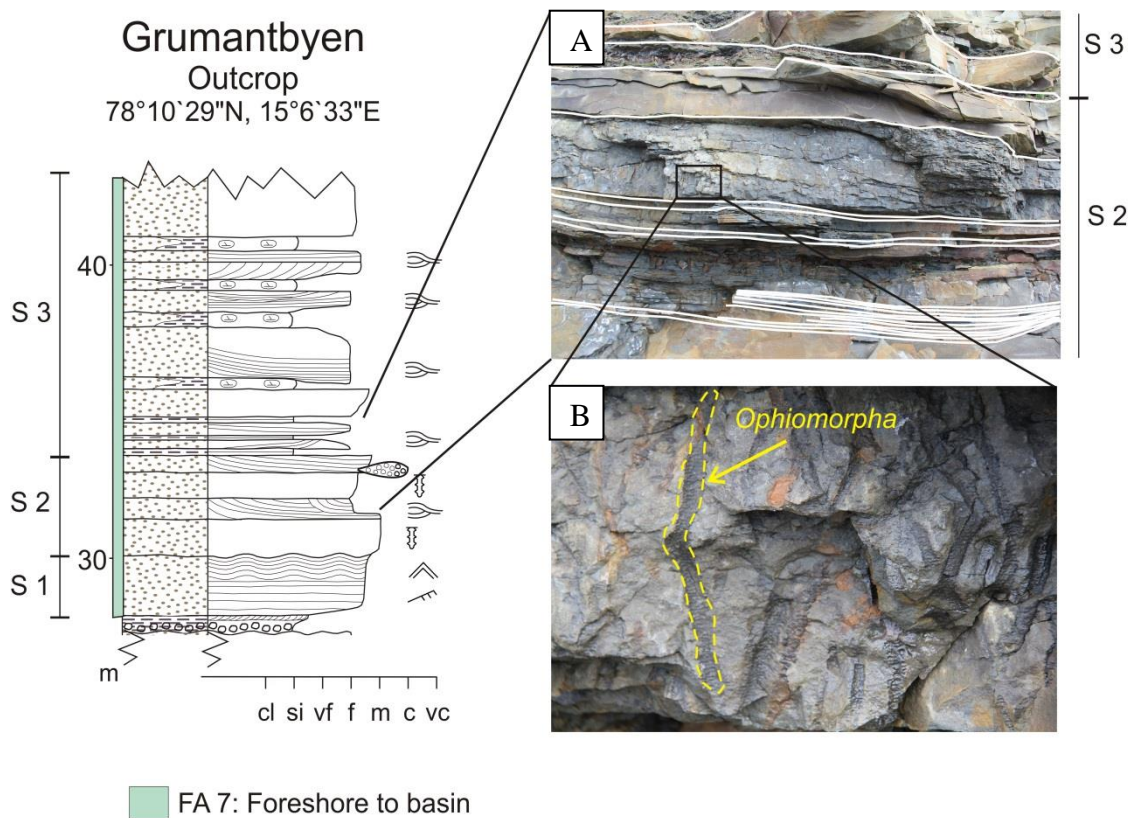


Figure 33: Facies association 7 in the Grumantbyen outcrop (Endalen Member). **A)** The upper photo display sequences 2 and 3. Sequence 2 consists of alternating beds of hummocky cross-stratified sandstones (HCS) and burrowed sandstones displaying *Ophiomorpha* trace fossils. Sequence 3 display alternating beds of HCS and mudrocks. Structures and boundaries are outlined in white. **B)** The lower photo shows the abundance of *Ophiomorpha*-type burrows in sequence 2 (one of which is outlined in yellow, ~30 cm long).

Interpretation

Hummocky cross-stratified sandstones (HCS) are characteristic for storm deposits on the lower shoreface between the fair-weather and storm wave base (Clifton 2006). *Ophiomorpha*-type burrows are commonly encountered in an upper shoreface to lagoonal setting (Gerrard and Bromley 2008). As HCS-beds are regarded as a lower shoreface parameter, and *Ophiomorpha*-type burrows as a parameter of shallower waters, the depositional setting of this sequence represents an overall shoreface environment.

Sequence 3 on the other hand, consisting of HCS-beds interbedded by mud rich carbonate cemented sandstones, may indicate fast shifts between the lower shoreface environment (HCS-beds) and the offshore environment (mud rich carbonate cemented sandstones) due to the soft sediment deformation which requires the sediments to be unconsolidated at the time of deposition of the overlying bed. The large mud-content in the mud rich carbonate cemented sandstone also indicates that the current regime was low, allowing clay-sized particles to settle out of suspension.

Sequence 1 consists of a sandstone unit with asymmetrical ripples in its lower part grading upwards into ripples with a symmetrical appearance in its upper part. Such a pattern is expected in a shoreface environment going from being under the influence of sharp-crested waves, to being under the influence of sinusoidal waves (Clifton 2006). Sharp-crested waves are characteristic of shallower water-depths (which causes the waves to “break” and become short-crested), while sinusoid waves requires deeper waters. This implies that Sequence 1 represents the start of an overall relative sea level rise which is continued in the overlying Sequence 2 and Sequence 3.

Overview of Occurrence from East to West

The facies association is present in the lower Endalen Member strata in the Grumantbyen outcrop. It is also present in the middle of the Todalen Member in the Endalen outcrop. No obvious delta front deposits are observed in the Todalen Member in the two logged cores.

5. Petrographical Results

A total of thirty-five thin sections displaying sandstone lithologies have been point counted from the Todalen Member and lower Endalen Member strata in Core 18-2009, Core 15-2010, the Endalen outcrop and the Grumantbyen outcrop. Each of these cores and outcrops are assigned to an individual subchapter which aims to demonstrate the essential petrographic observations. The results from the sandstone classification after Pettijohn (1972) are presented in Appendix 3.1.

5.1 Petrographic Composition of Core 18-2009

Modal Analysis Results

Nine petrographic thin sections have been analyzed from the logged section of Core 18-2009. The modal analysis results are presented in Table 2 (values are in percent). A stratigraphic overview of the thin sections is illustrated in Figure 34.

Table 2a: Modal analysis (detrital grains and matrix), values in percent.

Thin Section #	Elevation a.C.Fm. (m)	Firkanten Fm. Mb.	Quartz			Chert			Feldspar		Lith. Frag >2 mm	Matrix <0.03 mm	Org. Mat.
			Monocryst. qtz	Polycryst. qtz	Sheared qtz	Microcryst. qtz	Spicular chert	Chalcedony	Plagioclase	K-Feldspar			
18-3	11.00	Todalen	47,0	18,3	-	2,3	1,0	1,3	0,7	2,7	2,0	6,3	1,0
18-6	15.60	Todalen	53,7	21,7	-	3,3	0,7	1,0	0,3	2,3	1,7	2,7	0,3
18-8	22.20	Todalen	38,7	19,3	-	3,7	0,3	0,7	0,3	1,7	2,3	20,3	1,0
18-10	33.80	Todalen	52,3	13,3	-	1,3	0,7	0,7	trace	2,3	1,7	12,7	0,7
18-13	43.73	Todalen	54,3	22,7	-	2,0	0,3	0,3	0,3	3,7	1,7	6,7	0,7
18-16	47.10	Endalen	16,7	6,3	-	0,7	trace	trace	trace	0,3	65,7	5,3	0,7
18-17	50.45	Endalen	35,7	9,3	-	1,0	-	-	-	3,3	3,7	28,3	1,3

Table 2b: Modal analysis (diagenetic minerals, porosity and assecory minerals), values in percent.

Thin Section #	Elevation a.C.Fm. (m)	Firkanten Fm. Mb.	Cement		Porosity		Assecory Minerals				
			Carbonate	Quartz	Inter-granular	Intra-granular	Muscovite	Glauconite grains	Glauconite porefilling	Pyrite	Heavy minerals
18-3	11.00	Todalen	3,0	2,3	6,7	1,3	1,0	1,7	0,7	0,7	trace
18-6	15.60	Todalen	3,3	3,7	2,3	1,7	0,3	0,7	0,3	0,3	trace
18-8	22.20	Todalen	1,7	1,3	4,3	2,0	0,7	0,7	0,7	0,3	trace
18-10	33.80	Todalen	1,3	2,7	4,7	3,3	0,3	1,3	0,7	-	trace
18-13	43.73	Todalen	trace	2,0	3,7	0,3	0,3	0,7	0,3	-	trace
18-16	47.10	Endalen	0,3	0,7	1,3	0,7	-	trace	0,3	1,0	trace
18-17	50.45	Endalen	0,3	0,7	11,7	2,3	0,3	-	0,7	0,7	0,7

Table 2c: Textural parameters. See Appendix 3.2 for abbreviations.

Thin Section #	Elevation a.C.Fm. (m)	Firkanten Fm. Mb.	Wentworth size class	Sorting	Rounding	Lithology
18-3	11.00	Todalen	Fine	Moderate	Subangular to subrounded	Sandstone
18-6	15.60	Todalen	Fine	Well	Subangular to subrounded	Sandstone
18-8	22.20	Todalen	Very fine	Well	Subangular to subrounded	Sandstone
18-10	33.80	Todalen	Fine	Moderately well	Subangular to angular	Sandstone
18-13	43.73	Todalen	Fine	Well	Subangular to subrounded	Sandstone
18-16	47.10	Endalen	Granules & pebbles	Poor	Rounded & subrounded	Conglomerate
18-17	50.45	Endalen	Fine	Poor	Angular to rounded	Sandstone

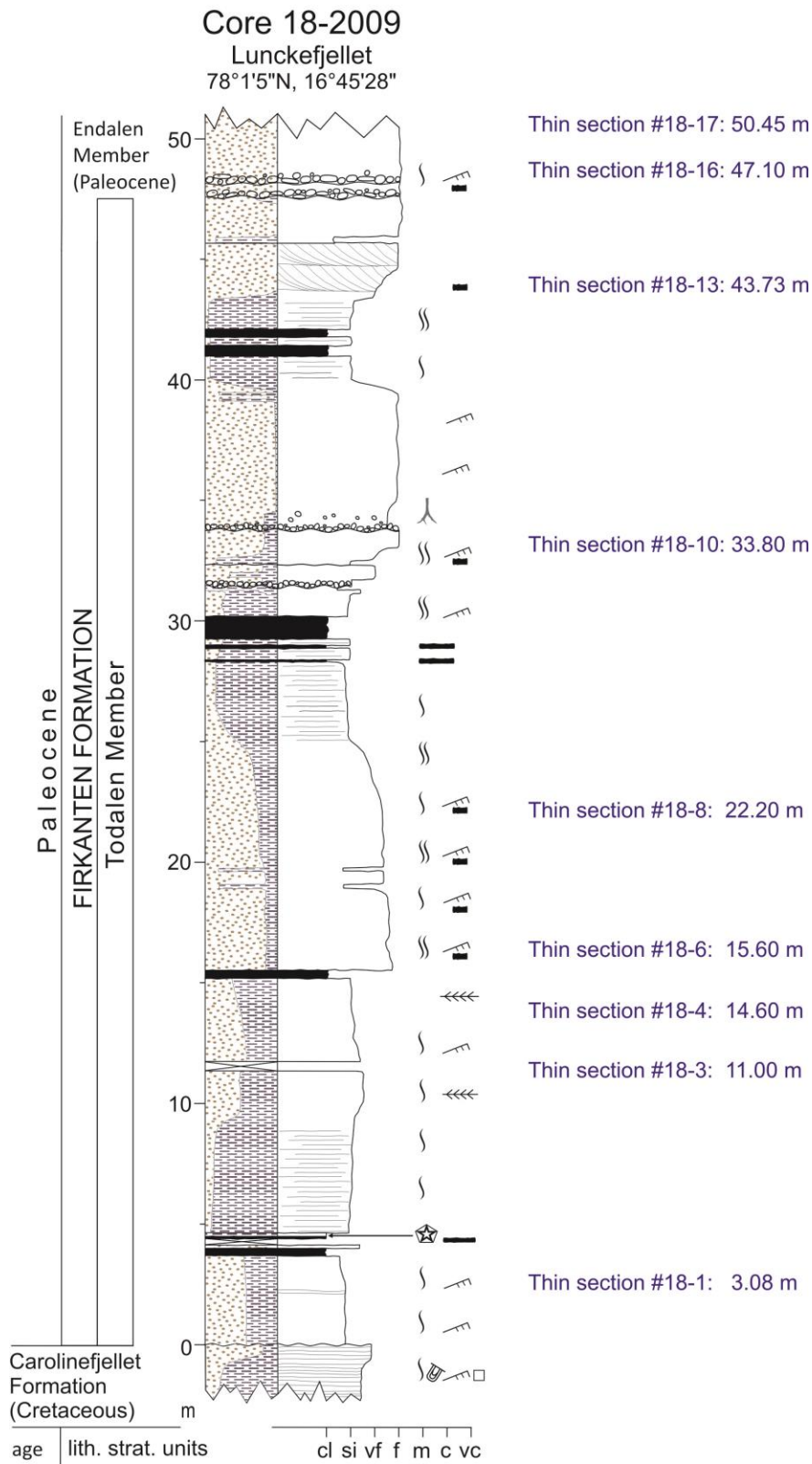


Figure 34: Stratigraphic overview of the point counted thin sections from Core 18-2009. For legend, see Appendix 2.1.

Lithology and Texture

Todalen Member

The point counted thin sections from Todalen Member consist of moderate to well sorted very fine and fine grained sandstones (Figure 35). The grains are mostly subangular to subrounded.

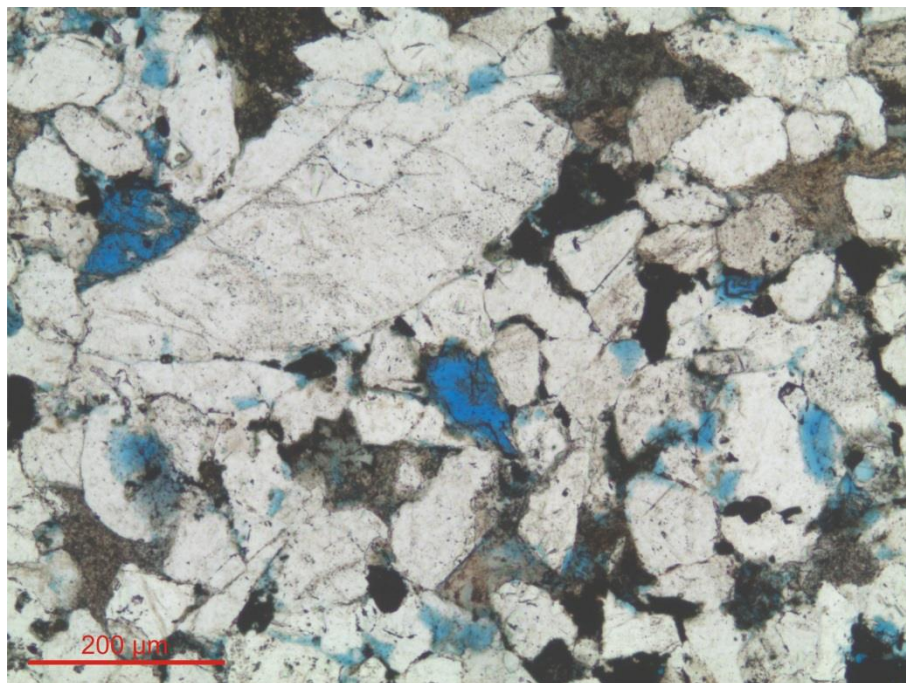


Figure 35: Moderately sorted sandstone. Note the lithic fragment to the left. Plane light micrograph of thin section 18-3, Todalen Member.

Endalen Member

The Endalen Member consists of poorly sorted sandstones and a conglomerate. The majority of the grain fraction in the poorly sorted sandstones are fine-grained and rounded whereas the minority is medium to coarse-grained and angular.

The conglomerate marks the boundary to the Todalen Member. The conglomerate clasts are polymictic (with polycrystalline quartz, monocrystalline quartz and microcrystalline quartz), bimodal (granule to pebble sized), well rounded and matrix supported. The matrix resembles the poorly sorted sandstones described above.

Detrital Grains

Todalen Member

The dominant detrital grain in Todalen Member is quartz. The volume of quartz makes up an average of 68.3% of the point counted thin sections in Table 2a-c . The ratio of monocrystalline to polycrystalline quartz is approximately 2:1. The majority of the monocrystalline quartz has uniform extinction under crossed-nichols, whilst the minority has undulose (“sweeping”) extinction.

Fluid and mineral inclusions are present in very small amount in the quartz grains; fluid inclusions are seen as dusty coatings whilst the very small mineral inclusions are mostly of zircon and apatite. Zircon is recognized by its high positive relief and high order interference colors. Apatite is recognized by its needle shaped morphologies and lack of high order interference colors. These two heavy minerals are often seen together in quartz grains. Zircon (Figure 36 a) may also be observed as free standing anhedral and euhedral minerals, and is together with apatite a part of the heavy mineral suite. Other heavy minerals observed in very small amounts include epidote (Figure 36 b), rounded tourmaline (Figure 36 c), rutile, garnet, chrome spinel, opaque minerals, microscopic siderite nodules and pyrite.

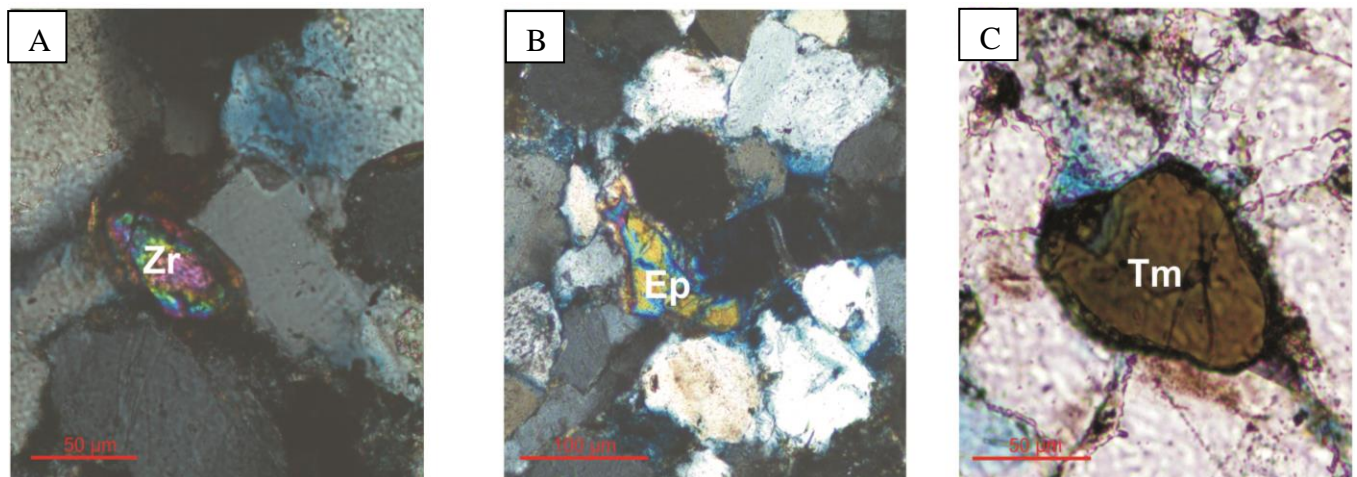


Figure 36: A) Rounded detrital zircon grain, crossed-nichols. **B)** Epidote, crossed-nichols. **C)** Rounded greenish brown tourmaline, plane light. A-C micrographs of thin section #18-3, Todalen Member.

The detrital grain fraction also includes cherts, feldspars and lithic fragments of microcrystalline quartz (chert) and polycrystalline quartz. Chert occurs in three forms; as microcrystalline quartz, spicular chert and chalcedony. The content of chert makes up an average volume of 3.9% of the thin sections. The amount of spicular chert and microcrystalline quartz remains fairly stable throughout the Todalen Member while the content of chalcedony decreases upwards in the section.

K-feldspars, primarily orthoclase but also some microcline, are present in volumes up to 3.7%. Plagioclase with albite twinning is present in volumes of 0-0.7% and is thus relatively rare to absent.

The amount of lithic fragments (>2 mm) in the Todalen Member is fairly steady, between 1.7-2.3%, and mostly in the form of polycrystalline and microcrystalline quartz (Figure 37 a-b).

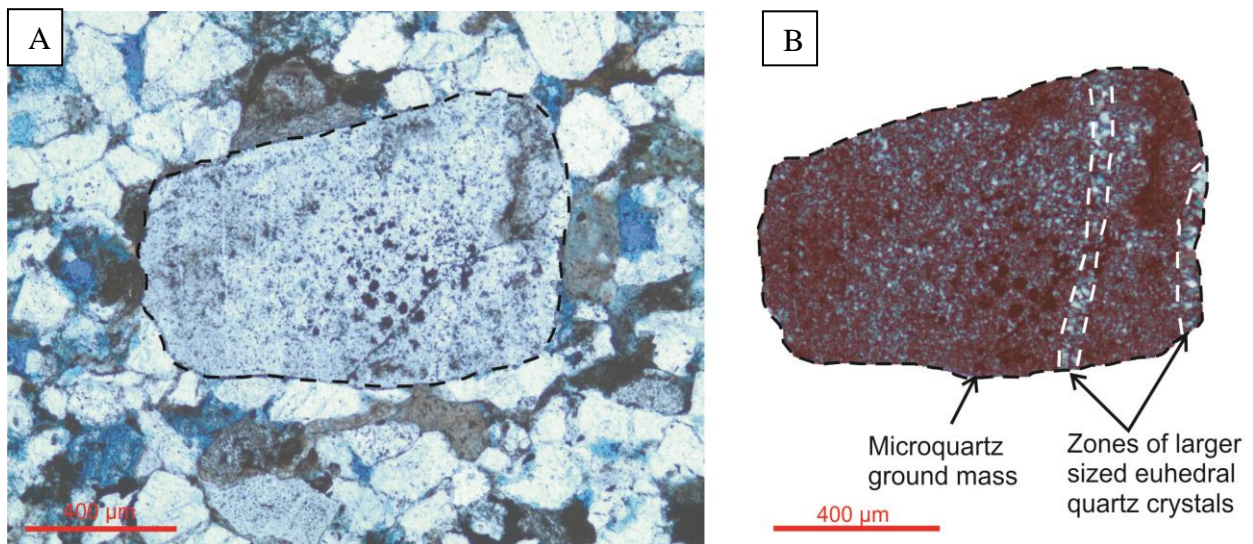


Figure 37: A) Plane light micrograph of lithic fragment of microcrystalline quartz (chert) outlined in black. **B)** Crossed-nichols micrograph of the same lithic fragment, note the microquartz ground mass and the zones of larger sized euhedral quartz crystals within the lithic fragment. A and b are from thin section #18-3, Todalen Member.

A significant amount of matrix (fragments smaller than <0.03 mm) is present in all the Todalen Member sandstones. The main components of the matrix are detrital and authigenic clay, organic material (original structures not recognizable) and small silt sized quartz grains. Deformed and

partly dissolved muscovite is often concentrated in the clay fraction (Figure 38). Accessory minerals observed in the thin sections, apart from the heavy mineral suit mentioned above include porefilling glauconite cement and detrital glauconite grains.

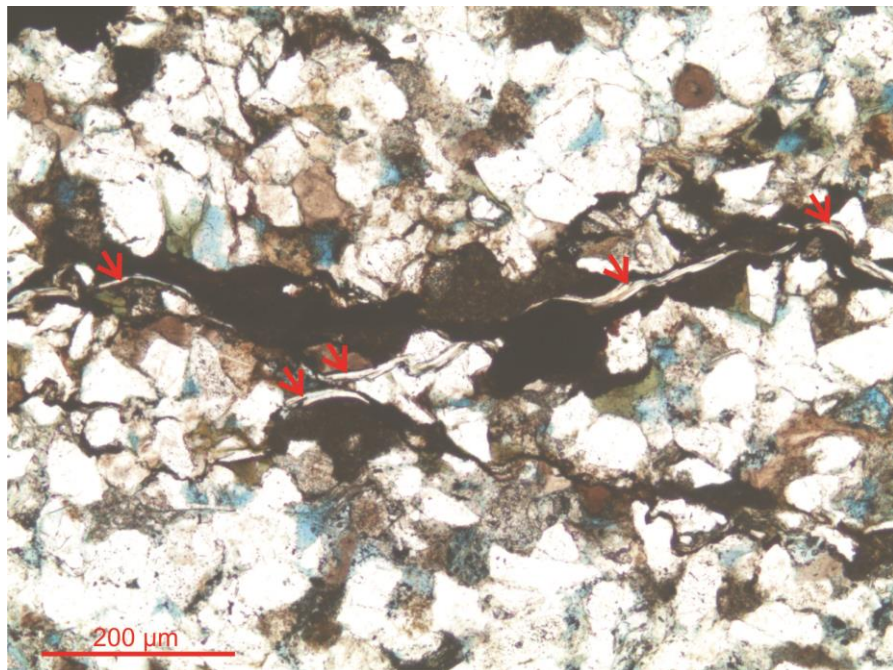


Figure 38: Mechanically deformed flaky muscovite concentrated in the clay fraction. Plane light micrographs of thin section #18-8, Todalen Member.

Endalen Member

The ratio of monocrystalline quartz grains to polycrystalline quartz grains in the Endalen Member sandstones is approximately 7:2. The vast majority of the quartz grains display uniform extinction under crossed-nichols whereas the minority displays undulose extinction.

The content of spicular chert and chalcedony is rare to absent. No feldspars are observed. The Endalen Member sandstones are generally more abundant in the heavy mineral suite seen in the Todalen Member.

Diagenetic Minerals

Todalen Member

The volumetric content of quartz and carbonate cement in the samples is low, on average 2.4% and 1.8% respectively. Quartz cement occurs in variable amounts (1.3%-3.7%) and is seen as continuous and discontinuous overgrowths on detrital grains (Figure 39).

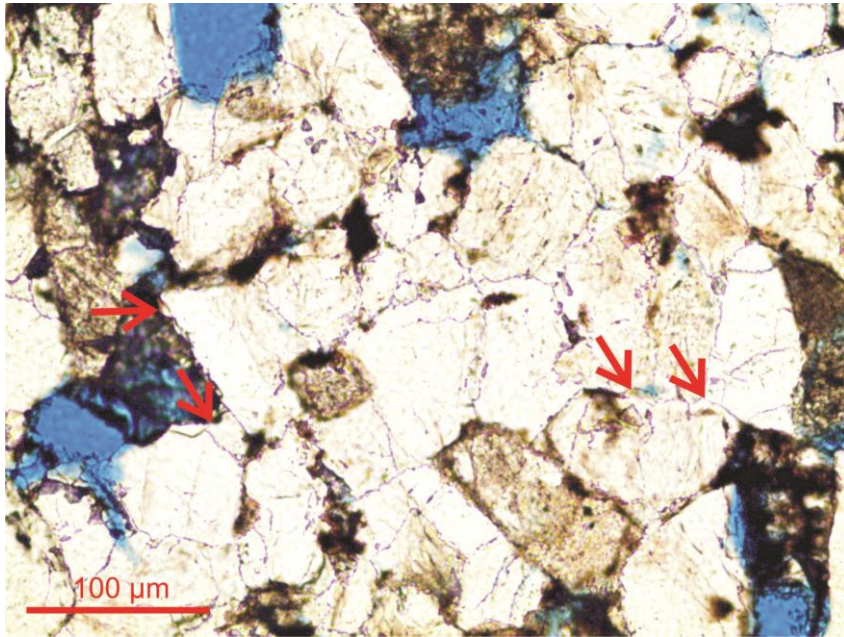


Figure 39: Quartz cement in the Todalen Member. The red arrows points on continuous and discontinuous quartz overgrowths. Plane light micrograph of thin section #18-3, Todalen Member.

The amount of carbonate cement is decreasing upwards in the Todalen Member section from 3.0% in the lowermost thin section to trace amounts in the uppermost thin section. The carbonate cement is mostly in the form of ferroan-dolomite/ ankerite (FDA) and appears as thin outer linings on quartz cement as well as inter- and intragranular porefilling cement patches. It is recognized by its high order interference colors under crossed-nichols, and by its brownish to transparent appearance in plane light.

Intergranular pyrite framboids are present in the lower part of the Todalen Member (0.3%-0.7%), but is completely absent in the upper part.

Microscopic rosette shaped morphologies are observed in a silty clay matrix in thin section #18-1 (Table 1 and Figure 40). They occur in abundance and are made up by pentagon shaped blades radiating outwards from the rosette center. Each rosette blade consists of bundled crystal fibers which provide each blade with an oriental fan-like texture. The distance between the outer edges of two opposite directed blades are ~100-200 μm . The color of the rosette blades in plane light is white, brown staining is concentrated in the central part of the rosette and appears to be partially smeared out over some of the rosette blades. Multiple black minerals, rectangular (length x width: ~30 μm x 10 μm) and circular (diameter: ~5-10 μm) in shape, are present in the center of the rosette. Floating individual rosette blades are also present; these appear to have a more rounded appearance than the pentagon shaped blades in the rosettes.

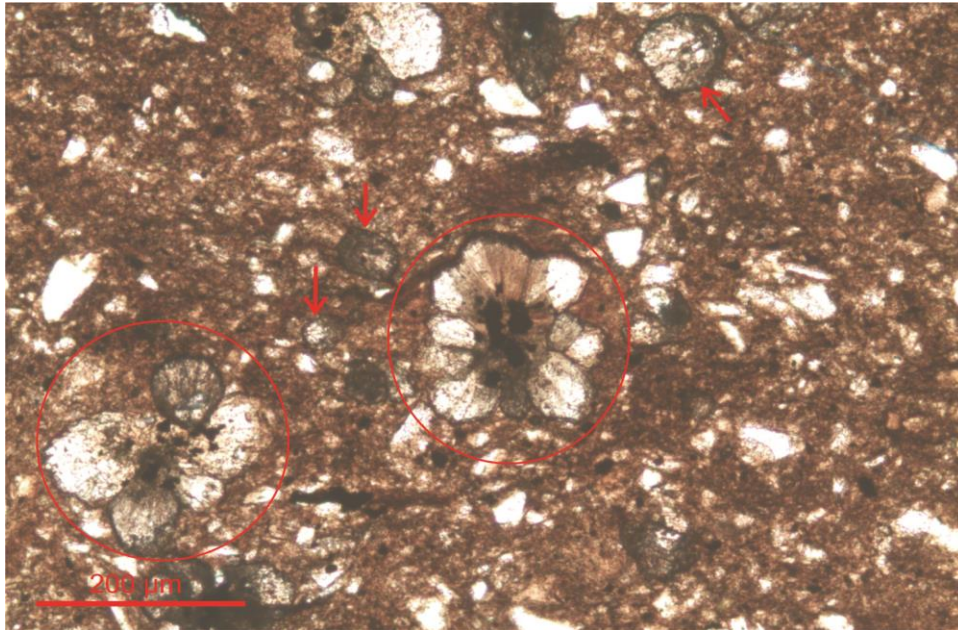


Figure 40: Microscopic siderite rosettes (red circles) in a silty clay matrix. Note the fan-like texture of each rosette blade caused by bundled fibers radiating outwards. Also notice the concentration of opaque minerals in the rosettes center. Floating rosette blades are pointed out by the red arrows. Plane light micrographs of thin section #18-1, Todalen Member.

EDS analysis uncovered that the white rosette blades consist of siderite (Figure 41 A, point 1) due to the ratio between iron (Fe) and oxygen (O) it also contains minor components of calcium (Figure 41 B1). The black minerals in the center of the rosette described from the plane light micrograph in Figure 40 A are pyrite and quartz (Figure 41 B2 and 3).

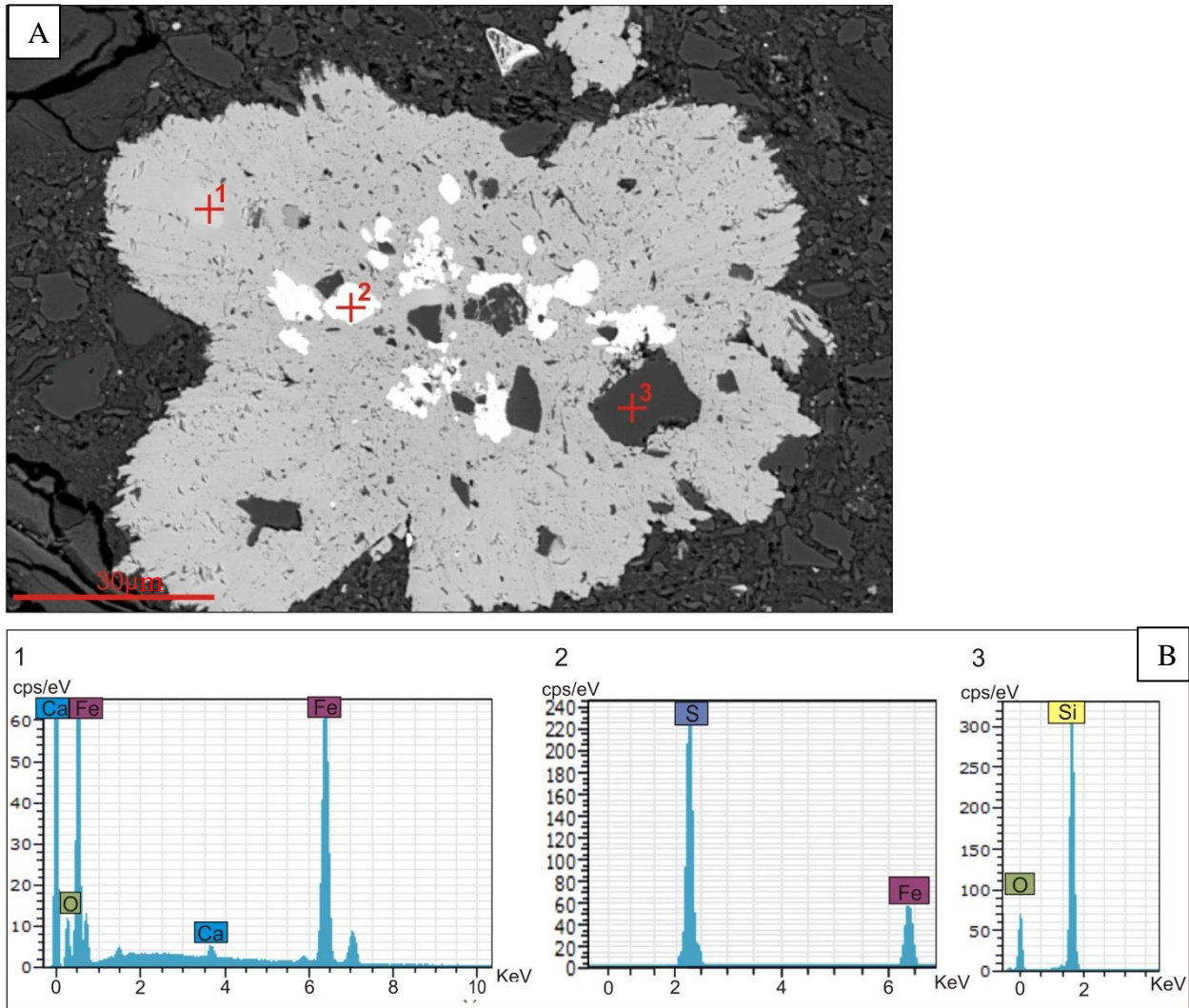


Figure 41: A) SEM backscattered electron image of siderite rosette marked with EDS sample points 1-3. B) 1: EDS of siderite (FeCO_3) with minor components of calcium, 2: EDS spectrum of pyrite (FeS_2), 3: EDS spectrum of quartz (SiO_2). Thin section #18-1, Todalen Member.

Endalen Member

Quartz and ferroan-dolomite/ ankerite cement accounts for respectively 0.7% and 0.3% of the sample volume in the Endalen Member thin sections. The quartz cement appears as thin, synthaxial overgrowths on detrital grains, the carbonate cement is seen as a few porefilling patches which post-dates the quartz cement formation as it is partially enveloping the quartz cement.

Porosity

Todalen Member

The majority of the Todalen Member samples have low to moderate intergranular porosity volumes close to the average which is 4.3 %. This intergranular porosity is inferred to be primary as it bears signs of mechanical deformation with horizontally squeezed and asymmetric porosity voids. They contain little to some diagenetic/ detrital clay residues. The intragranular porosity (secondary porosity) is on average 1.7 % due to dissolution of grains. The nature of the almost completely dissolved grain is challenging to establish. The partially dissolved grains, however, are seen to display cleavage/ twinning together with low order (grey) interference colors, it is implied that feldspars accounts for at least some of the intragranular porosity volumes (Figure 42 a and b).

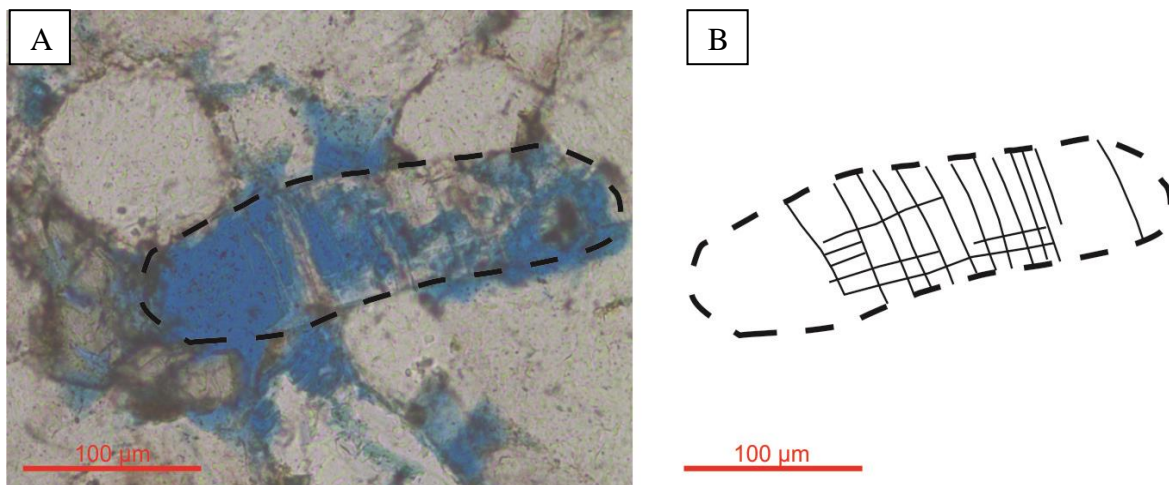


Figure 42: A) The area within the dotted line is a partially dissolved detrital K-feldspar grain with microcline twinning. **B)** Illustration of a) with outlined twinning planes (cross-hatch pattern). Plane light micrograph of thin section #18-3, Todalen Member.

Endalen Member

The porosity of the sandstones in the Endalen Member is variable. The lowest total porosity (both intergranular and intragranular) is 1.7 % while the highest recorded total porosity is 14% (11.7% intergranular porosity, 2.3% intragranular porosity). The intergranular porosity is secondary and due to complete dissolution of detrital clay assemblages. This highest recorded porosity is more than twice than the average total porosity of the Todalen Member.

5.2 Petrographic Composition of Core 15-2010

Modal Analysis Results

The seven point counted thin sections from Core 15-2010 are presented in Table 3. A stratigraphic overview of these is given in Figure 43.

Table 3a: Modal analysis (detrital grains and matrix), values in percent.

Thin Section #	Elevation a.C.Fm. (m)	Firkanten Fm. Mb.	Quartz			Chert			Feldspar		Lith. Frag >2 mm	Matrix <0.03 mm	Org. Mat.
			Monocryst. qtz	Polycryst. qtz	Sheared qtz	Microcryst. qtz	Spicular chert	Chalcedony	Plagioclase	K-Feldspar			
15-2	0,72	Todalen	66,7	8,3	-	3,3	1,3	0,7	-	3,3	5,3	8,4	0,7
15-5	7,30	Todalen	73,7	5,7	-	4,7	2,7	0,3	-	2,3	2	3,4	0,3
15-6	14,29	Todalen	72,3	2,0	-	0,3	0,3	0,7	-	1,2	-	21,3	0,3
15-8	21,05	Todalen	73,3	3,7	-	0,7	-	1,0	-	4,7	1,0	11,7	0,3
15-9	33,50	Endalen	68,3	4,7	-	1,3	-	-	trace	4,3	0,7	15,3	0,7
15-10	37,75	Endalen	83,3	5,3	-	1,3	-	-	trace	5,3	0,3	3,2	0,7
15-11	38,92	Endalen	83,3	2,7	-	1,7	-	-	2,3	4,7	0,3	2,4	0,3

Table 3b: Modal analysis (diagenetic minerals, porosity and assecory minerals), values in percent.

Thin Section #	Elevation a.C.Fm. (m)	Firkanten Fm. Mb.	Cement		Porosity		Assecory Minerals				
			Carbonate	Quartz	Inter-granular	Intra-granular	Muscovite	Glauconite grains	Glauconite porefilling	Pyrite	Heavy minerals
15-2	0,72	Todalen	0,7	0,3	trace	trace	-	0,7	0,3	trace	trace
15-5	7,30	Todalen	0,7	0,3	2,3	1,0	-	0,3	0,3	trace	trace
15-6	14,29	Todalen	0,3	trace	0,3	0,7	trace	0,3	trace	trace	trace
15-8	21,05	Todalen	0,3	trace	0,3	1,7	trace	0,3	0,7	trace	0,3
15-9	33,50	Endalen	0,3	0,7	0,7	0,7	trace	0,7	1,3	trace	0,3
15-10	37,75	Endalen	trace	trace	0,3	0,3	-	trace	trace	trace	trace
15-11	38,92	Endalen	trace	0,3	0,7	0,3	-	0,7	0,3	trace	trace

Table 3c: Textural parameters. See Appendix 3.2 for abbreviations.

Thin Section #	Elevation a.C.Fm. (m)	Firkanten Fm. Mb.	Wentworth size class	Sorting	Rounding	Lithology
15-2	0,72	Todalen	Medium	Poor	Rounded	sandstone
15-5	7,30	Todalen	Very fine	Moderately well	Subrounded	sandstone
15-6	14,29	Todalen	Very fine	Moderately well	Subangular	sandstone
15-8	21,05	Todalen	Very fine	Moderately well	Subrounded	sandstone
15-9	33,50	Endalen	Very fine	Moderately well	Subrounded	sandstone
15-10	37,75	Endalen	Fine	Well	Subangular	sandstone
15-11	38,92	Endalen	Fine	Well	Subangular	sandstone

Core 15-2010
 Bassen on Operafjellet
 78°12'36"N, 16°5'54"E

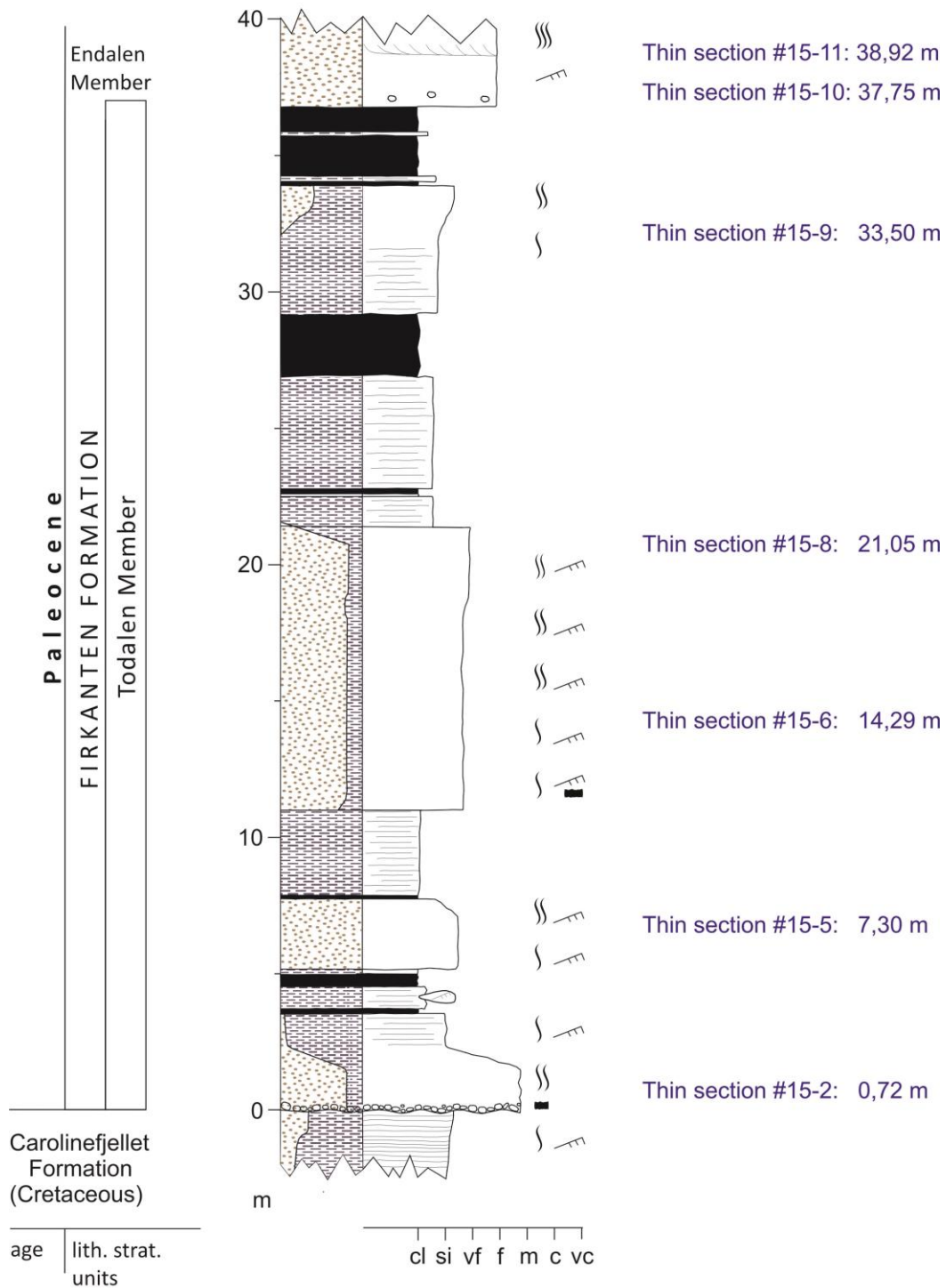


Figure 43: Stratigraphic overview of the modal analyzed thin sections from Core 18-2009. For legend, see Appendix 2.1.

Lithology and Texture

Todalen Member

The samples obtained from the Todalen Member consist of poorly (Figure 44) and moderately well sorted sandstones. The dominant grain fraction of the latter is very fine sand. The matrix content is on average 11.2% of the point counted volume. Grains are typically subangular to rounded.

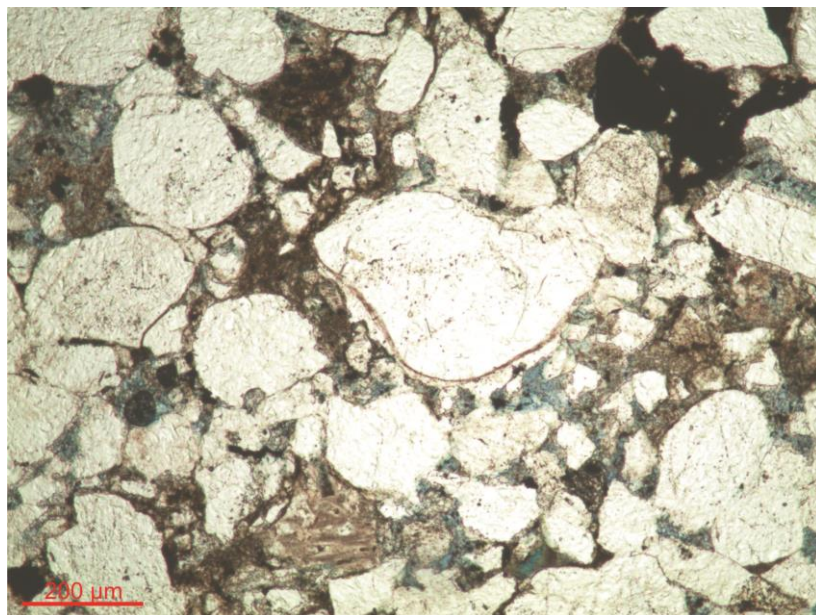


Figure 44: Poorly sorted sandstone with a matrix consisting of clay and silt-sized quartz grains. Plane light micrograph of thin section #15-2, Todalen Member.

Endalen Member

Samples obtained from the lower Endalen Member sandstones are moderately well and well sorted. The dominant grain size is very fine and fine sand (Figure 45). The volume of matrix is on average 7.2%. The grains are subangular to subrounded.

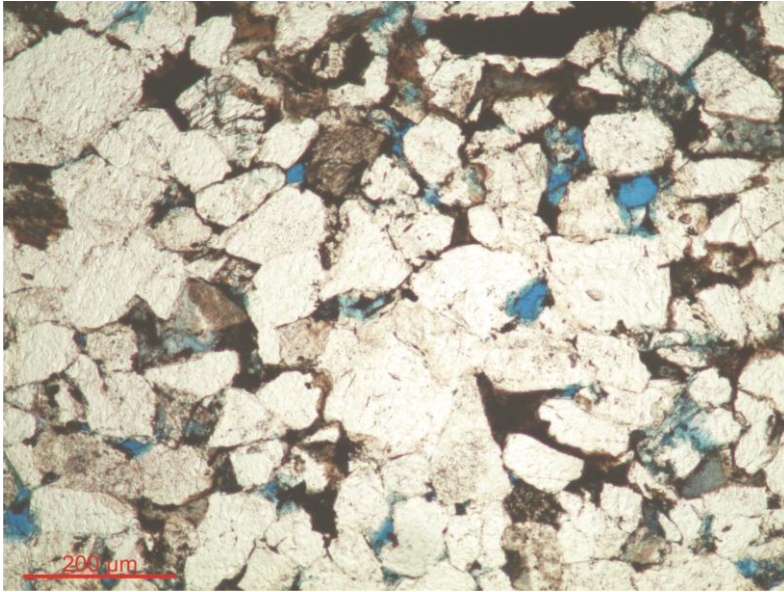


Figure 45: Subangular to subrounded grains in an Endalen Member sandstone. Plane light micrograph of thin section #15-10, Endalen Member.

Detrital Grains

Todalen Member

Quartz is the dominant detrital grain in the Todalen Member sandstones with an average volume of 76.4%. The ratio of monocrystalline to polycrystalline quartz is approximately 30:4 (Figure 46). The majority of the monocrystalline quartz grains display uniform extinction. Sheared quartz grains are not observed. Fluid and mineral inclusions as described in Core 18-2009 are common within the quartz grains.

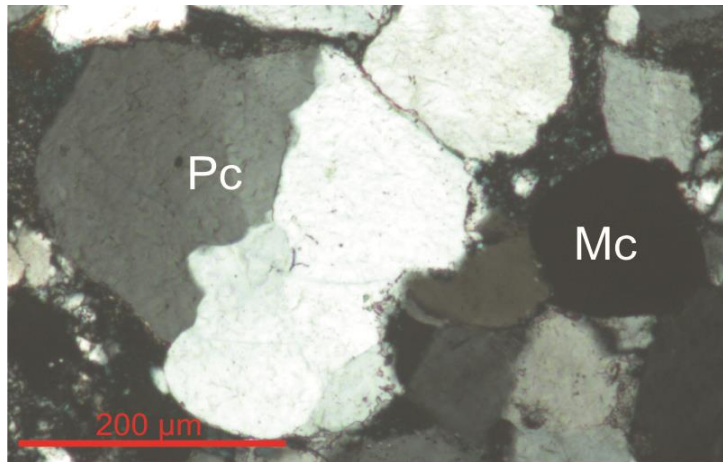


Figure 46: Polycrystalline quartz grain (Pc) with sutured boundaries between the crystals which goes into extinction at different orientations. Monocrystalline quartz grain (Mc), the whole crystal goes into extinction at one orientation. Crossed-nichols micrograph of thin section #15-2, Todalen Member.

Chert is present in the form of microcrystalline quartz, spicular chert and chalcedony (Figure 47). The total volume of chert varies between 1.3% and 7.7%. The trend is a decreasing upwards volume of all the chert types in the Todalen Member section.

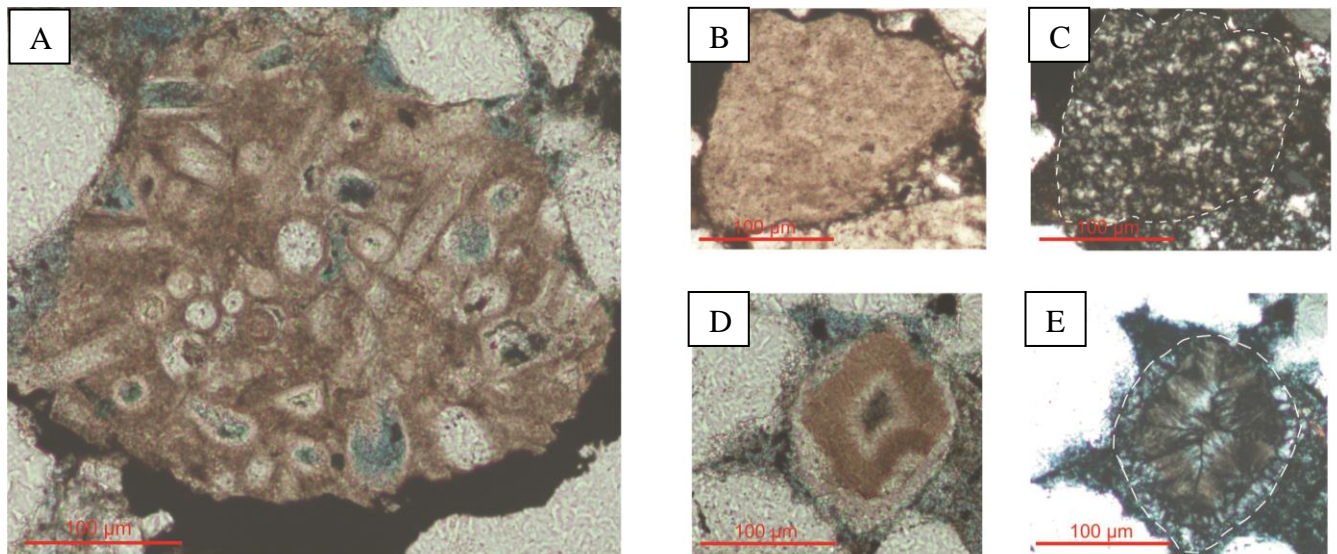


Figure 47: Micrographs of chert. **A)** Spicular chert fragment in plane light. **B)** Microcrystalline quartz grain, plane light. **C)** Microcrystalline quartz grain (same as in b), crossed-nichols. **D)** Chalcedony grain in plane light. **E)** Chalcedony grain (same as in d) under crossed-nichols. A-E micrographs of thin section #15-2, Todalen Member.

In regards to feldspars, no plagioclase is observed. K-feldspar however, in particular orthoclase, but also some microcline, are seen in volumes between 1.2-4.7% (Figure 48).

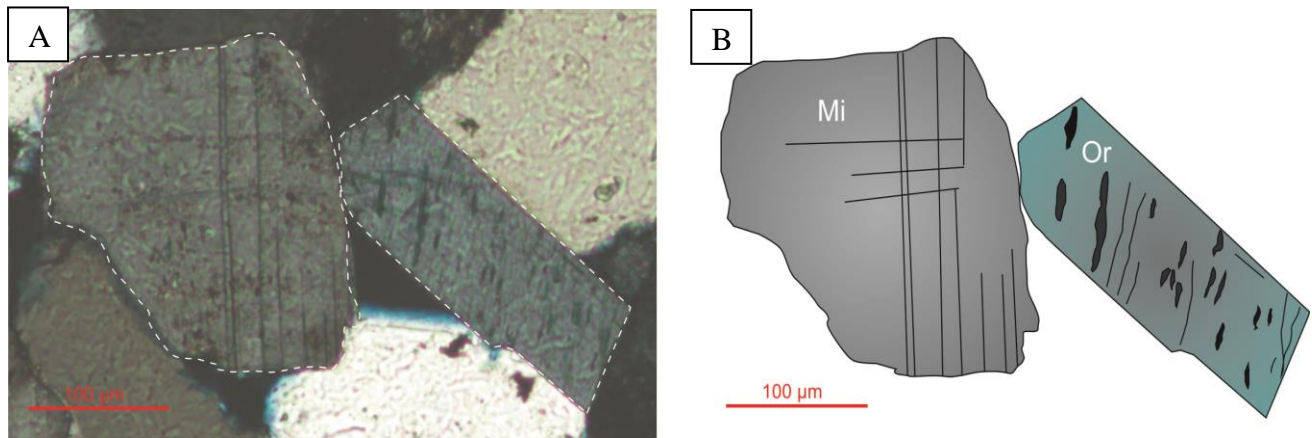


Figure 48: A) Crossed-nichols micrograph of K-feldspar grains (microcline and orthoclase). **B)** Illustration of microcline (Mi), which display twinning upon rotation under the microscope. Illustration of orthoclase (Or) which is partly dissolved along the cleavage planes. Thin section #15-2, Todalen Member

Lithic fragments occur as monocrystalline and polycrystalline quartz and are seen in variable amounts between 5.3% to none. The frequency of appearance is decreasing upwards in the section.

The occurrence of grains with glauconitic morphology, green in color and with an internal mottled texture, is stable throughout the section (0.7%-0.3%). Glauconitic pore filling cements are present in trace amounts to 0.7%.

The matrix consists of angular quartz grains smaller than 0.03 mm and clay. The clay is both detrital and diagenetic. The detrital clay is seen between the grain-to-grain contacts, and is dark brown to black in color and of an apparently homogenous texture. Diagenetic clay occurs as scattered pore fillings as well as thin linings between detrital grains. As a porefilling substance, it is generally light brown to transparent in color, and often clustered in and around partially dissolved feldspar grains.

Organic material makes up an average volume of 0.4% of the samples. It is most often seen as black, elongated “blobs” apparently subjected to ductile deformation due to its plastic-like

deformation appearance. The cell texture of the organic material may occasionally be recognized (Figure 49).

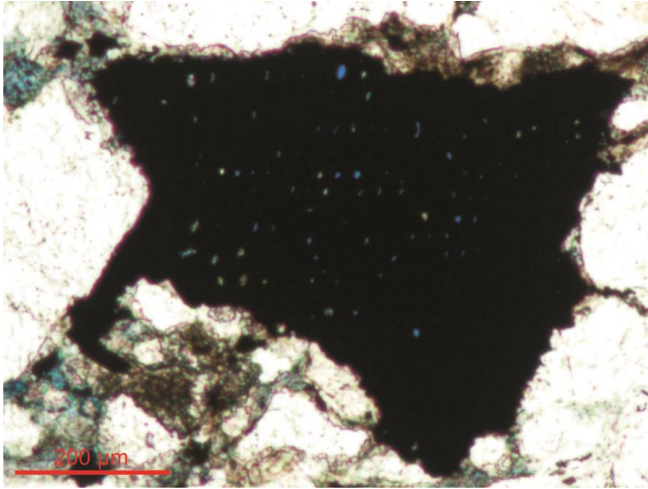


Figure 49: Organic material with recognizable cell-framework (blue epoxy spots in the dark matter). Plane light micrograph of thin section 15-2, Todalen Member.

Small amounts of framboid pyrite is scattered in the matrix, the rounded appearance suggest that it is occurring as diagenetic mineral.

The heavy mineral suite is seen in trace amounts, and is comprised by apatite, zircon, epidote, tourmaline, rutile, garnet, chrome spinel (Figure 50), opaque minerals, microscopic siderite nodules and pyrite. The most frequently encountered ones are tourmaline, pyrite, opaque minerals and chrome spinel. Microscopic siderite nodules are only observed in the uppermost sample.

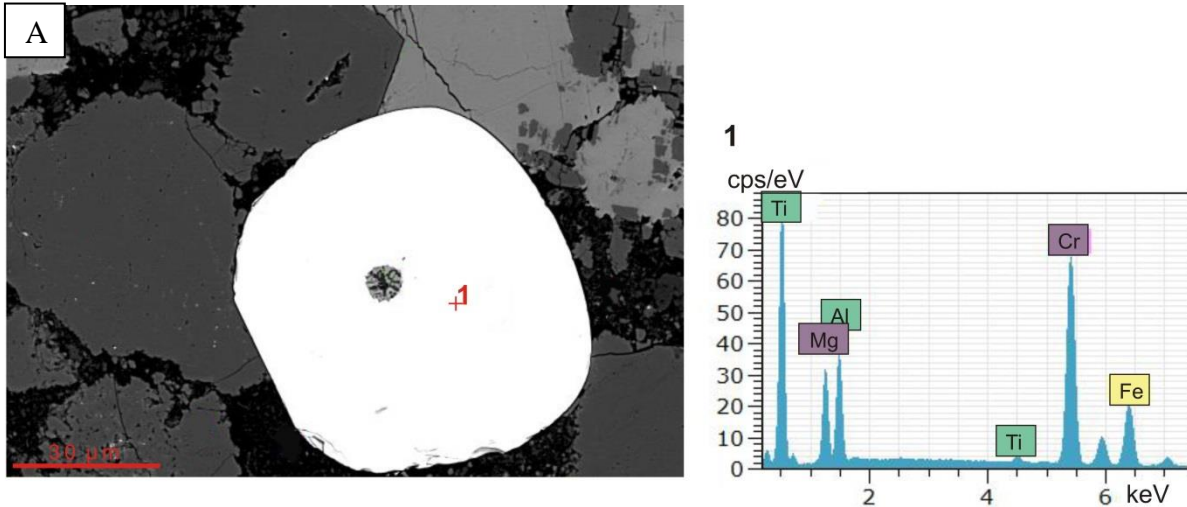


Figure 50: SEM backscattered electron image of chrome spinel (white), 1: EDS analysis of chrome spinel. Thin section #15-2, Todalen Member.

Endalen Member

The average point counted volume of quartz grains is 82.5%. The ratio of monocrystalline quartz grains to polycrystalline quartz grains is approximately 18:4. A majority of the monocrystalline quartz grains display uniform extinction whereas a minority displays undulose extinction.

Microcrystalline quartz is the only type of chert observed in the samples.

Feldspars are present in volumes between 4.3 and 5.7%, almost exclusively as the K-feldspars orthoclase and microcline. A small amount of plagioclase is however observed in the uppermost sample.

The volume of lithic fragments is low and stable, between 0.3% and 0.7%, and only in the form of polycrystalline quartz.

Glaucitic grains, as well as porefilling glauconite cement, occur in variable amounts, thus never exceeding a total sample volume >1.0%.

The nature of the matrix is similar to the Todalen Member samples, though generally in smaller volumes around 7.2% on average.

Organic material is present in volumes between 0.3% and 0.7%, no original cell-framework could be recognized.

The most frequently occurring heavy minerals, though still in trace amounts, are pyrite, garnet, epidote, microscopic siderite nodules and tourmaline. The shape of the pyrite is framboid, and it is seen to be dispersed in the matrix. The microscopic siderite nodules are occurring on the edges of detrital grains, and are sometimes enveloped in quartz cement. The tourmaline is typically greenish brown in plane light, fine grained and well rounded.

Diagenetic Minerals

Todalen Member

Quartz cement makes up a small part of the sample volume, from trace amounts to 0.3%. It is seen as discontinuous overgrowths which are in optical continuity with the detrital quartz grains from which it nucleated. Some of the cemented quartz grains also have a thin lining of iron-oxide on the detrital quartz grain surface (Figure 51).

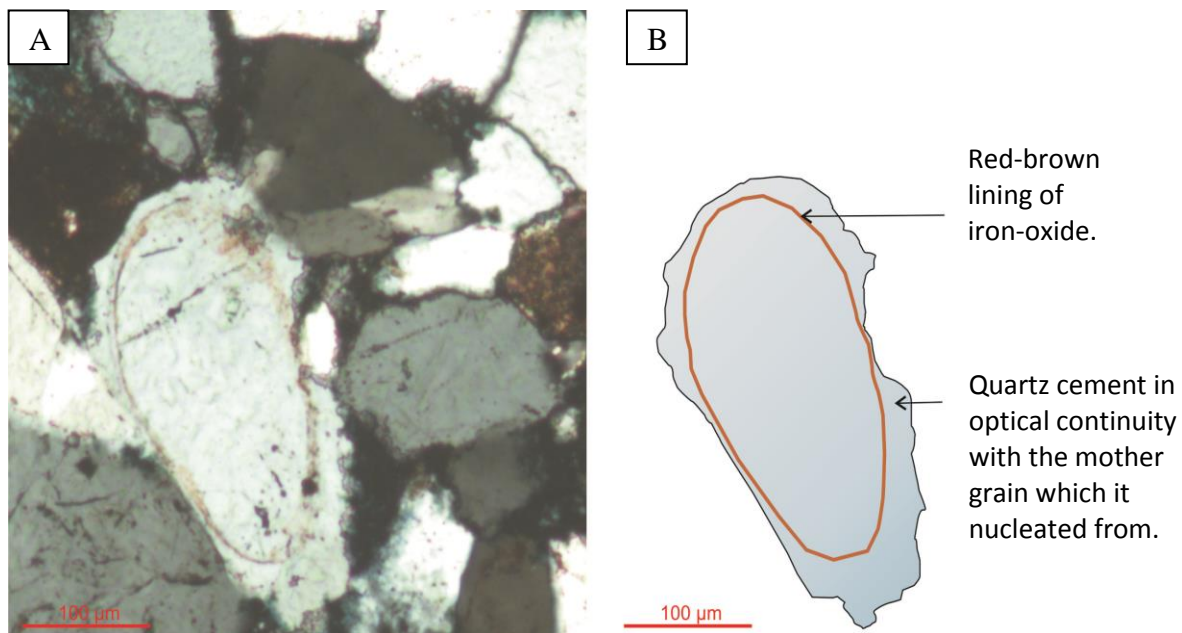


Figure 51: A) Crossed-nichols micrograph of a rounded detrital quartz grain, the surface of the grain is lined by a thin layer of iron-oxide. Note that the cement is in optical continuity with the grain it nucleated from. **B)** Illustration of A with the iron-oxide lining drawn in orange. Thin sectino #15-2, Todalen Member.

Carbonate cement occupy the pore space and is recognized by its high order yellow to pink interference colors. EDS analysis disclosed the composition to be calcite with a small ferroan component (Figure 52). The volumetric content of the calcite cement is slightly decreasing upwards from 0.3% to 0.7% in the Todalen Member section.

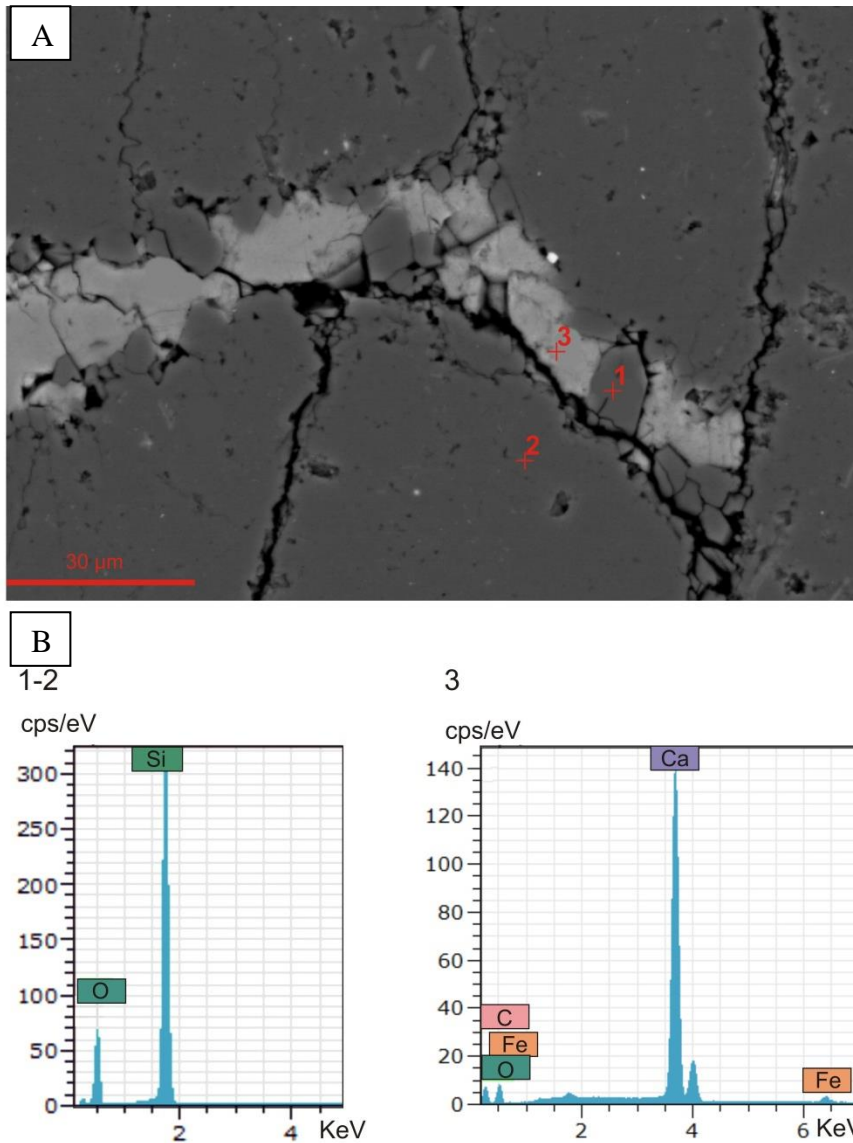


Figure 52: A) Reflected light micrograph, note the euhedral quartz cement crystal (1) enveloped by calcite cement (3). 2) Detrital quartz grain (dark grey color). Note the jig-saw boundaries between the two detrital quartz grains in the left corner. **B)** EDS analysis results: 1,2) quartz (SiO_2), 3) calcite with a small ferroan component (CaCO_3). Thin section #15-2, Todalen Member.

Endalen Member

The content of cement is also low in the lower Endalen Member sandstones. Quartz overgrowths accounts $\leq 0.7\%$ of the sample volume. Whereas small patches of calcite cement only accounts for trace volumes.

Porosity

Todalen Member

The overall average porosity is low, 1.7%, as the pore space is by large occupied by matrix. The maximum observed intergranular and intragranular porosity volumes are 2.3% and 1.7% respectively, whereas the matrix rich samples display close to no porosity, hence the overall low average number of 1.7%.

Endalen Member

The counted intergranular and intragranular porosity volumes both varies between 0.3% and 0.7% in the Endalen Member samples (Figure 53).

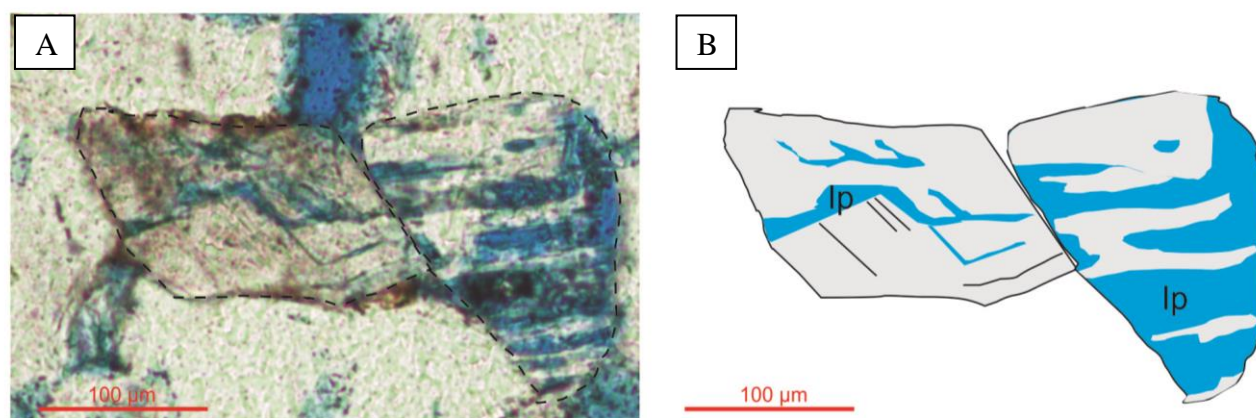


Figure 53: A) Plane light micrograph of intragranular porosity development along cleavage planes within detrital grains resembling K-feldspar. B) Illustration of a), the intragranular porosity (Ip) is colored in blue, the grain relics are colored in grey. Thin section 15-10, Endalen Member.

5.3 Petrographic Composition of the Endalen Outcrop

Modal Analysis Results

Five thin sections have been analyzed from the logged section in the Endalen Outcrop. The modal analysis results are presented in Table 4. A stratigraphic overview of the thin sections is presented in Figure 54.

Table 4a: Modal analysis (detrital grains and matrix), values in percent.

Thin Section #	Elevation a.C.Fm. (m)	Firkanten Fm. Mb.	Quartz			Chert			Feldspar		Lith. Frag >2 mm	Matrix <0.03 mm	Org. Mat.
			Monocryst. qtz	Polycryst. qtz	Sheared qtz	Microcryst. qtz	Spicular chert	Chalcedony	Plagioclase	K-Feldspar			
EN 1-2	1,00	Todalen	59,7	4,7	-	0,3	-	-	-	4,7	1,3	6,0	2,0
EN 1-3	9,70	Todalen	63,3	6,3	-	3,0	-	trace	0,3	3,7	1,0	3,3	2,7
EN 1-5	22,90	Todalen	72,3	3,7	0,3	2,3	-	-	-	4,7	0,3	0,3	0,3
EN 1-6	31,70	Todalen	76,0	0,7	-	2,7	-	trace	0,7	3,3	0,7	0,4	trace
EN 1-7	43,05	Endalen	68,7	4,3	-	3,7	-	3,0	1,3	5,0	0,3	1,2	0,3

Table 4b: Modal analysis (diagenetic minerals, porosity and assecory minerals), values in percent.

Thin Section #	Elevation a.C.Fm. (m)	Firkanten Fm. Mb.	Cement		Porosity		Assecory Minerals				
			Carbonate	Quartz	Inter-granular	Intra-granular	Muscovite	Glauconite grains	Glauconite porefilling	Pyrite	Heavy minerals
EN 1-2	1,00	Todalen	7,3	3,7	2,0	5,7	trace	0,3	2,3	trace	trace
EN 1-3	9,70	Todalen	2,3	3,0	0,3	2,3	0,5	4,8	3,3	-	trace
EN 1-5	22,90	Todalen	1,0	7,3	0,7	4,0	-	0,3	2,3	-	0,3
EN 1-6	31,70	Todalen	0,7	3,5	4,7	5,3	0,3	-	0,3	trace	0,7
EN 1-7	43,05	Endalen	0,7	2,3	0,3	8,3	trace	-	0,3	-	0,3

Table 4c: Textural parameters. See Appendix 3.2 for abbreviations.

Thin Section #	Elevation a.C.Fm. (m)	Firkanten Fm. Mb.	Wentworth size class	Sorting	Rounding	Lithology
EN 1-2	1,00	Todalen	Very fine sand	Moderately well	Subangular	Sandstone
EN 1-3	9,70	Todalen	Very fine sand	Moderately well	Subangular	Sandstone
EN 1-5	22,90	Todalen	Fine sand	Well	Subrounded	Sandstone
EN 1-6	31,70	Todalen	Fine sand	Well	Subangular	Sandstone
EN 1-7	43,05	Endalen	Fine sand	Well	Subangular	Sandstone

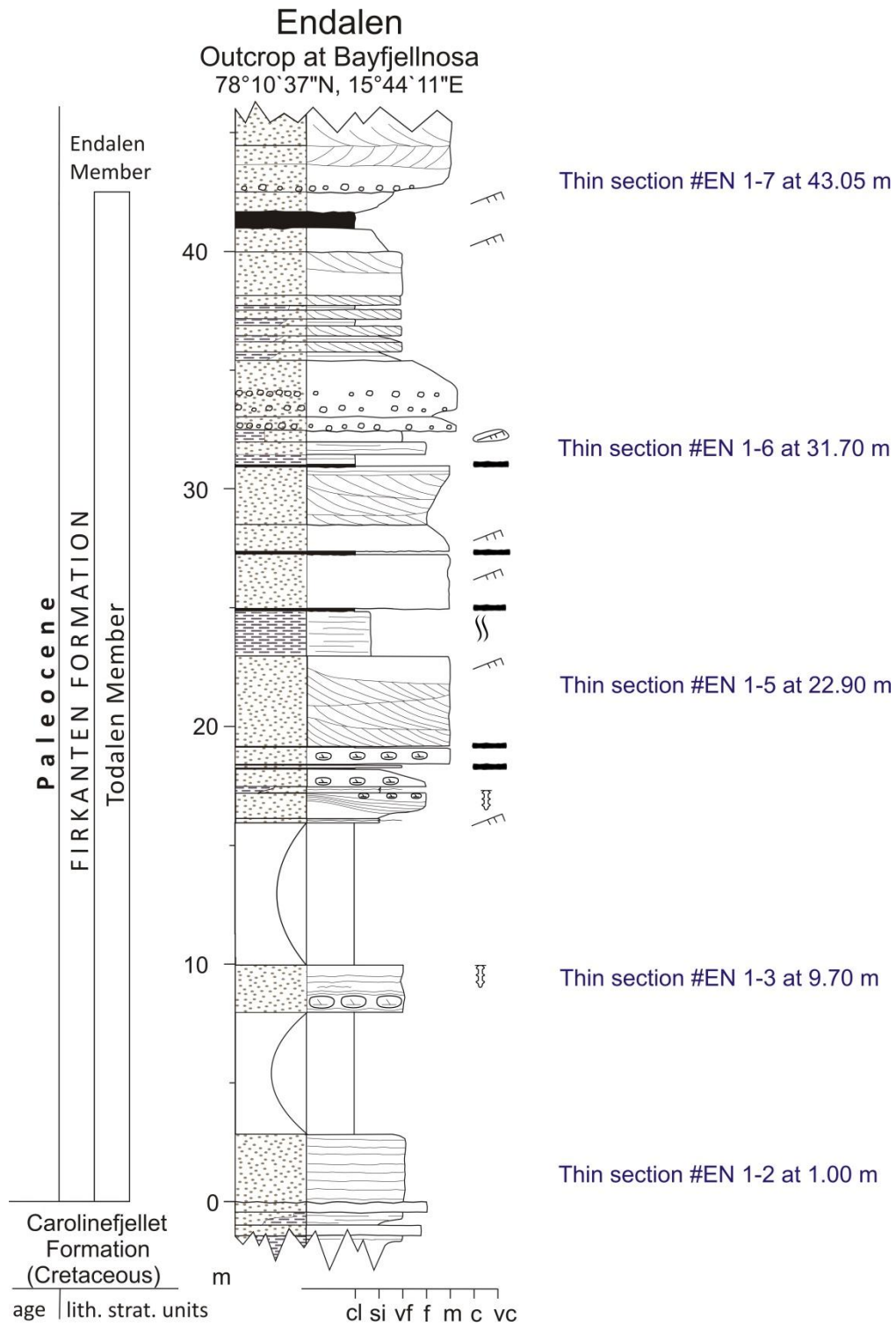


Figure 54 Stratigraphic overview of the modal analyzed thin sections from the Endalen outcrop. For legend, see Appendix 2.1.

Lithology and Texture

Todalen Member

The two lowermost point counted thin sections are predominantly very fine grained and moderately well sorted. Samples from above this are well sorted and of fine grain size (Figure 55).

The matrix content varies between 6% and 0.3%. The grains are typically subangular to subrounded.

Endalen Member

The Endalen Member sample consists of a fine grained and well sorted sandstone with an organic content of 0.3% (Figure 56).

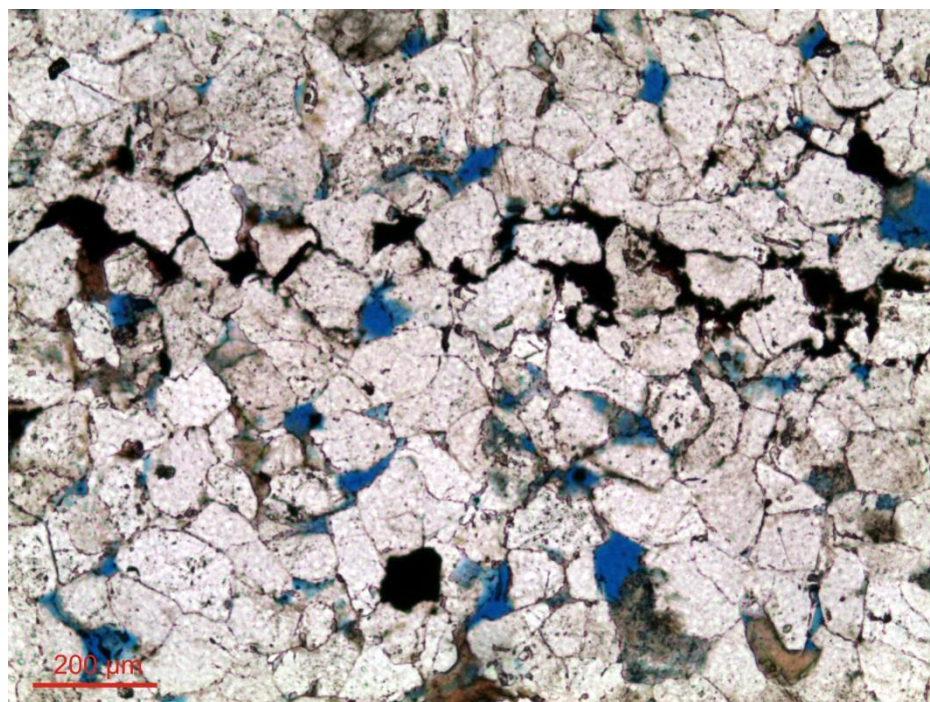


Figure 55: Well sorted fine grained sandstone representing the lithology of the upper part of the Todalen Member. Plane light micrograph of thin section EN 1-5, Todalen Member.

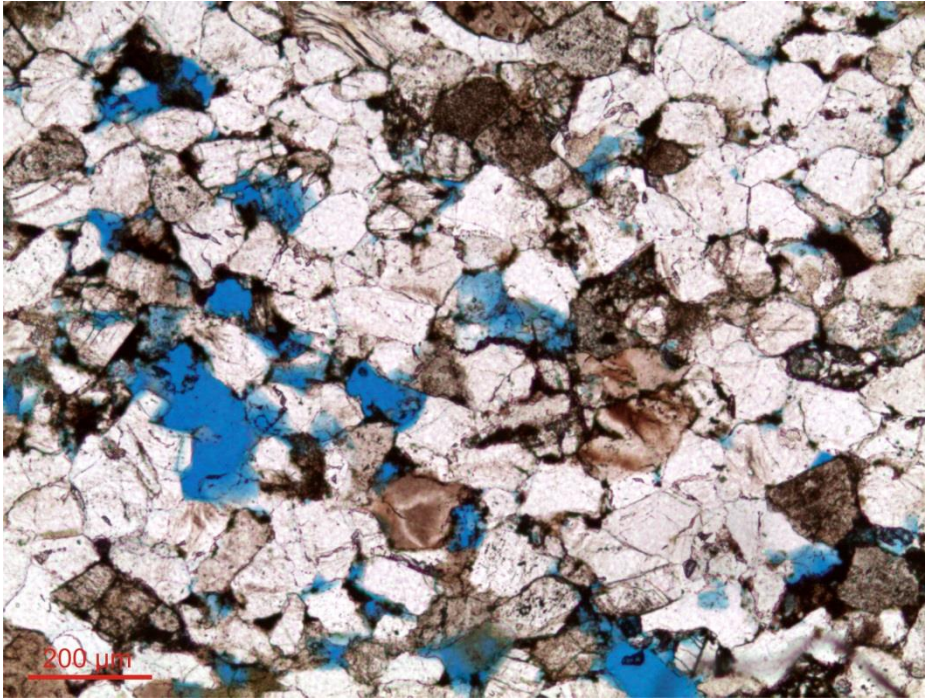


Figure 56: Well sorted fine-grained sandstone with a low content of organic material. Endalen Member. Plane light micrograph of thin section EN 1-7, Endalen Member.

Detrital Grains

Todalen Member

Quartz is the most common detrital grain which on average, accounts for 71.7% of the sample volume. The majority of the monocrystalline quartz display uniform extinction. The average content of polycrystalline quartz is 3.9%. Only a few sheared quartz grains are observed in the uppermost Todalen Member thin section.

Detrital chert is present in very small volumes, on average 2.1%. Most of the chert is in the form of microcrystalline quartz. Spicular chert is completely absent while chalcedony is only observed in trace amounts in some of the thin sections.

K-feldspar, predominantly in the form of orthoclase, is present in volumes between 3.3% and 4.7%. Plagioclase with albite twinning is present in some of the thin sections, but the volumetric content never exceeds 0.7% (Figure 57).

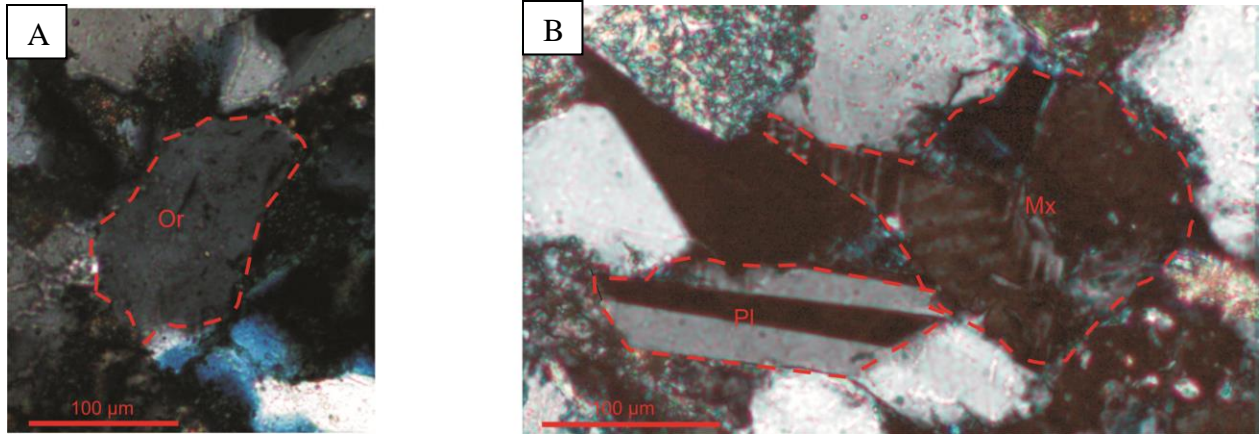


Figure 57: Crossed-nichols micrograph of thin section EN 1-2, Todalen Member. **A)** Outlined detrital orthoclase (Or) grain with similar low order interference color as quartz. **B)** Outlined plagioclase (Pl) with albite twinning and K-feldspar with microcline twinning (Mx), note the internal cross-hatch pattern of the twinning.

The occurrence of lithic fragments varies between 0.3% and 1.7%, the lithic fragments are all monocrystalline quartz with uniform extinction. The amount of muscovite is scarce (Figure 58). The content of organic material decreases upwards in the section from 3.3% to 0.3%.

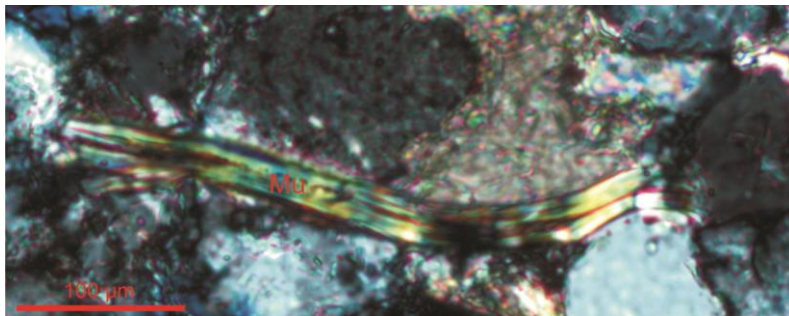


Figure 58: Mechanically deformed flaky muscovite (Mu). Crossed-nichols micrograph of thin section EN 1-2, Todalen Member.

Heavy minerals (Figure 59) are seen in amounts up to 0.7% and include tourmaline, epidote, zircon, opaques, microscopic siderite clusters and garnet. Pyrite, chrome spinel and apatite are only seen in trace amounts in some of the samples.

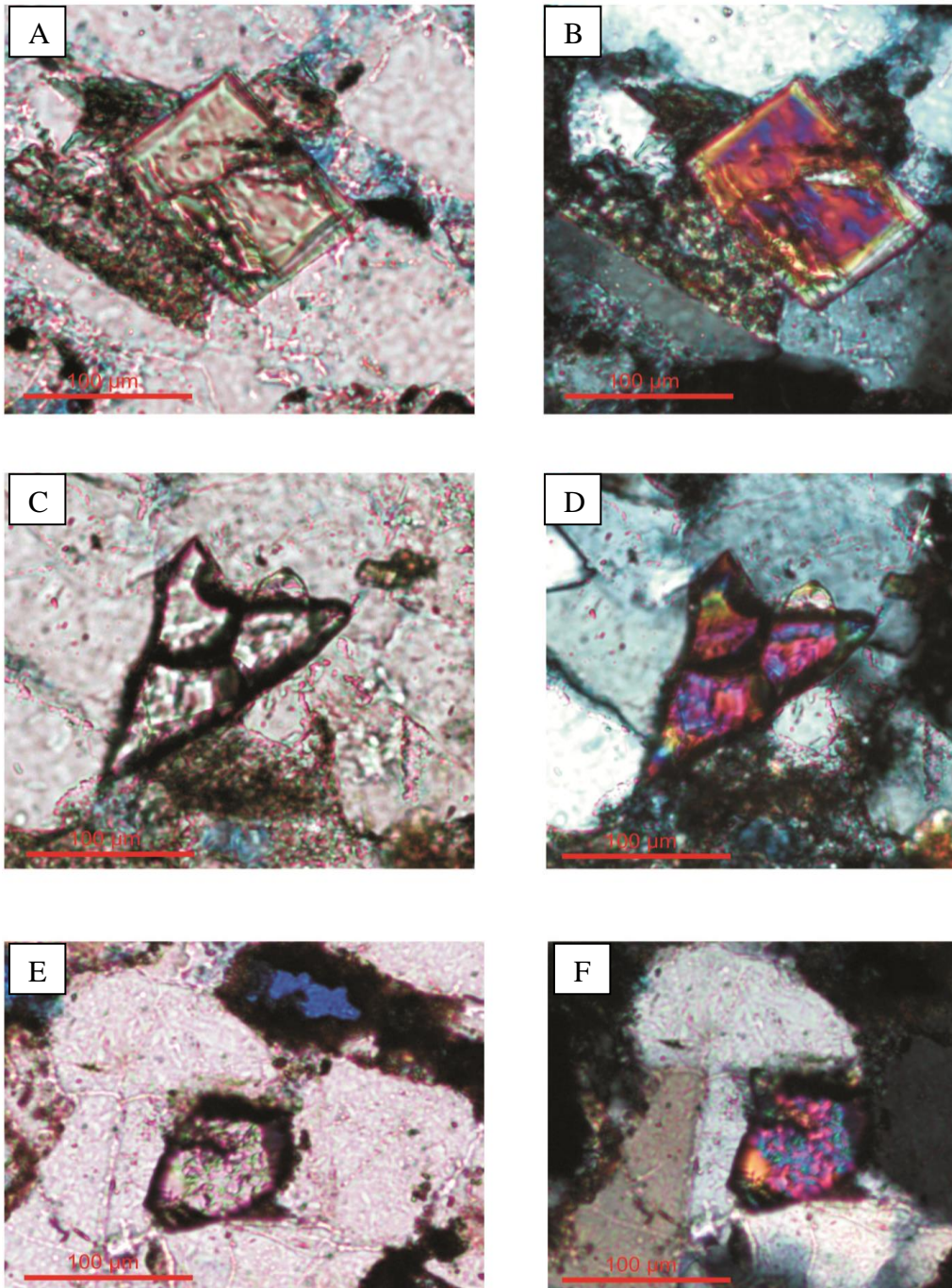


Figure 59: Heavy minerals. **A)** Euhedral epidote crystal with yellowish green pleochroism in plane light. **B)** Crossed-nichols micrograph of a), note the high order interference colors. **C)** Euhedral zircon crystals in plane light. **D)** Same as c) under crossed-nichols. **E)** A more anhedral zircon crystal in plane light. **F)** Same as e) under crossed-nichols. Micrographs of thin section EN 1-2, Todalen Member.

Endalen Member

Monocrystalline quartz with uniform extinction is abundant and accounts for 68.7% of the sample volume while polycrystalline quartz only accounts for 4.3%. No sheared quartz is detected.

Chert is seen in small amounts, mostly as microcrystalline quartz. Chalcedony (0.3%) is also present. Spicular chert grains are completely absent.

Feldspars account for 6.3% of the sample volume; 5% K-feldspar (mostly orthoclase, but also some with microcline twinning) and 1.3% plagioclase with albite twinning. The K-feldspar content is similar to the Todalen Member thin sections while the content of plagioclase is somewhat larger. Only a few lithic fragments are observed. The amount of muscovite is sparse. Detrital glauconite grains are not present. The variety of heavy minerals is low as only zircon and garnet are observed.

Diagenetic Minerals

Todalen Member

Optical continuous irregular quartz overgrowths on detrital quartz grains are present in the majority of the thin sections. The overgrowth cement display one or more planar faces. Anhedral quartz cement patches are also observed. The quartz cement accounts on average for 4.4% of the sample volume (Figure 60).

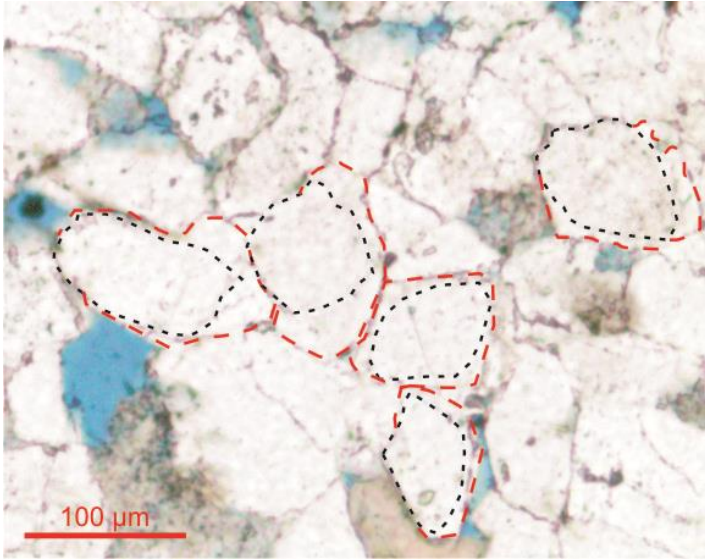


Figure 60: Quartz cement overgrowth (red dotted lines) on detrital grains (black dotted lines). Note the irregular overgrowth development on most of the outlined grains as well as the in part planar faced appearance of the cement. Plane light micrograph of thin section EN 1-5, Todalen Member.

The amount of ferroan dolomite/ ankerite cement is decreasing upwards in the Todalen Member section from 7.3% to 0.3% (Figure 61).

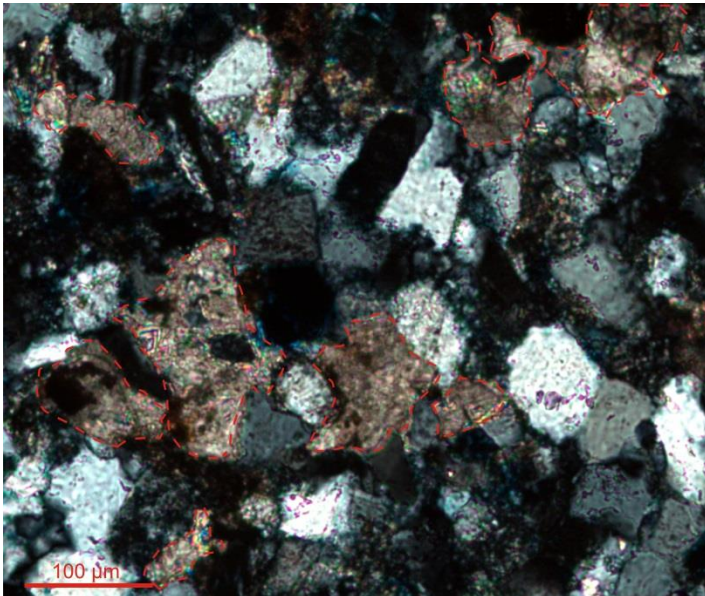


Figure 61: Patchy ferroan dolomite/ ankerite cement in the lowermost Todalen Member thin section. Crossed-nichols micrograph of thin section EN 1-2, Todalen Member.

The abundance of small scattered clusters of siderite is increasing upwards in the Todalen Member section (Figure 5.3.11).

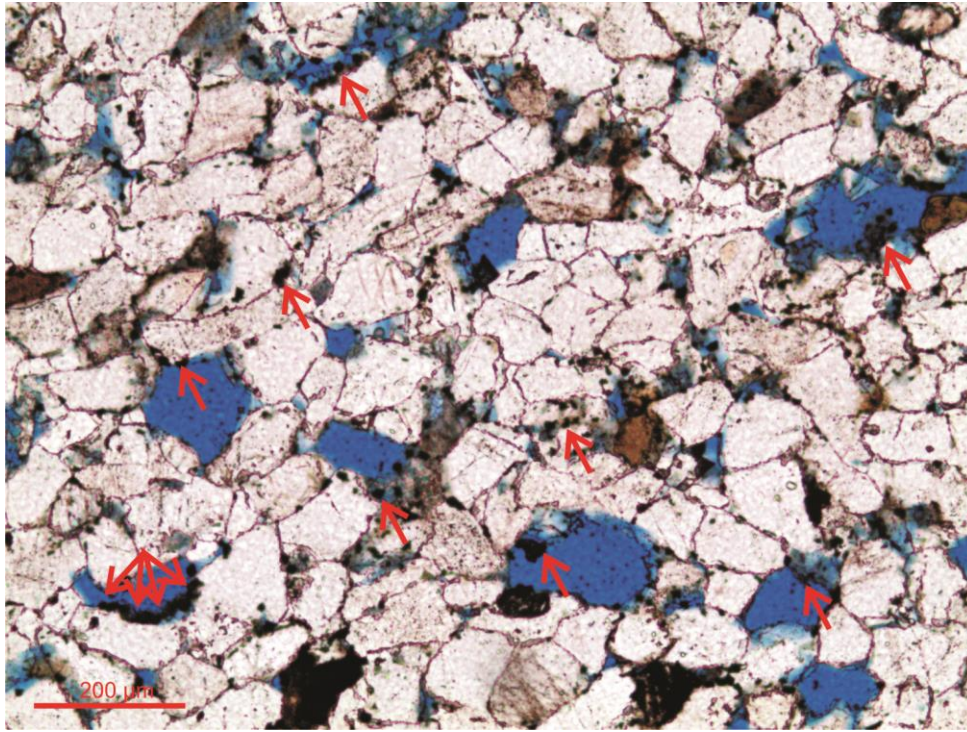


Figure 62: Dark brown scattered clusters of siderite. Red arrows points on a few examples. Plane light micrograph of thin section EN 1-6, Todalen Member.

Porefilling glauconite cement is present in volumes between 0.3%-3.3%. It is recognized by its brownish green color. From time to time, the porefilling glauconite appears to be more brown in color than green (Figure 63). It may however still be recognized as glauconite by the internal mottled texture under crossed-nichols.

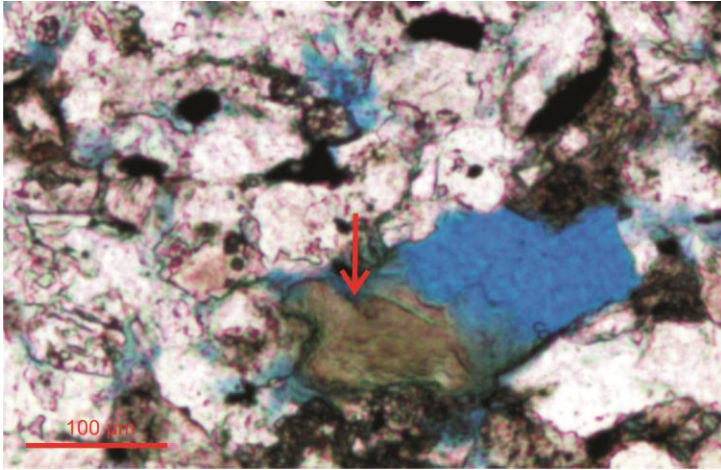


Figure 63: Brownish green porefilling glauconite. Note the secondary porosity void to the right postdating the glauconite formation. Plane light micrograph of thin section EN 1-2

Endalen Member

Quartz and ferroan dolomite/ ankerite cement is present in small volumes, 2.3% and 0.7% respectively. Feldspars are heavily altered, in parts dissolved, but not sericitized. Porefilling glauconite is close to rare, 0.3%, while pyrite is completely absent.

Porosity

Todalen Member

The average porosity is 6.2%. Secondary porosity accounts for the majority of this volume. The secondary porosity is seen as macro-pores formed by dissolution of assemblages consisting of what resembles feldspars and perhaps also clay.

Intergranular porosity voids are typically very small in size and bear sign of mechanical deformation.

Endalen Member

The total porosity is 8.6%. Secondary porosity accounts close to all of this. These porosity voids are markedly larger in size than those encountered in the Todalen Member and appears to have

been induced by complete/ partial dissolution of assemblages of clay, detrital grains and porefilling glauconite (Figure 64)

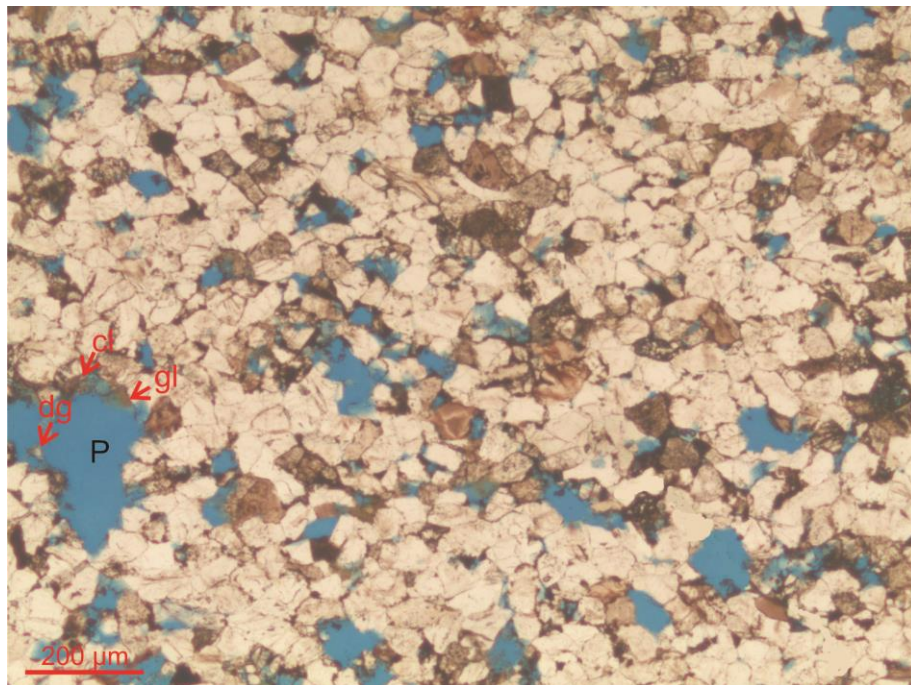


Figure 64: Relatively large intergranular porosity (e.g. “P”) volumes due to dissolution of assemblages consisting of authigenic glauconite cement (gl), clay (cl) and detrital grains (dg). The porosity is stained by blue epoxy. Plane light micrograph of thin section EN 1-7, Endalen Member.

5.4 Petrographic Composition of the Grumantbyen Outcrop

Modal Analysis Results

Seven thin sections have been analyzed from the logged Grumantbyen Outcrop. The results of the modal analysis is presented in Table 5a-c. A stratigraphic overview of the thin sections are presented in Figure 65.

Table 5a: Modal analysis (detrital grains and matrix), values are in percent.

Thin Section #	Elevation a.C.Fm. (m)	Firkanten Fm. Mb.	Quartz			Chert			Feldspar		Lith. Frag >2 mm	Matrix <0.03 mm	Org. Mat.
			Monocryst. qtz	Polycryst. qtz	Sheared qtz	Microcryst. qtz	Spicular chert	Chalcedony	Plagioclase	K-Feldspar			
GR 1-2	1,80	Todalen	38,7	15,7	4,3	8,3	11,3	2,0	3,3	-	1,7	0,7	0,4
GR 1-3	2,87	Todalen	36,3	17,3	2,7	14,3	8,7	2,7	0,3	1,3	1,0	3,7	0,5
GR 1-4	16,67	Todalen	49,7	8,7	3,3	5,3	2,7	0,7	0,7	3,7	0,7	8,0	2,8
GR 1-7	23,13	Todalen	63,3	12,3	0,3	4,0	1,3	0,3	0,3	3,0	0,3	4,3	0,7
GR 1-9A	27,87	Endalen	19,0	4,7	-	0,7	-	-	1,3	0,7	52,7	2,3	2,3
GR 1-9	28,45	Endalen	56,7	19,7	-	0,7	0,3	-	1,7	0,3	0,3	3,3	1,7
GR 1-10	32,42	Endalen	62,0	20,3	-	1,3	-	-	1,0	2,7	2,0	2,7	0,4

Table 5b: Modal analysis (diagenetic minerals, porosity and assecory minerals), values are in percent.

Thin Section #	Elevation a.C.Fm. (m)	Firkanten Fm. Mb.	Cement		Porosity		Assecory Minerals				
			Carbonate	Quartz	Inter-granular	Intra-granular	Muscovite	Glauconite grains	Glauconite porefilling	Pyrite	Heavy minerals
GR 1-2	1,80	Todalen	10,7	1,3	-	0,3	0,7	0,3	0,3	-	trace
GR 1-3	2,87	Todalen	3,3	5,7	-	0,3	1,3	0,3	-	trace	0,3
GR 1-4	16,67	Todalen	2,7	3,3	1,7	2,3	1,7	-	1,3	0,7	trace
GR 1-7	23,13	Todalen	trace	3,3	1,3	3,7	1,3	trace	-	0,3	trace
GR 1-9A	27,87	Endalen	4,7	3,7	0,3	1,3	0,3	0,3	3,0	2,7	trace
GR 1-9	28,45	Endalen	2,3	3,0	0,7	1,7	1,0	1,7	2,3	2,3	0,3
GR 1-10	32,42	Endalen	1,3	0,3	0,7	2,7	trace	0,3	1,7	0,3	0,3

Table 5c: Textural parameters. For abbreviations, see Appendix 3.2.

Thin Section #	Elevation a.C.Fm. (m)	Firkanten Fm. Mb.	Wentworth size class	Sorting	Rounding	Lithology
GR 1-2	1,80	Todalen	Medium sand	Moderately well	Angular to subrounded	Sandstone
GR 1-3	2,87	Todalen	Medium sand	Moderately well	Angular to subrounded	Sandstone
GR 1-4	16,67	Todalen	Very fine sand	Well	Subangular	Sandstone
GR 1-7	23,13	Todalen	Fine sand	Well	Subangular	Sandstone
GR 1-9A	27,87	Endalen	Granules, pebbles & cobbles	Poor	Rounded & subrounded	Conglomerate
GR 1-9	28,45	Endalen	Fine sand	Moderately well	Subangular	Sandstone
GR 1-10	32,42	Endalen	Fine to coarse sand	Poor	Subangular	Sandstone

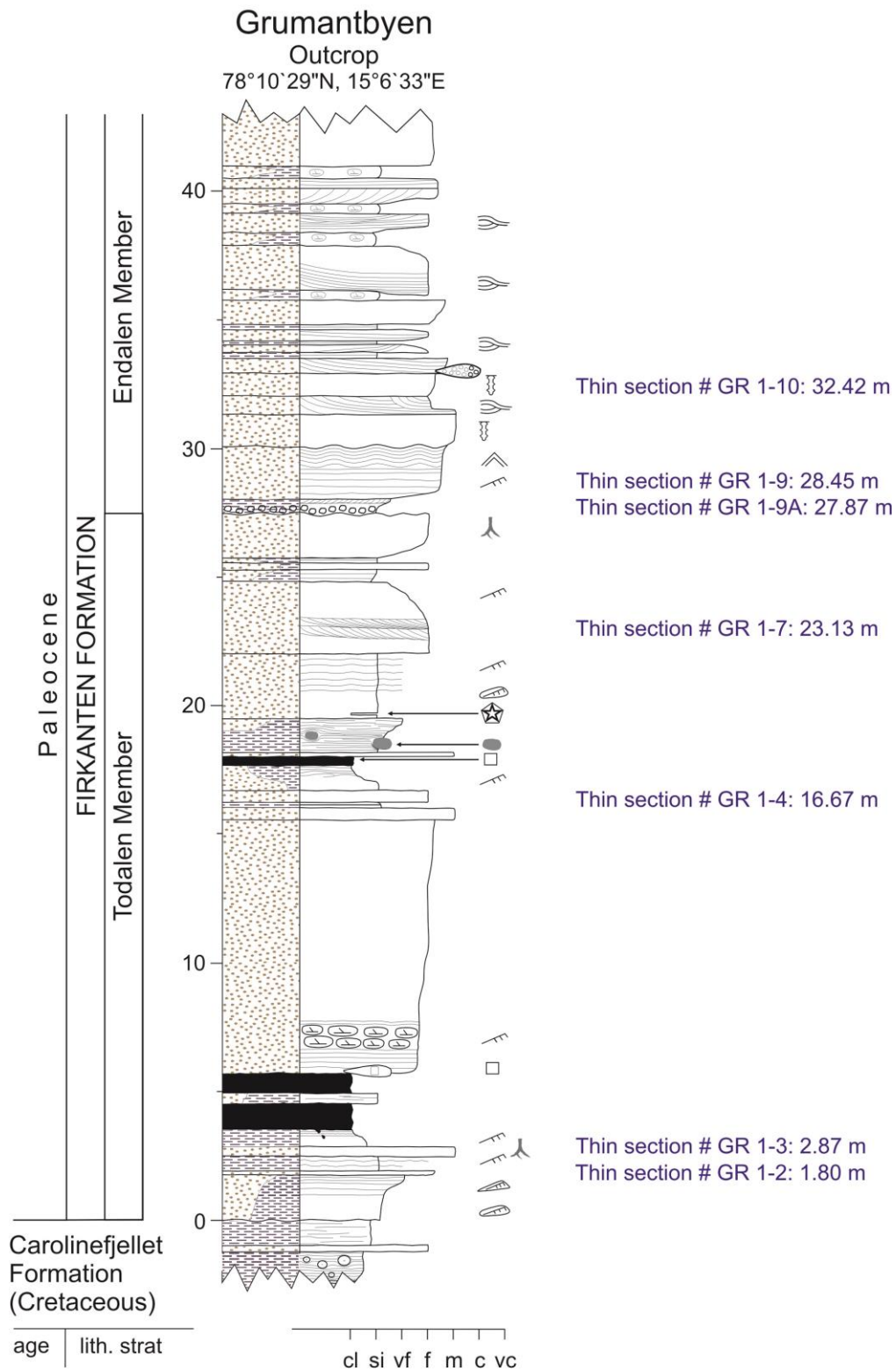


Figure 65: Stratigraphic overview of the modal analyzed thin sections from the Grumantbyen Outcrop. For legend, see Appendix 2.1.

Lithology and Texture

Todalen Member

The lower part of the Todalen Member (thin section GR 1-2 and GR 1-3) consists of predominantly medium-grained, moderately well sorted sandstones with a mixture of angular to subrounded grains (Figure 66). The upper part of the Todalen Member (thin section GR 1-4 and GR 1-7) display moderately well sorted very fine and fine clay rich sandstone lithologies. The majority of the grains are subangular (Figure 67).

Endalen Member

Endalen Member thin sections consist of poorly to moderately well sorted sandstones and a conglomerate. The sandstones are fine to coarse-grained and subangular in nature. The conglomerate is matrix supported, bimodal and polymictic (Figure 68).



Figure 66: Moderately well sorted sandstone representing the lithology and texture of the lower part of the Todalen Member. Plane light micrograph of thin section GR 1-3, Todalen Member.



Figure 67: Well sorted very fine-grained clay rich sandstone representing the lithology and texture of the upper Todalen Member. Plane light micrograph of thin section GR 1-4, Todalen Member.

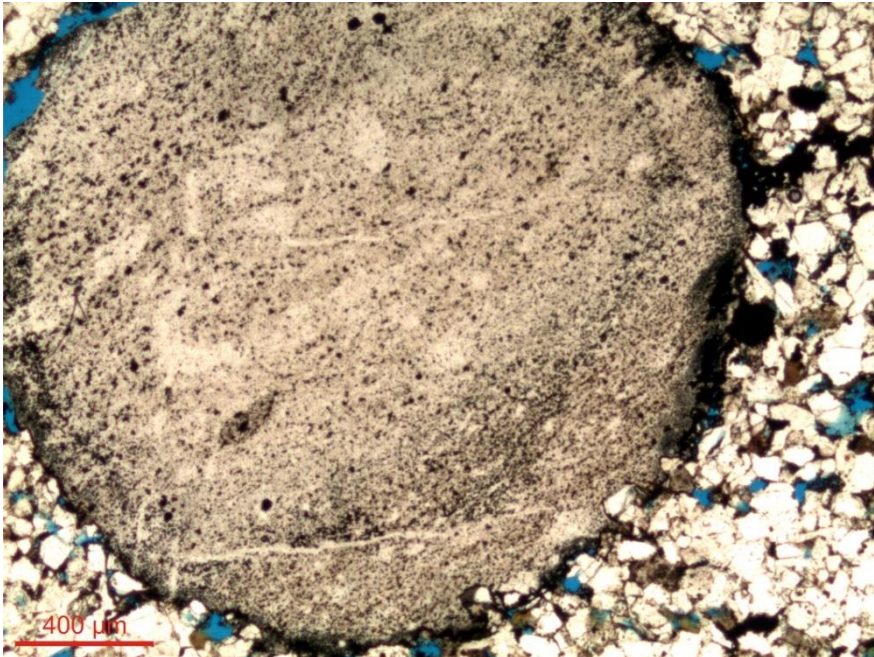


Figure 68: Well rounded matrix supported clast in the conglomerate marking the boundary between the Todalen and Endalen Members. Plane light micrograph of thin section GR 1-9A, Endalen Member.

Detrital Grains

Todalen Member

Quartz is the most abundant detrital grain in the Todalen Member sandstones. The average volumetric content of monocrystalline (MC), polycrystalline (PC) and sheared (S) quartz is 63.3%. The monocrystalline quartz grains display both undulose and uniform extinction.

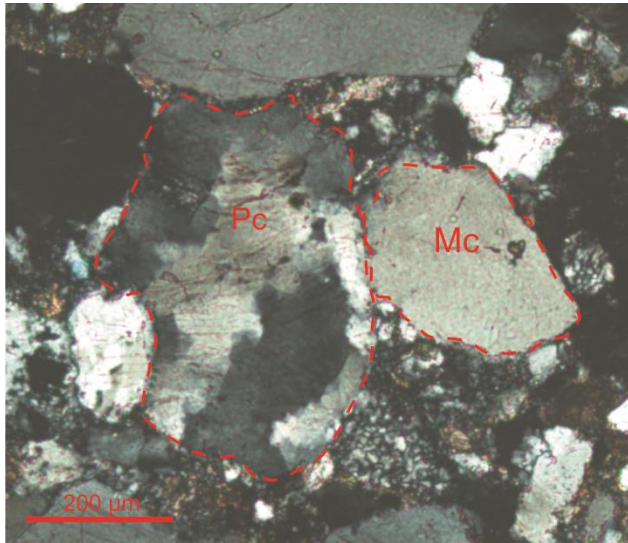


Figure 69: Polycrystalline quartz grain (PC) note the different orientations of the quartz crystals and the sutured boundaries between them. Monocrystalline quartz grain (MC) with zircon and apatite inclusions. Crossed-nichols micrograph of thin section GR 1-3, Todalen Member.

The approximate average ratio of the detrital quartz grains (MC:PC:S) in the lower part of the Todalen Member is 12:6:1.5, while it in the upper part is 12:4:0.5. The amount of both polycrystalline and sheared quartz are thus decreasing upwards in the Todalen Member.

Detrital chert is present in volumes up to 25.7 % and includes spicular chert (Figure 70a-b), chalcedony (Figure 70c-d) and microcrystalline quartz (Figure 70 e-f). Microcrystalline quartz and spicular chert makes up the majority of the chert fraction, chalcedony grains are only present in small volumes (0.3-2%). The amount of chalcedony and spicular chert is decreasing upwards in the Todalen Member. This combined with a low microcrystalline quartz content is responsible for a significantly lower than average volume of chert, ~7%, in the upper Todalen Member.

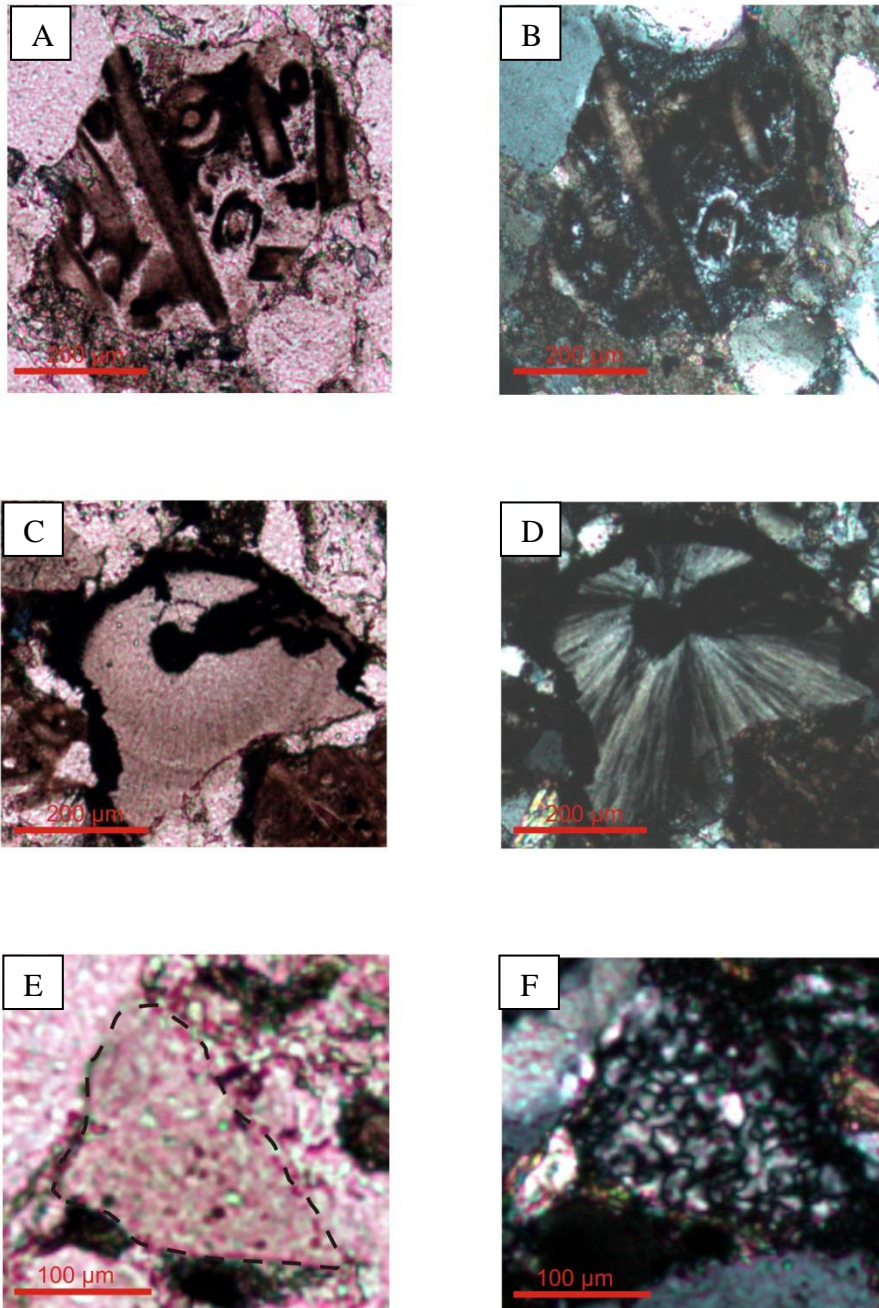


Figure 70: **A)** Spicular chert grain in plane light. **B)** Same as a) with crossed-nichols. **C)** Chalcedony in plane light. **D)** Same as c) with crossed-nichols. The chalcedony grain displays a radially rotating extinction pattern when the thin section is rotated under crossed-nichols. **E)** Microcrystalline quartz (chert) in plane light. **F)** Same as e) under crossed-nichols. Note the mottled internal texture of the grain and first order grey interference colors. A-b from thin section GR 1-2, c-f from thin section GR 1-3. Todalen Member.

Plagioclase with albite twinning and K-feldspars (microcline twinning and orthoclase) are present in volumes up to 3.3%. The content of lithic fragments is low ($\leq 1.7\%$). Muscovite is observed in small amounts (0.7-1.7%) in all thin sections. The occurrence of detrital glauconite grains is overall sparse.

The content of organic material is variable, but never exceeds 2.7%. The original framework of the organic material can be outlined in some thin sections. The heavy mineral suit is compromised by pyrite, zircon, epidote, chrome spinel, apatite, garnet and rutile. Pyrite, zircon and garnet are the most frequently encountered ones. The amount of heavy minerals is seldom exceeding 0.3%.

Endalen Member

In the Endalen Member sandstones, monocrystalline quartz accounts for 59.5% of the sample volume while polycrystalline quartz accounts for 20.0%. Sheared quartz is absent. The chert fraction is scarce; the average content of microcrystalline chert is 1.0% while spicular chert and chalcedony are rarely encountered to completely absent.

The average amount of feldspars is 2.9%, which includes plagioclase with albite twinning and orthoclase. K-feldspar with microcline twinning is observed in trace amounts.

Lithic fragments are sparse and never accounts for more than 2% of the sample volume. The amount of detrital glauconite grains is stable, on average 2%, and thus more abundant than in the Todalen Member sandstones.

The Endalen conglomerate (thin section GR 1-9A) is matrix supported, bimodal and polymictic (Figure 71). The matrix is predominantly very fine to fine grained quartz. The conglomerate clasts consist of polycrystalline quartz, microcrystalline quartz (chert), spicular chert and organic material with intact cell structures.

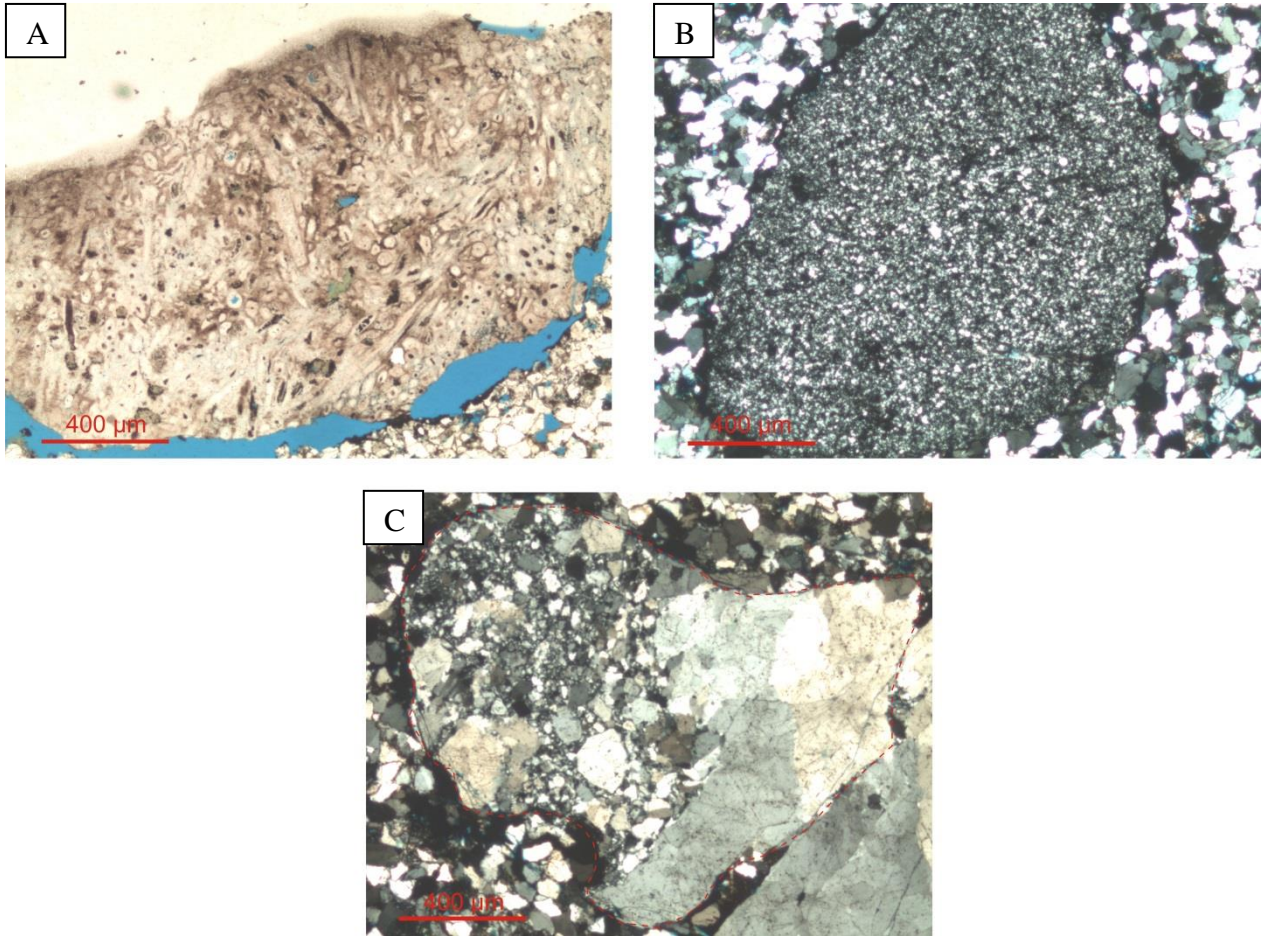


Figure 71: **A)** Plane light micrograph of a spicular chert fragment. Note the light brown color and spiculite needle texture. **B)** Crossed-nichols micrograph of microcrystalline quartz (chert) fragment made up by very small quartz crystals. **C)** Crossed-nichols micrograph of partly chertified polycrystalline quartz, note the larger sized quartz crystals on the right hand side of the fragment. A-C from thin section GR 1-9A, Endalen Member.

Diagenetic Minerals

Todalen Member

Quartz cement accounts for 1.3%-5.7% of the sample volume. The cement is predominantly seen as synthaxial overgrowth on detrital grains, but also as tiny euhedral quartz crystals (Figure 72).

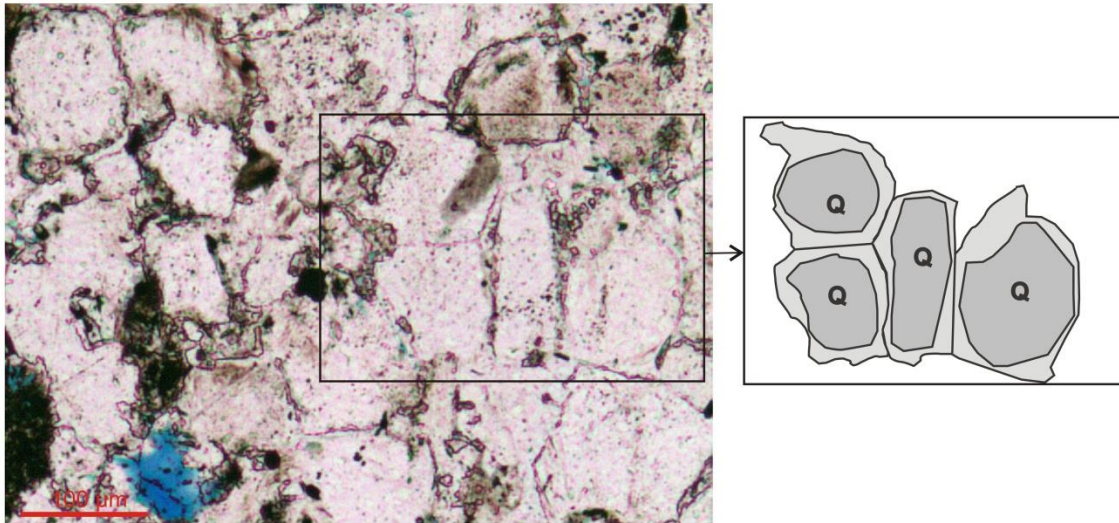


Figure 72: Synthaxial quartz cement overgrowth on detrital quartz grains, note the straight cement boundaries. Plane light micrograph of thin section GR 1-7, Todalen Member.

The most abundant carbonate cement is non-ferroan calcite cement, but patches of ferroan dolomite/ ankerite are also present. The carbonate cement is present in all samples, but is especially abundant in the lowermost sample of Todalen Member (10.7%) (Figure 73).

Porefilling glauconite is encountered in some of the thin sections.

Alterations of feldspars are common, and accounts for a significant part of the matrix fraction. Sericitization of K-feldspar, in particular K-feldspar with microcline twinning, into fine-grained mica is observed (Figure 73). Calcite replacement along microcline twinning planes is also present in some of the thin sections (Figure 74). Trace amounts of diagenetic pyrite is scattered in the matrix, and often clusters in areas of the matrix which are rich in organic material.

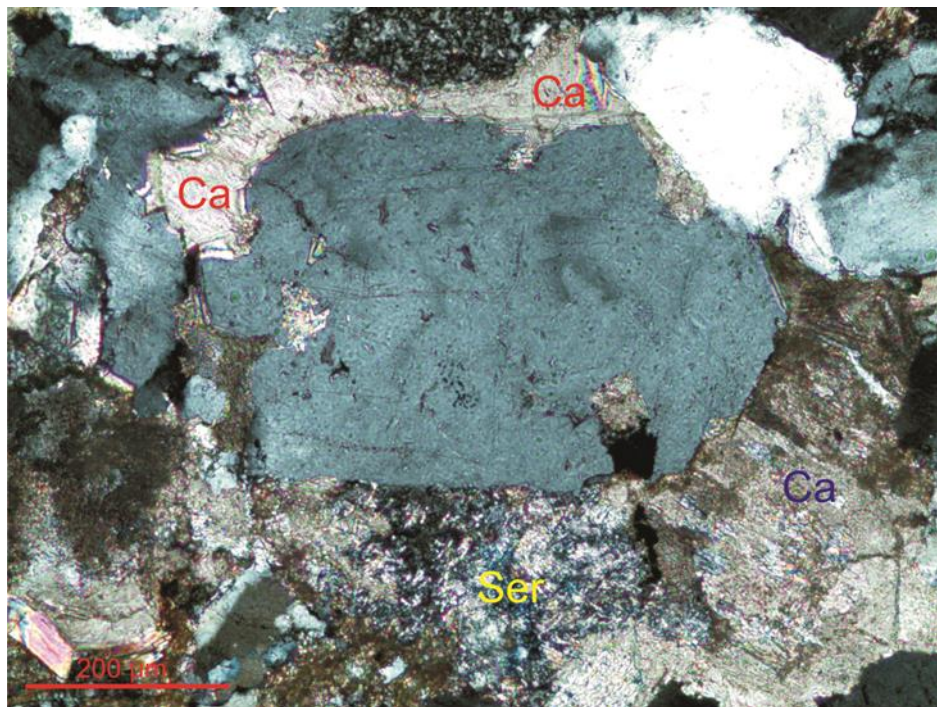


Figure 73: Carbonate cemented sandstone. Red colored “Ca” : non-ferroan calcite cement, note the high-order interference colors. “Ser”: Sericitization of K-feldspar with microcline twinning. Note that the small mica flakes are oriented parallel to the original cross-hatch pattern of the twins. Blue colored “Ca”: Calcite cement replacement of detrital plagioclase grain. Crossed-nichols micrograph of thin section GR 1-3, Todalen Member.

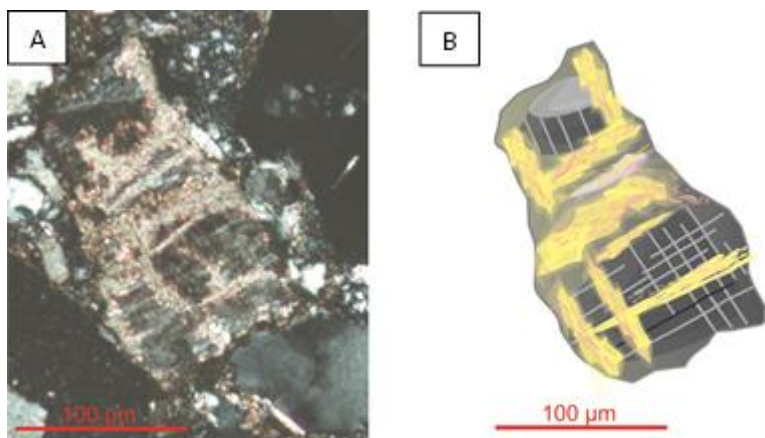


Figure 74: **A)** Micrograph under crossed-nichols of microcline K-feldspar grain with cross-hatch pattern and low order grey interference colors. Calcite replacement has taken place along the twinning planes and is recognized by the yellow to pink high order interference colors. **B)** Illustration of a, yellow colored zones mark the parallel orientation of calcite to the twinning planes (light grey and black lines).

Endalen Member

Porefilling glauconite, as well as pyrite (Figure 75), is observed in amounts up to 2.3%. Cement of quartz and ferroan-dolomite/ ankerite are the dominant in the Endalen Member thin sections, on average 2.3% quartz and 2.8 % ferroan-dolomite/ ankerite cement (Figure 76).

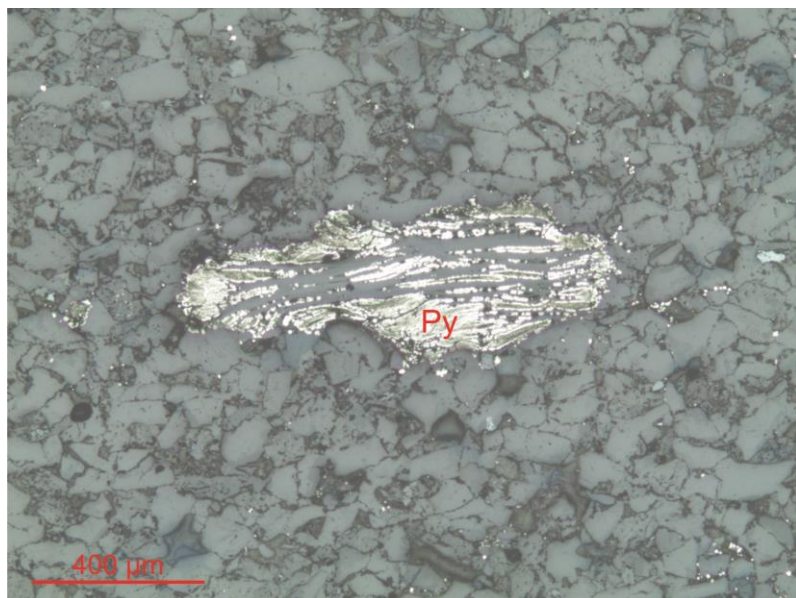


Figure 75: Reflected light micrograph of thin section GR 1-9. Massive pyritization (Py) around organic material, also note the scattered pyrite in the matrix.

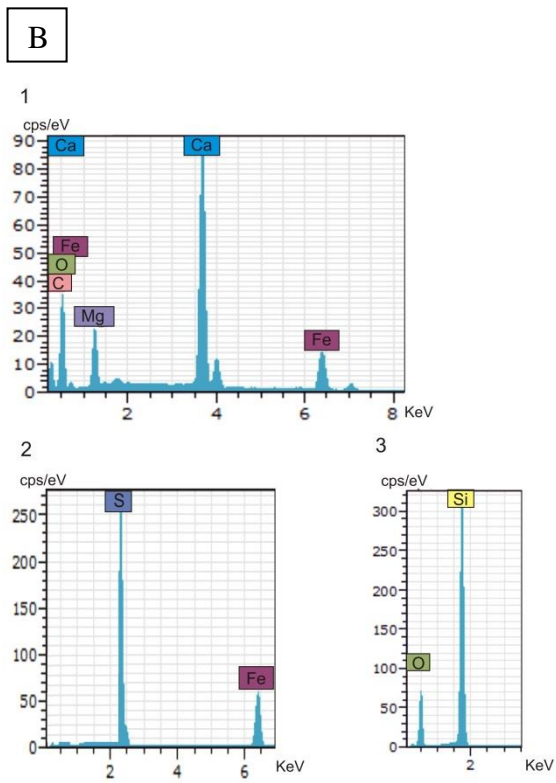
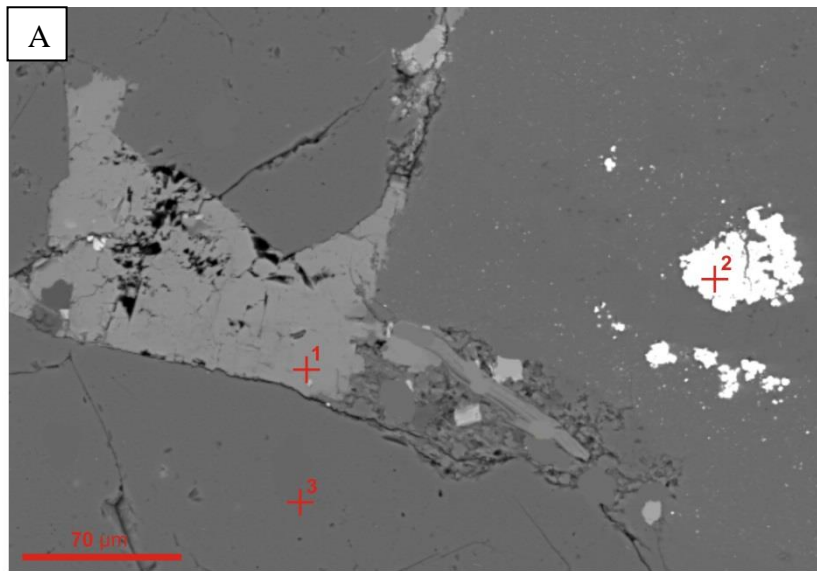


Figure 76: A) SEM backscattered electron image of thin section GR 1-9A. **B)** EDS analysis yielding the following results for the analyzed points (1-3) , 1) Ferroan-dolomite/ ankerite cement, $\text{CaMg}(\text{CO}_3)_2 / \text{Ca}(\text{Fe,Mg})(\text{CO}_3)_2$. 2) Pyrite, FeS_2 (very bright patches). 3) Quartz, SiO_2 (dark grey).

Porosity

Todalen Member

The total average porosity of the Todalen samples is low (2.4%). A majority of this porosity is secondary and due to partial/ total dissolution of detrital grains like feldspars and clay.

Endalen Member

The porosity in the Endalen Member resembles the Todalen Member in both type and amount. On average, the total porosity is 2.9%, the majority of this volume is due to dissolution of feldspars.

6. Discussion

6.1 Sedimentology of Todalen Member and the Endalen Boundary Beds

Introduction

The interpreted facies and facies associations in Chapter 4 are subjected to further discussion in this chapter which aims to propose the nature of the depositional environment.

The sedimentological observations from the investigated locations (Figure 7, localities 1, 4, 5 and 7) are discussed individually from the base up with the appendix logs 2.3-2.6 as a reference point. The discussed localities will then be placed in an overall context from which the depositional environment will be concluded.

Core 18-2009

See Appendix 2.3 for log referrals in the text.

A sharp boundary separates the base of the Todalen Member from the Carolinefjellet Formation. The boundary to the Carolinefjellet Formation was identified by the observation of *Zoophycos* burrows in the top of the silty unit below the sharp boundary beneath the lowermost coal seam. *Zoophycos*-type burrows are present in Carolinefjellet Formation, but not in the Todalen Member (M. Jochmann, pers. comm., 2011).

Above the boundary and up to the 30 m mark in the log, follows three stacked fining-upwards units consisting of intertidal- and supratidal flat deposits (FA 4) and mire deposits (FA 3). The intertidal- and supratidal flat deposits are interpreted from bidirectional ripples, unidirectional ripples with mud drapes on the ripple crests, combined with an overall increase in the proportion of clay to sand upward, pointing towards a tidally influenced environment (Reading and Collinson 2006a; Longhitano et al. 2012). The mire deposits were established from the presence of coal seams (Thomas 2002).

The thicknesses of the stacked fining-upwards units (FA 4-FA 3) are increasing upwards in the logged section, from 4.5 m to 14.5 m. This upwards increasing thickness trend and repeating

sedimentation pattern of the two facies associations suggests a cyclicity in the depositional environment which was interconnected with relative sea-level changes, the available accommodation space and humid conditions for mires to form. Furthermore, the upwards increase in thickness may perhaps be extended into a suggestion of the subsidence pace starting to accelerate already during the start of the deposition the Todalen Member, and not during the deposition of the Grumantbyen Formation close to the Paleocene-Eocene boundary, as proposed by Bruhn and Steel (2003). However, more cores would have to be investigated to validate such a suggestion.

Distributary channels features of (FA 1) are separated from the uppermost fining-upwards unit by a bed of intertidal- and supratidal flat deposits (FA 4), which implies that distributary channel deposits perhaps protuberated a fourth deposition cycle of a FA 4-FA 3 unit (see 30 m-40 m in the log) as two coal seams are situated further above. The inferred distributary channel deposits both contains conglomerate bases, whereof the lowermost conglomerate display a gradual upwards shift into a sandstone with bidirectional ripples and mud drapes (Figure 25), which suggests that the distributary channel was under tidal influence (Reading and Collinson 2006a). The conglomerate above, located slightly below the 35 m mark in the log, grades upwards into a rippled sandstone with in-situ rootlets, thus confirming a close affiliation to a subaerial environment.

Next in the log follows the two uppermost coal seams which are, like all the Todalen Member coal seams, indicative of a peat forming mire were the organic material was preserved either by anoxic conditions in the mire itself, or by rapid burial (McCabe and Parrish 1992; Thomas 2002). The coal seams are both under- and overlain by planar laminated mudrocks which have been interpreted to represents the muddy supratidal part of the intertidal- and supratidal flat facies association (FA 4) due to the rhythmic slit laminae in the mudrock (Longhitano et al. 2012) as well as the immediate proximity to the coal seam. The mudrock between the two coal seams is also assigned to the intertidal- and supratidal flat facies association, but do in addition mark a flooding of the mire (Thomas 2002). Two thick split coal seams are also present on a similar stratigraphic level in Core 15-2009, and the correlation potential between these will be discussed later.

A thick cross-bedded sandstone unit is present above this (see 45 m mark in the log). It is however hard to distinguish the nature of cross-beds in a core, but the gradational boundary to the mudrock below advocate that it represents a sandy sub-environment which forms adjacent to supratidal flats (Walther`s law), and thus a perhaps a distributary channel bar of some sorts.

The boundary between the Todalen Member and Endalen Member is located at the first conglomerate above the cross-bedded sandstone unit. The clasts of this conglomerate, and the conglomerate situated 1 meter above, are larger than those of the Todalen Member, which indicates higher flow velocities. These observations alone are however insufficient to suggest any change in the depositional environment across the Todalen Member-Endalen Member boundary since they might as well be from another event of distributary channels on the tidally influenced delta plain.

Core 15-2010

See Appendix 2.4 for log referrals in the text.

A basal conglomerate marks the boundary between Todalen Member and the Carolinefjellet Formation. It consists of a 0.3 meter thick conglomerate which translates upwards into a mud rich sandstone. The well-rounded shape of the conglomerate pebbles strongly suggests a high energy subaqueous environment (Nichols 2009). Even though this conglomerate has been inferred to represent a distributary channel deposit (FA 1) due to its rounded pebbles and upwards translation into a mud rich sandstone, a more possible suggestion is that the basal conglomerate in Todalen represents the Grønfjorden Bed, and thus of a braided river origin (Bruhn and Steel 2003; Nagy 2005).

Situated above this are two thin coal seams (mire deposits of FA 3), which are separated by a laminated mudrock indicating flooding of the mire (Thomas 2002). It is possible that the rippled sandstone with increasing bioturbation above (with its base at 5 m mark in the log) represent a delta lobe which was reworked by marine processes inferred from the presence of asymmetrical ripples and bioturbation.

Three stacked, and to an extent fining-upwards units of intertidal- and supratidal flat deposits (FA 4) and mire deposits (FA 3) are situated above this possible delta lobe unit (from the 7.5 m to 47 m in the log). These stacked units are similar to the FA 4-FA 3 units described in Core 18-2009, apart from the mud rich sandstone of FA 4, which in this core only is seen to comprise asymmetric ripples with mud drapes on the ripple crests and foresets, instead of bidirectional ripples which are seen in Core 18-2009. Nevertheless, asymmetric ripples with mud drapes points towards a tidally influenced environment, though with one direction of flow stronger than the other. The overall clay to very fine grain size of these stacked units, and the absence of conglomerates and *in-situ* rootlets, implies that the overall tidally influenced depositional setting of this core alone is not clearly a delta plain environment (Bhattacharya 2006). However, due to the correlative coal seams between this core and Core 18-2009 which contains several inferred delta plain indicators like distributary channel features and *in-situ* roots, it is interpreted as a delta plain. A correlation of these two cores will be handled in detail in the comparison subchapter. The absence of distributary channel in this core, in spite of it being a delta plain, is not surprising as several different subenvironments may operate on different part a delta plain.

The uppermost FA 4 unit of these (with its base above the 29 m mark in the log) terminates into three split coal seams separated by two centimeter thick mudrocks, thus implying two periods of flooding of the same mire.

The boundary between Todalen Member and Endalen Member is at the base of the first whiteish colored sandstone above the last coal seam, which is considered to be an identification criteria in the absence of a conglomerate here (Dallmann et al. 1999). This unit has been regarded as a distributary channel feature, although the medium grain size, cross-beds and degree of bioturbation above the cross-beds also may imply a shift to a delta front (shoreface) environment (Collinson 2006). Yet again, the nature of the Endalen Member remains unclear from the cores alone as the nature of cross-beds hardly can be established.

The Endalen Outcrop

See Appendix 2.5 for log referrals in the text.

The lowermost exposed unit in the Endalen outcrop consist of a whiteish, planar bedded sandstone of very fine grain size. It is separated from the overlying unit by a scree covered section measuring 5 meters, and is therefore of little use alone from a depositional environment perspective. However, this unit is very useful in establishing the lower boundary to the Carolinefjellet Formation, which is recognized by an irregular contact to the underlying dark red colored and platy rocks of the Carolinefjellet Formation (as described by Dallmann et al. (1999) and in Chapter 2.3 on the Firkanten Formation).

A very fine grained sandstone with siderite concretions in its lower part, and *Ophiomorpha* burrows and planar beds in the upper part, is located above the scree covered section with its top at the 10 m mark in the log. Siderite concretions may be a sign of brackish waters, or a diagenetic feature (Boggs 2006). Due to the combination of siderite concretions and *Ophiomorpha* burrows, this unit was initially presented as a brackish interdistributary bay in Chapter 4.2, but another and more favorable interpretation is for it to represent a foreshore environment, with the planar beds representing the swash zone (Clifton 2006), this is supported by the *Ophiomorpha* burrows as these are common in such an environment.

This foreshore deposit is overlain by another scree covered section. Above follows a 3 meter thick segment, located between 16 and 19 m in the log, composed by three fine grained sandstone beds with siderite concretions interbedded by centimeter thick beds of mudrocks and coal. The lowermost sandstone bed is coarsening upwards and comprises low angle concave-up cross-beds and *Ophiomorpha* burrows in addition to the siderite concretions.

Ophiomorpha is a burrow commonly encountered in the upper shoreface-, beach- and lagoonal environments (Gerard and Bromley 2008). This implies that the low angle, concave-up cross-beds represent swaley cross-stratification, and deposition on the shoreface (Clifton 2006). The next fine grained sandstone bed is fining upwards and does not display any distinct structures or features apart from siderite concretions. The third fine grained sandstone bed of this section is separated from the sandstone bed below by a thin coal seam measuring a few centimeters in thickness. This thin coal seam, and the thin coal seam above (at 19 m in the log) combined with

the siderite concretions within the sandstones, gave way to the interdistributary bay/ marsh interpretation of FA 5 after the description of such by Reading and Collinson (2006a). Though, as it turns out, a shoreface interpretation is more favorable due to the outlined arguments above.

This change in interpretation of the depositional environment of the lower half of the Todalen Member questions the interpreted facies association above between 19 and 31 meters in the log. The sandy beds here were initially interpreted to represent distributary channel features (FA 1) like middle ground bars, based on the observations two sandstone units at ~19 m and ~30 m in the log displaying cross-beds gradually translating upwards into rippled/ planar bedded sandstones (Reading and Collinson 2006b). The absence of channel incision was already pointed out in this early interpretation, but was attempted explained by a laterally limited exposure. Now, in the light of the new interpretation described in the section above, these inferred middle ground bars are most likely indicative of an upper shoreface environment which do produce similar structures (Clifton 2006). Nevertheless, this does not exclude the fact that the thin coal seams may have been deposited in a bay-like environment. The lenticular bedded mud rich sandstone above the coal seam at 31 m in the log supports a tidally influenced environment (Longhitano et al. 2012).

The upper part of the Todalen Member, from the first conglomerate in the log to the last, display fluvial evidence, seen as sandstone units with irregular bases and well rounded pebbles on top of the base (Reading and Collinson 2006b). Another fluvial indicator is the inferred crevasse splays, seen alternating thin beds of cross-laminated sandstone and planar laminated mudrock (Reading and Collinson 2006b). The thickest recorded coal seam in the Todalen Member is situated above these fluvial deposits, and confirms an affiliation to the subaerial environment. This coal seam is situated on a similar stratigraphic level as the uppermost coal seams in the two logged cores, and will be further discussed later. Nøttvedt (1985) pointed out in his investigation of the upper part of the Todalen Member around Adventdalen (Endalen is a side valley to Adventdalen) that the lower part of the Todalen Member was dominated by shoreline/ delta front deposits, while the upper part is by large comprised by delta plain deposits. The observations of Nøttvedt (1985) is in line with the observations and interpretations presented above since the Todalen Member is seen to display marine indicators in its lower part (like *Ophiomorpha* burrows, swaley cross-stratification and swash zone deposits), while the upper part contains fluvial channel deposits.

Moreover, it is observed that the lowermost Endalen Member strata in the Endalen Outcrop contains a 5 meter thick unit of channel deposits (Figure 77 A, B). The lowermost unit, outlined in shades of blue and green in Figure 77 C, consists of cross-bed sets of a bidirectional orientation, which points towards an inlet channel under tidal influence (Reading and Collinson 2006a, 2006b). Another channel is present above, this is outlined in orange color in Figure 77 C, the base of this incises the two uppermost beds of the channel below. This channel display lateral accretion surfaces which implies a meandering fluvial origin (Boggs 2006). Though the apparent shallowness and limited width of this channel, combined with the fact that the underlying channel was deposited in proximity to the subaerial environment, indicates that it might be more likely to have been distributive, and not meandering (Reading and Collinson 2006a). Above this is a wedge shaped unit, outlined in pink in Figure 77 C, which pinches out to the right. The top of this is eroded, but due to the nature of the underlying channels, and its display of a unidirectional cross-bed set, it might also be a distributary channel.



Figure 77: A) Channels in the lower part of the Endalen Member in the Endalen outcrop.

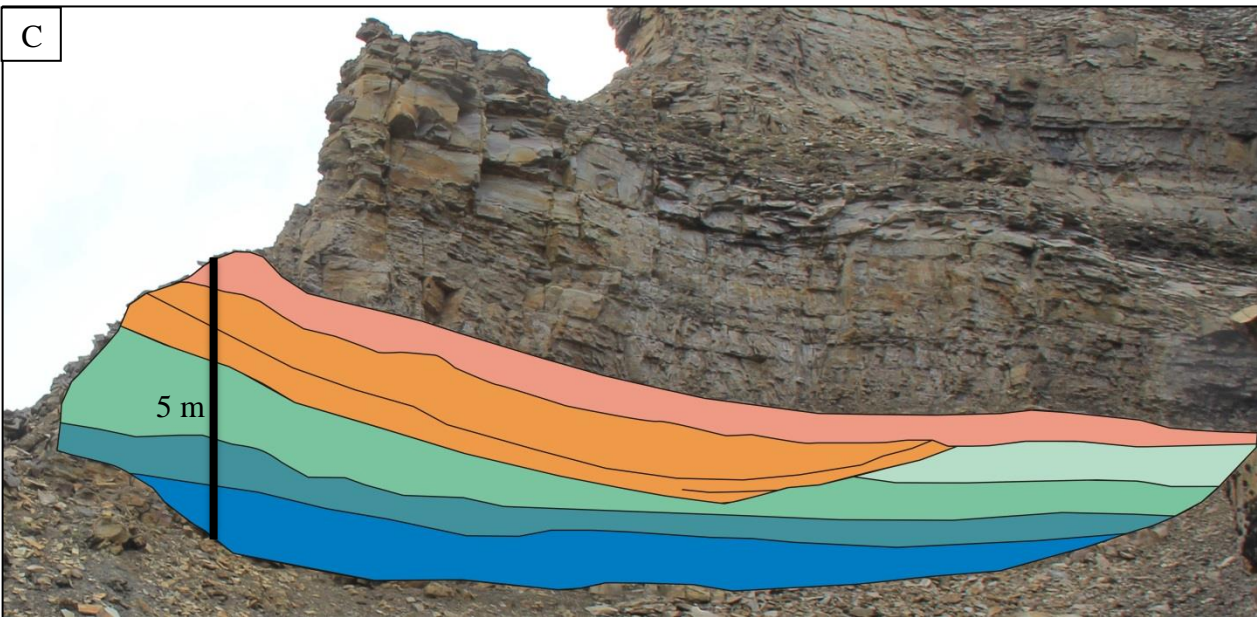
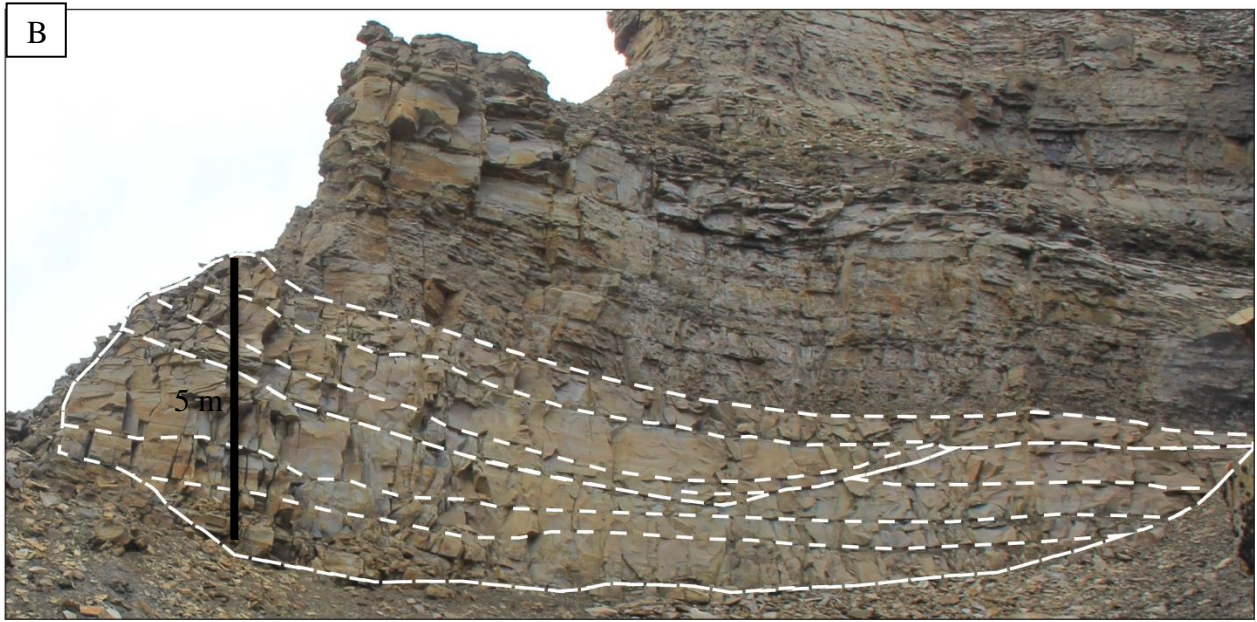


Figure 77: B) Outlined channels in the lower part of Endalen Member. C) Blue to green shades illustrates the lowermost channel with bidirectional co-bed sets which points towards an inlet channel under tidal influence. Note that it is pinching out to the right. The channel, possibly distributary due to its limited width and depth, is outlined in orange. Note the lateral accretion surfaces and erosive base to the underlying channel unit. The uppermost unit is outlined in pink and might also be represent a channel, possibly distributary, due to its unidirectional cross-bed set and relation to the channels below.

Observation of distributary channels/ tidal inlet channels in the lower part of the Endalen Member in the Endalen outcrop does not coincide well with the findings of Steel et al. (1981) at this location who referred to the Endalen Member sandstones as barrier bars on the delta front. Even though the interpretation of Steel et al. (1981) does not match the described findings of the sandstones in the lower part of the Todalen Member, it does not rule out the fact that it might be applicable to the sandstones above. These sandstones were not investigated as the aim of this thesis was to investigate the Todalen Member and lower Endalen Member strata. But, it would be interesting to return to the Endalen outcrop, and make a complete log of the Endalen Member.

The Grumantbyen Outcrop

See Appendix 2.6 for log referrals in the text.

The boundary between the Carolinefjellet Formation and Todalen Member is easily recognized in the Grumantbyen Outcrop due to the “cannon ball” (clay-ironstone concretions) in the Carolinefjellet Formation. The boundary is sharp, and no conglomerate is present at the base of the Todalen Member.

Above the boundary follows a mud rich sandstone which translates upwards from a lenticular bedding style to a wavy bedding style (Figure 16), this feature is often regarded as diagnostic of tidal influence (Selley 2000), and the apparent bidirectional orientation of the ripples supports such a bidirectional flow regime and the intertidal- and supratidal flat (FA 4) assignation. The unit above is regarded as a crevasse splay (FA 2) due to 1) thin beds of very fine sand in a silty mudrock and 2), the presence of *in-situ* rootlets in the upper most medium grained sandstone bed, confirming a relation to the subaerial environment. A laminated mudrock bed separates this unit from the overlying coal seam which is separated from the next overlying coal seam by another thin mudrock unit, which indicates flooding of the mire (Thomas 2002). This coal seam, with its base at the 5 meter mark in the log, displays several pyrite lenses in the top (Figure 29 B).

Pyrite lenses in the coal supports the interpretation of the mire being flooded, as flooding is a mechanism which can bring ferric ions, Fe^{3+} , in the form of colloidal assemblies (or absorbed onto clay) into the mire, which during early diagenetic stage of the peat formation becomes

reduced to Fe^{2+} , and reacts with the sulphide released from the peat. The iron-monosulphide precipitated from this process is assumed to produce pyrite later on during continued diagenesis (Berner 1970; Reidenouer et al. 1979; Boggs 2006). According to Boggs (2006), wooden fragments are often favored to become pyritized.

A thick, laterally extensive (traceable over 40+ meters), massive sandstone unit is present immediately above the second lowermost coal seam. It does not display channel incision or cross-beds, and is thus inferred to represent a delta lobe with its sheet-like geometries owed to marine reworking by waves/ burrowing organism.

The uppermost coal seam is underlain by crevasse splay deposits (FA 2) and a fining upwards mud rich sandstone with ripples assigned to the intertidal and supratidal flat facies associations (FA 4). This coal seam also hold pyrite lenses in the upper part, which is evident of a marine water incursion. Another evidence for marine waters, and a distinct flooding event, is the laminated mudrock unit above with erratic clasts which represents a major flooding-event as well as a "climatic shift", going from a humid peat forming conditions, to cold conditions with ice-sheets floating around. Nevertheless, this "climatic shift" could have been from seasonal variations like mid-Norway today. Erratic clasts have been reported in the Firkanten Formation before by Spielhagen and Tripiati (2009).

A bentonite horizon is present below the 20 m mark in the log within the FA 4 unit. As far as the author have been able to find out, few studies have focused on bentonites horizons in the Firkanten Formation, but the presence thereof have been mention by authors like Dypvik and Nagy (1979), Grenard (2002) and Jochmann (2004). The overlying units are features of distributary channel deposits (FA 1) and crevasse splays (FA 5). A sandstone unit with *in-situ* roots confirms this proximity to a subaerial environment.

The boundary between the Endalen Member and the Todalen Member reflects an obvious change in the depositional setting of the delta, going from being under the influence of delta plain processes, to be influenced by delta front processes (shoreface-basin environment) reflected by 1) alternating sequence of hummocky cross-stratified sandstones and *Ophiomorpha* burrowed sandstones and 2) alternating sequences of hummocky cross-stratified sandstone and mud rich sandstones with siderite concretions.

6.2 The Depositional Environment

Deltas can be described as “discrete shoreline protuberances formed where rivers enters oceans, semi-enclosed seas, lakes or lagoons and supply sediments more rapidly than they can be redistributed by basinal processes” Bhattacharya (2006).

The recognized facies associations in the investigated locations, and the sequences which they occur, shows that the Todalen Member on the northeastern flank of the Central Basin was deposited in an overall delta plain environment where the different investigated locations records different amounts of tidal, fluvial and shoreface (delta front) influence.

The following subchapters refers to Figure 78 unless other is specified.

Sedimentological Variations, Correlation Potential and Depositional Environment of the lower part (<~25 m) of the Todalen Member, from North to South and East to West

Core 18-2009 and Core 15-2010 are situated almost 30 kilometers apart (Figure 7, loc.1 and 4). If a line is drawn between these two locations, it will run almost parallel to the easternmost exposed flank of the Central Basin, and thus from south to north. Even though the distance between the cores are significant, the encountered facies associations are almost identical as they both display fining upward sequences of intertidal-and supratidal flat deposits capped by mire deposits (FA 4-FA 3 sequences).

A suggested correlation of the two lowermost coal seams between the two cores is illustrated in Figure 78. These display a high correlation potential since they both are split and of similar thickness, located on the same stratigraphic level, and underlain by the same facies association. In addition, the coal seam number two from the base is overlain by a bentonite horizon in Core 18-2009. Whereas the coal seam number two from the base in Core 15-2010 is overlain by a thin, grey and flaky mudrock, which implies that it can contain volcanic ash as well, thus further supporting the correlation.

A continued correlation of the two lowermost coal seams between the two cores towards the two outcrops to the west is questionable. It may however not be ruled out in the Endalen outcrop, as the same stratigraphic level here is completely covered by scree, however, as the facies

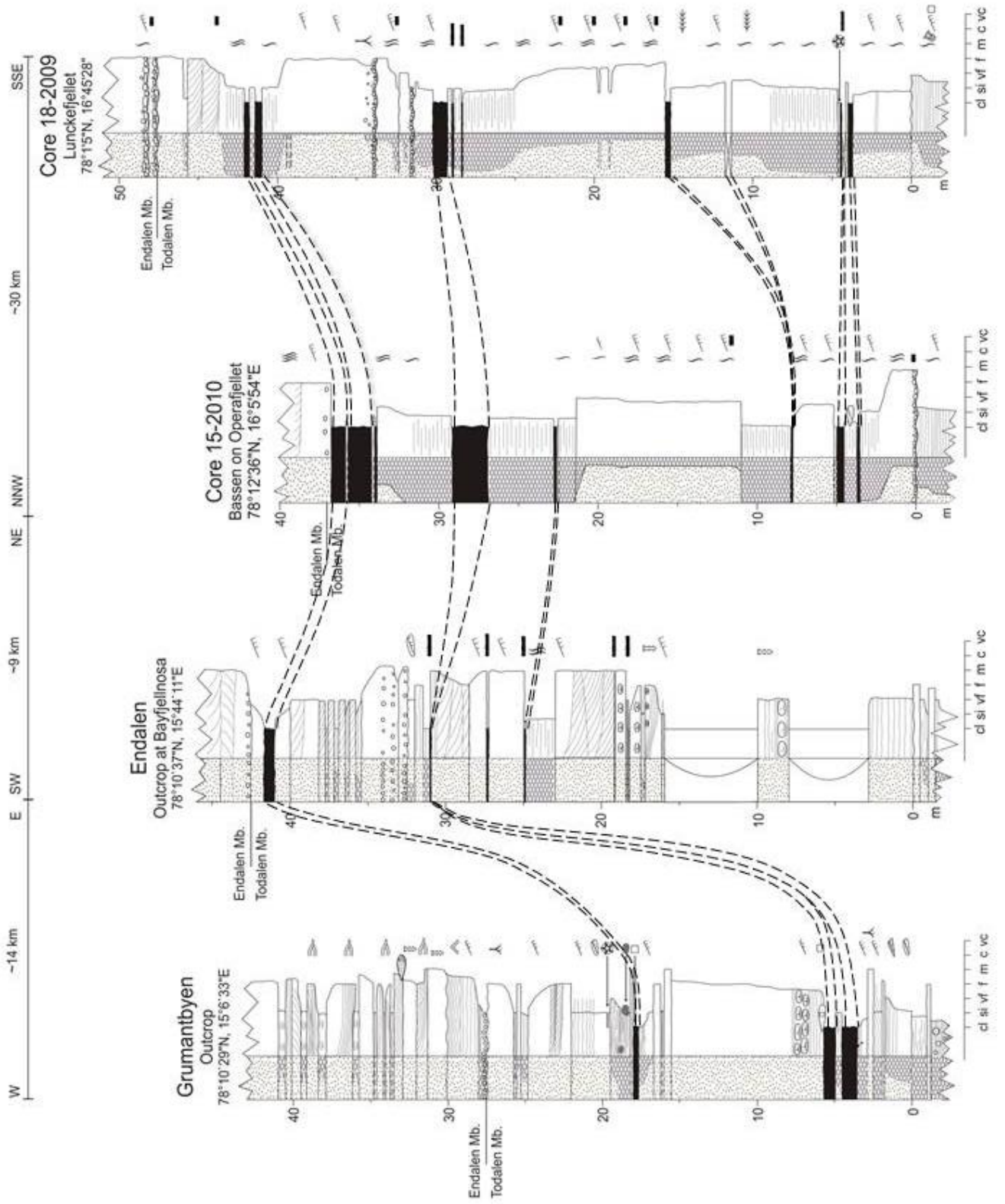
associations above display affiliations to the foreshore (delta front) environment, as indicated by the *Ophiomorpha* burrowed sandstones and swaley cross-stratification, it seems rather unlikely since this is a quite different from setting the intertidal- and supratidal flat deposits above in the two cores. This makes a further correlation to the west, and an extended correlation to the two lowermost coal seams in the Grumantbyen outcrop even more doubtful (Figure 78). It must also be pointed out that the Todalen Member in the Grumantbyen section only measures about 27 meters in thickness, versus the Endalen outcrop and the two cores where the Todalen Member measures between ~37-47 meters.

The limited thickness of the Todalen Member in Grumantbyen may be explained by several active thrust- and normal faults in this area (Figure 28), and even though the placement of the Carolinefjellet Formation-Firkanten Formation boundary appeared to be correct in the field, it is seen from pictures that the faults were quite conspicuous, which led to a too high placement of the boundary. Therefore, the Grumantbyen outcrop will be handled as the upper part of the Todalen Member, and thus be excluded from the discussion of the lower part

A piece of core was lost during drilling of Core 18-2009, since coal is brittle, it can be questioned whether it was a piece of coal. In that case, it could be suggested to be correlated to the third coal seam from the base in Core 15-2010, since they both are overlain by the intertidal- and supratidal flat facies association (FA 4) and not too far off on a stratigraphic level. Nevertheless, as the inclination of this correlation line is higher than the correlation lines above and below, it seems like an unfavorable suggestion.

Starting from the east and Core 18-2009; the coal seam at the 15 m mark in the log appear not to correlate to Core 15-2010 as no coal seam are present on a similar stratigraphic level here. However, two thin coal seams are present below the 20 m mark in the log from the Endalen outcrop. These have however attributed to be nearshore bay deposits, due to the presence of shoreface deposits in-between, which combined with the limited lateral extent of these coal seams strongly suggests that they indeed are deposited in such an environment.

Figure 78: Suggested correlation between the logged cores and outcrops. Dotted lines features the correlation suggestions.



The delta front (shoreface) deposits in the lower part of the Todalen Member in the Endalen outcrop, combined with the abundance of intertidal- and supratidal flat deposits in the cores, suggests that the delta plain during the lower Todalen Member deposition was under the influence of shoreline processes. The poorly correlative coal seams, apart from the two lowermost coal in the two cores, suggests a sporadic mire development. This is in line with the interpretation of Orheim et al. (2007), which stated the same conclusion about mire development in the lower Todalen Member.

Sedimentological Variations, Correlation Potential and Depositional Environment of the Upper Part (>~25 m) of the Todalen Member, from North to South and East to West

Starting with the three split coal seams at the 30 m mark in Core 18-2009; The splitting of these coal seams indicate a flooding of the mire. The uppermost one correlate well with the thicker and un-split coal seam right below the 30 m mark in Core 15-2010. This suggests that a laterally continuous mire development, as the two cores are separated by a distance of 30 km. A very thin coal seam is present on a similar stratigraphic level in the Endalen outcrop at about 31 m. The correlation between these three locations are supported by the fact that the coal seam is overlain by a laminated mudrock at all locations, which is assigned the intertidal- and supra tidal flat facies association. This coal seam is probably correlative with the split coal seam at the base of the Grumantbyen outcrop as the coal seam here also is split by a laminated mudrock like those in the two cores, and since it is inferred represent the upper part of the Todalen Member (as explained in Chapter 6.1). Another indication of flooding here is the pyrite lenses in the top of the coal seam with its base at the 5 m mark in the log.

Again from Core 18-2009; the sandy section between 32 and 40 meters contains conglomerates, *in-situ* rootlets and ripples, and, as thoroughly described and interpreted in the individual discussion of this core, is a great fluvial indicator. The bidirectional ripples (Figure 25) above the lowermost conglomerate here points towards a tidally influence distributary channel, while the rooted and rippled unit above the conglomerate above (at ~34 m) indicate a more fluvially dominated regime. The mudrock unit on the similar stratigraphic level in Core 15-2010, between 29-34 m, does not display a fluvial influence, but this does not disregard the correlation between the uppermost coal seams between the two cores as different delta plain sub-environments are

known to operate on different parts of the delta plain. Furthermore, the section between ~31-41 m in the Endalen outcrop displays fluvial indicators like conglomerates and crevasse splays (FA 2). These observations support the results of Nøttvedt (1985) by verifying a more fluvially dominated delta plain during the deposition of the upper part of the Todalen Member.

Moving over to the Grumantbyen outcrop, and starting where it was left in the discussion the last time (at the second coal seam at the 5 m mark in the log, Figure 78), follows a thick, laterally extensive reworked delta lobe deposits. The uppermost coal seam is situated a few meters above. This coal seam displays pyrite lenses too, and thus strongly implies an incursion of marine water.

The east to west, proximal to distal shift in facies during the deposition of the upper Todalen Member may also be expressed as a story; if one were to walk from Operafjellet via Endalen to Grumantbyen in the Paleocene, one would start walking on the muddy delta plain on Operafjellet (which was certainly not a mountain) in waters not reaching much over the ankle, if any. When one came to Endalen one would have to cross a few channels, though assuming one managed to avoid an unfortunate encounter with a Pantodont on the way. At the time one reached Grumantbyen, one could cool down with a swim in the foreland basin. If one were to take this exact same route during the lower Todalen Member deposition, one would be swimming quite hard already in Endalen.

Sedimentological Variations, Correlation Potential and Depositional Environment of the Lower Endalen Member

In Core 18-2009, the boundary between the Endalen Member and Todalen Member is marked by a conglomerate, and little may be inferred from this alone.

In Core 15-2010, the Todalen Member is thinner, and the boundary is situated lower than the boundary in Core 18-2009, which supports the downwards correlation choice. Furthermore, the lower Endalen Member sandstone displays both cross-beds and burrows.

Several channel complexes are observed in the lower Endalen Member strata (Figure 77), and the character of these indicates both tidal and fluvial channels. The Grumantbyen outcrop on the

other hand display a clear shoreface nature with *Ophiomorpha* burrows and hummocky cross-stratification (Figure 33).

These differences may have several explanations, like for instance an undulating shoreline, or that some deposited units are missing. The latter is probably of importance, as the boundaries are generally sharp. Regardless, the present obtained and interpreted sedimentological data of the lower part of the Endalen Member is inadequate to establish an overall interpretation of the member. What is certain, however, is that the lower Endalen Member strata represents shoreface (delta front) deposits in Grumantbyen and delta plain deposits in the Endalen outcrop, seen as stacked channel complexes (Figure 77 C).

6.3 Petrographic Composition and Provenance

The Todalen Member Sandstones

Nearly all the point counted thin sections from the Todalen Member sandstones in Core 18-2009 are classified as quartz rich subarkoses (Figure 79). The samples from Core 15-2010 are in contrast classified as sublitharenite, quartz arenite, quartz wacke and quartz rich subarkose. This span in classification is not due to huge compositional differences within the detrital grain fraction, but owing to minor variations in the ratio of lithic fragments to feldspars, as noted by the cluster of points in Figure 79. The Endalen outcrop sandstones are on the other hand exclusively comprised by quartz rich subarkoses, whereas the Grumantbyen sandstones chiefly consist of quartz arenites (Figure 79).

Even though it seems as the Todalen Member sandstones are widely different in composition, the cluster of sample points in the QFL-diagram in Figure 79 illustrates that the wide classification span is indeed a result of the sample point cluster being located at the intersecting lines of the mentioned rock classes.

The matrix content seldom exceeds 15% in all of the sampled Todalen Member sandstones. The matrix consists of silt-sized grains <0.03 millimeters and clay. Both authigenic and diagenetic clay is recognized. The authigenic clay is recognized by its intergranular appearance and its presence between grain-to-grain contacts (Wilson and Pittman 1977) as well as occasional ripple structures in the thin sections.

Detrital quartz grains are present as monocrystalline quartz (MQ), polycrystalline quartz (PQ) and sheared quartz (SQ) (Figure 46). The majority of the monocrystalline quartz grains display uniform extinction in the Todalen Member samples from all locations, whereas the minority displays undulose extinction. However, the differentiation between quartz grains with undulose and uniform extinction becomes ambiguous with decreasing grain size (Blatt 1967; Basu et al. 1975; Young 1976).

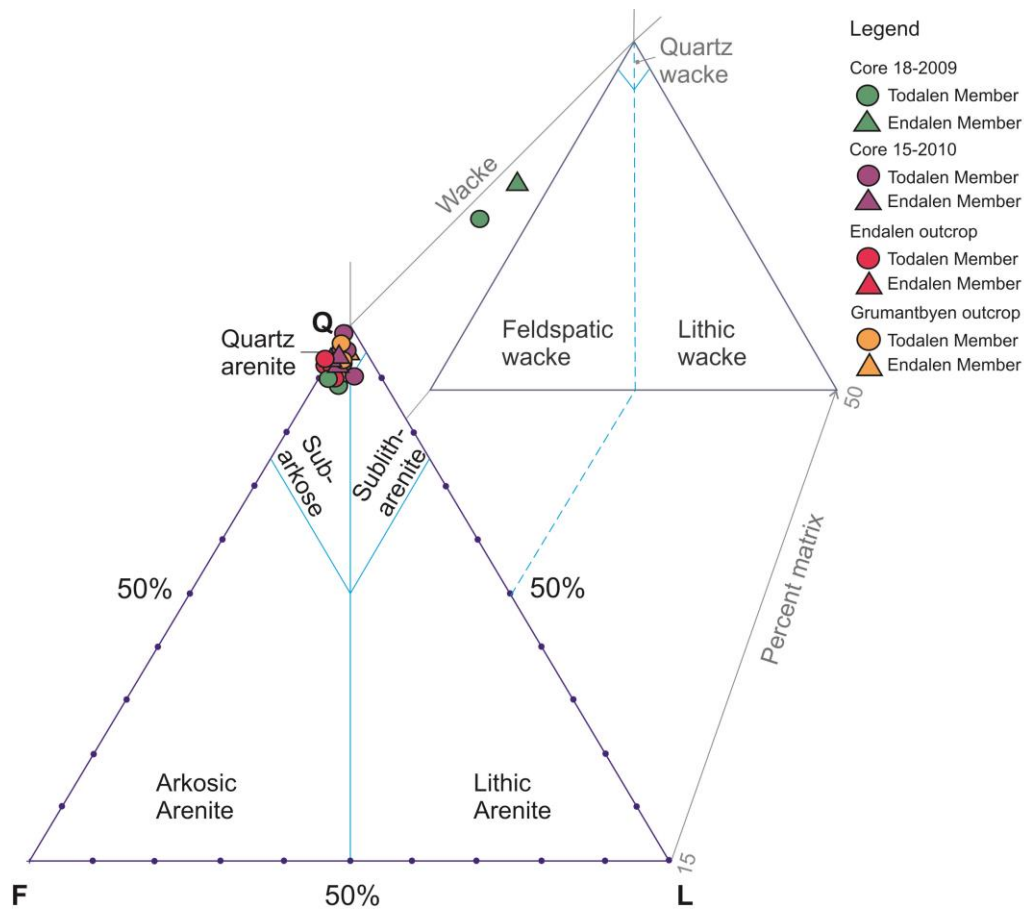


Figure 79: QFL-triangle (Pettijohn 1972) showing sandstone composition based on modal analysis results. Q = monocrystalline quartz, polycrystalline quartz and sheared quartz. F = K-feldspar and plagioclase. L = Lithic fragments.

Another interesting observation in regards to the detrital quartz grain fraction is the absence of inherited cement overgrowths on detrital grains, which indicates that the Todalen Member sandstones represent a first order cycle of deposition. The abundance of angular zircon grains within the heavy mineral suit supports this (Nichols 2009). Nevertheless, the presence of a few well rounded detrital zircon and tourmaline grains suggests a minor influence from a sedimentary source rock, and thus a secondary deposition cycle (Nichols 2009).

The polycrystalline quartz grains consist of 2, sometimes 3 quartz crystals of different orientations with sutured crystal boundaries. The nature of the extinction is slightly undulose

within each crystal. The sheared quartz grains are similar to the polycrystalline grains, but with elongated crystals. Some of the monocrystalline quartz grains also display undulose extinction.

The combination of quartz grains with undulose extinction and uniform extinction suggests that the quartz grains are either derived from two (or multiple) different source rocks, or one single source rock. The first can be explained by one source rock which has been subjected to metamorphism, as undulose extinction is very common in all metamorphic rocks (Adams et al. 1982), and one source rock which has not. A single source rock yielding grains with different extinction can be explained by e.g. a granite (yielding quartz grains with uniform extinction) with local deformation zones (yielding quartz grains with undulose extinction). The most favorable suggestion for the grains with undulose extinction is that they are derived from the metamorphic basement rocks exposed north of the Central Basin due to a slight southward topographic dip of the Cretaceous Unconformity on which the Todalen Member rests (Harland and Kelly 1997; Maher 2001; Bruhn and Steel 2003).

Fluid and mineral inclusions are common within the quartz grains, and the observed combination of apatite and zircon inclusions in the monocrystalline quartz grains point towards an acidic igneous source rock (Nichols 2009) like granite or rhyolite. As no rhyolites have been reported on the Svalbard mainland (Steel et al. 1989), it is reasonable to propose granite as a source rock for at least the monocrystalline quartz grains due to the zircon and apatite inclusions, and the lack of inherited cement. Post-Caledonian granite intrusions are cropping out north of the Central Basin around Hornemanntoppen, Rjipfjorden and Newtontoppen (Steel et al. 1989), and thus in the elevated northern areas of Svalbard in the Paleocene (Harland and Kelly 1997; Maher 2001; Bruhn and Steel 2003). This verifies a component of north to south directed sourcing of sediments into the Central Basin during the Todalen Member deposition.

Microcrystalline quartz (MQ), spicular chert (SC) and chalcedony (Ch) constitute the detrital chert grain fraction which accounts for, on average, 6.4% of the total point counted volume in all the Todalen Member samples. Microcrystalline chert, followed by spicular chert is generally most abundant in all samples and only minor volumes of chalcedony are present.

The relative abundances of MQ, SC and Ch are plotted in Figure 80. The lack of spicular chert and chalcedony grains in the Endalen outcrop results in a cluster of points in the MQ corner of

the triangle. Grains with spiculite and chalcedony morphologies are however not eye-catching in very fine grains (Figure 81), and the very fine grain size of the Endalen outcrop samples are therefore a more likely reason for this deviating cluster than modifications in the source rock assembly.

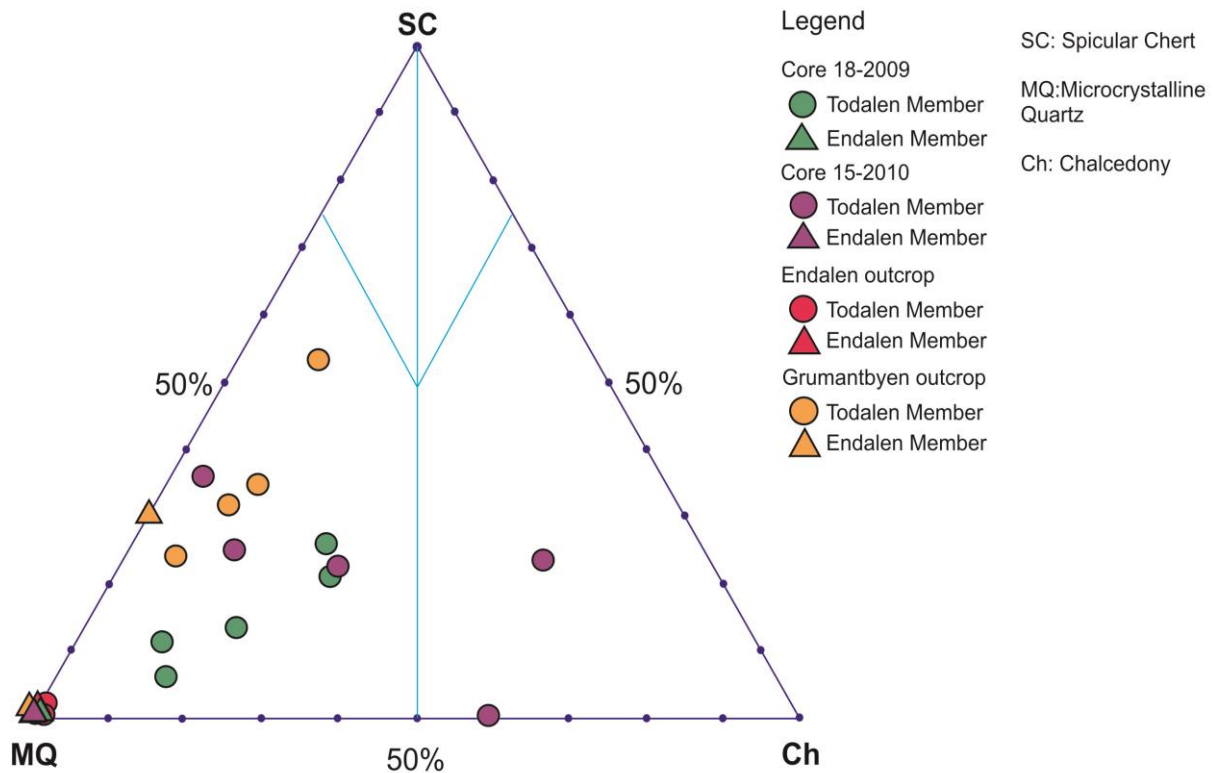


Figure 80: Plot illustrating the relative composition of detrital chert grains in the Todalen and Endalen Member sandstones calculated from modal analysis results (SC+MQ+Ch = 100%).

Siliceous shales with spiculites are only recognized in rocks of the late Permian Tempelfjorden Group (Worsley 2008). The spicular chert grains are therefore diagnostic of the Tempelfjorden Group being a part of source rock assembly. The Tempelfjorden Group is exposed along the West Spitsbergen Fold and Thrust Belt, west of the Central Basin, and north to northeast of the eastern flank of the Central Basin (Steel et al. 1989). Previous studies have suggested sediment transport from the north during the early stages of the infilling of the Central Basin, and thereafter predominantly from the north and east towards the south and west respectively (Kalgraff 1978; Tønseth 1981; Nøttvedt 1985; Bruhn and Steel 2003). Bruhn and Steel (2003) also pointed out that the north-south trending topography controlled drainage into the Central Basin due to uplifted northern areas. Hence the spicular chert grains do in all likelihood originate from the Tempelfjorden Group rocks situated north east of the eastern flank of the Central Basin (Figure 82).

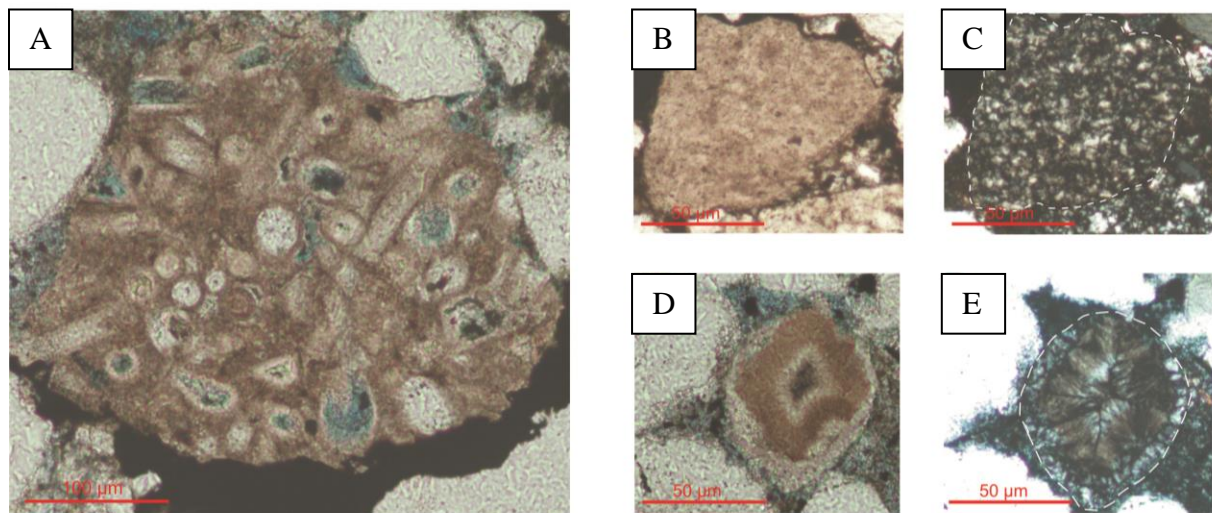


Figure 81: Micrograph of chert grains. **A)** Spicular chert grain in plane light. **B)** Microcrystalline quartz grain in plane light. **C)** Crossed-nichols micrograph of B. **D)** Chalcedony grain in plane light. **E)** Crossed-nichols micrograph of D.

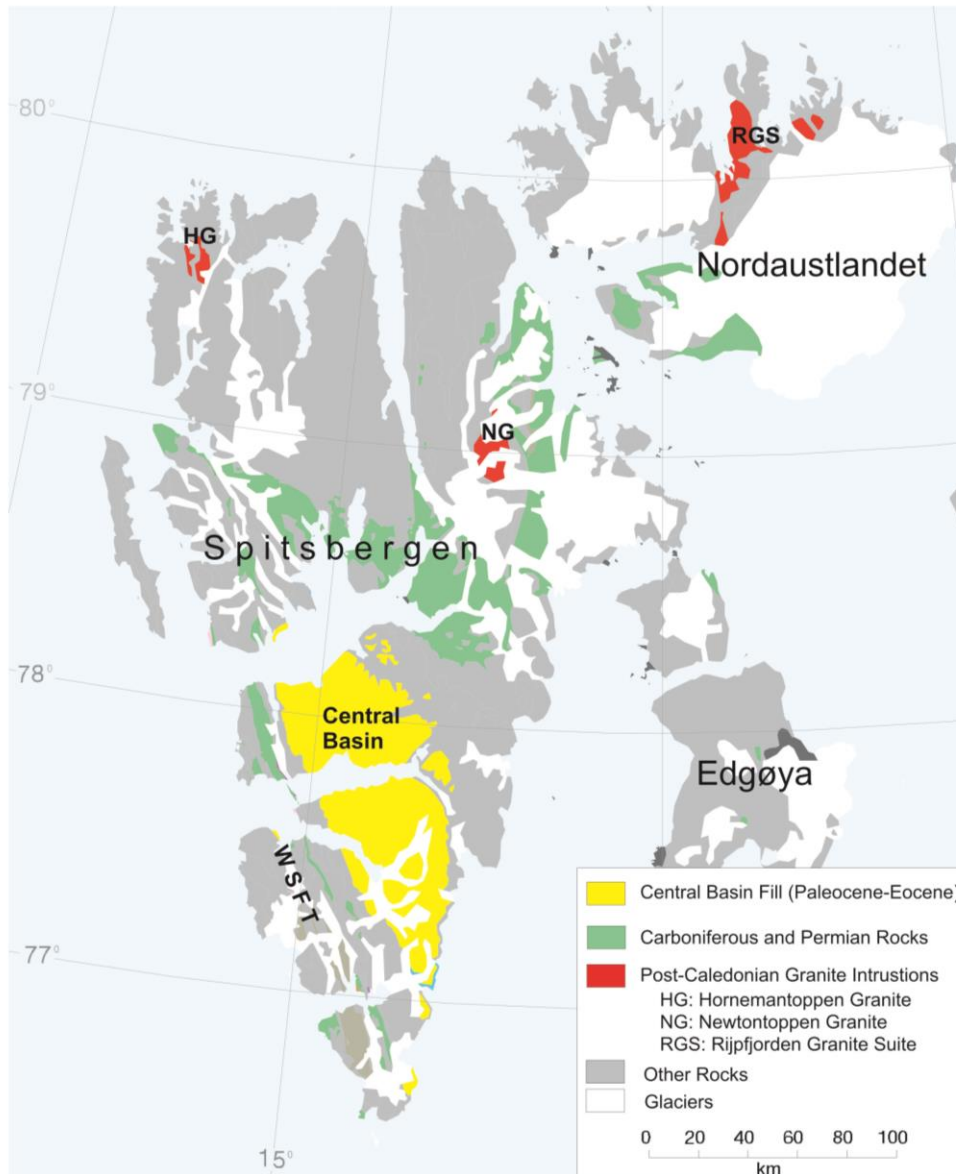


Figure 82: Present day location of two of the source rocks of the Todalen Member sandstones in the Central Basin. The green colored areas marks outcropping Carboniferous and Permian rocks; it is the Permian Tempelfjorden Group which contains siliceous (spicular) shales, and as the only rock containing spiculites, it is regarded to be regarded a source rock fingerprint on the Todalen Member sandstones. Due to the southwards dipping topography during the time of deposition of the Todalen Member (Harland and Kelly 1997; Maher 2001; Bruhn and Steel 2003), the green colored rocks north of the Central Basin are proposed to be the source rock of the chert grains. Red color marks outcropping granitic rocks, all of which are situated north of the basin, which suggest that the source rock location for the monocrystalline quartz grains with zircon and apatite inclusion, is north of the Central Basin. Color modified map after Dallmann et al. (2002).

Feldspars accounts for on average 3.5% of the point counted volume in all samples, and is primarily present as the K-feldspars orthoclase and microcline. The low amount of feldspars can be due to its susceptibility to be altered during transport/ diagenesis, or due to a feldspar-poor source rock.

Angular to rounded rock fragments are present in small volumes and occur in the form of microcrystalline-, monocrystalline- and polycrystalline quartz, as well as spicular chert. The first and latter type is proof of the siliceous Tempelfjorden Group, the remaining rock fragments have already been discussed under the quartz grain section.

The heavy mineral suite is alike for the investigated locations, and comprised by zircon, apatite, epidote, tourmaline, rutile, garnet, chrome spinel, opaque minerals, microscopic siderite nodules and pyrite. Zircon, apatite, tourmaline and garnet are the most abundant ones. Tourmaline and garnet are often regarded as indicators of metamorphic source rocks, but as these grains commonly are rounded to well rounded (Figure 36c), they do more likely represent secondary sedimentation cycle (Nichols 2009).

The Endalen Member Sandstones

The point counted Endalen Member samples from Core 15-2010 and the Endalen outcrop are exclusively composed by quartz rich subarkoses. The samples from Core 18-2009 consist of a polymictic, bimodal and matrix supported conglomerate in addition to a lithic wacke. The Grumantbyen outcrop samples also contain a conglomerate which is polymictic, bimodal and matrix supported, whereas the remaining Grumantbyen samples are classified as quartz arenite and quartz rich subarkose.

Despite the span in rock class, most of the Endalen Member samples plots within the Todalen Member cluster in Figure 79 which again is a result of slight variations in the ratio of feldspar to lithic fragments as the relative content of quartz remains high.

Matrix makes up a significantly smaller part of the sample volume in the Endalen Member thin sections compared to the Todalen Member, which seldom contained less than 5% matrix. This may reflect the changes in the depositional environment, which is going from being a very fine

and fine grained delta plain, to a fine to medium grained delta front (shoreface) (See Chapter 6.1.3).

The detrital quartz fraction, as well as the feldspar fraction, are similar to the Todalen Member samples. Lithic fragments are composed by monocrystalline and polycrystalline quartz, the heavy mineral inclusions of apatite and zircon indicates that the Post-Caledonian granite intrusions north of the basin still are involved in the source rock assembly, and thus still a component of north to south sourcing of sediments into the Central Basin during the Endalen Member deposition. In regards to heavy minerals, no new types are encountered, but neither chrome spinel or rutile have been observed. To test the relevance of this difference, more samples would have to be examined. Nonetheless, the overall absence of spicular chert and chalcedony grains in the samples obtained stratigraphically above the Endalen Member conglomerates is suggestive of modifications within the source rock assembly as these grains are diagnostic of the Tempelfjorden Group (As discussed in Chapter 6.2.1).

The conglomerate in Core 18-2009 and the Grumantbyen outcrop contain largely the same sorts of lithic fragment: microcrystalline quartz, polycrystalline quartz and spicular chert fragments (Figure 71a-c). This indicates that the Tempelfjorden Group was involved as a sediment source rock in at least in the lowermost part of the Endalen Member strata in these locations.

Summary of Composition and Provenance

The point counted Todalen and Endalen Member sandstones plots within the same cluster in the QFL triangle in Figure 79. The location of this cluster is on the intersecting lines for the different rock classes due to an overall high content of quartz (85%-98% of the normalized QFL values) and small variations in the proportions of feldspar to lithic fragments. This therefore leads to a large span in classification, in spite of the compositional difference in fact being rather small. The most frequently encountered rock classes for both members are subarkoses, quartz arenites and sublitharenites.

The content of matrix is generally higher in the Todalen Member sandstones where it can reach values up to 15% of the sample volume than in the Endalen Member sandstones which overall

display a low matrix, seldom exceeding 5%. The matrix is similar for both Members, and consists of small silt grains as well as detrital and diagenetic clay.

The majority of the quartz grains are monocrystalline with uniform extinction. Minor abundances of undulose quartz, both polycrystalline, undulose and sheared, are observed. These may have been derived from the metamorphic basement rocks north of the basin. Due to the overall lack of inherited cement and presence of angular heavy minerals (Figure 59), the quartz grains are by large inferred to represent a first cycle deposit (Nichols 2009). Apatite and zircon mineral inclusions are seen within the monocrystalline quartz grains with uniform extinction, which point towards the acidic igneous source rock like granite (Nichols 2009). Granites are cropping out north of the Central Basin in which the two members were deposited, and suggest that these are the most probable source rocks (Figure 82). This also coincides with previous authors statements about the northern Spitsbergen being slightly elevated in respect to the southern areas in the Paleocene, and hence with the bottom topography dipping gently down towards the south (Harland and Kelly 1997; Maher 2001; Bruhn and Steel 2003).

Microcrystalline quartz (chert), spicular chert and chalcedony grains accounts for 6.4% of the sample volume in the Todalen Member sandstones. Spiculite shales are only reported in the Permian Tempelfjorden Group on Svalbard (Worsley 2008), and are therefore to be regarded as a source rock fingerprint of this group. Due to the southwards dip of the bottom topography, the Tempelfjorden Group rocks situated north of the Central Basin is the most favorable provenance location (Figure 82). The Tempelfjorden grains are absent in the samples obtained stratigraphically above the lowermost conglomerates of the Endalen Member, which may suggest an alteration of the source rock assembly across the Todalen Member – Endalen Member boundary.

Lithic fragments are present in small volumes, and comprised by microcrystalline-, monocrystalline- and polycrystalline quartz, as well as spicular chert. And thus identical to the grains encountered in the detrital grain fraction.

The heavy mineral suite is comprised by zircon, apatite, epidote, tourmaline, rutile, garnet, chrome spinel, opaque minerals, microscopic siderite nodules and pyrite in the Todalen Member samples. As mentioned, more samples must be obtained and analyzed from the Endalen Member

to verify any changes in this assembly and thus of the source rock. Regardless, heavy minerals tend to accumulate in finer grained sandstones (Nichols 2009), and the coarser grained sandstones of the Endalen Member would therefore perhaps not display all the encountered heavy minerals, regardless of number of thin sections investigated.

6.4 Diagenesis

The Todalen Member Sandstones

Quartz cement is present as both continuous and discontinuous overgrowths on detrital grains (Figure 60 and 72). Small anhedral and euhedral quartz crystals are also detected. The volume of quartz cement accounts for on average 2.4%-4.4% of the point counted sample volume in all locations, and no obvious stratigraphic dependent quartz cement trend are seen. Anomalous low volumes of quartz cement, on average 0%-0.3%, are recorded in Core 15-2010. This low volume can be due to the high amount of clay in the matrix, which may result in a retardation of quartz cement overgrowth (McBride 1989). Quartz overgrowths are considered to be linked to late stage diagenesis at temperatures above 70°C (Bjørlykke et al. 1986; Walderhaug 1994).

Various carbonate cements are present in the samples. Scattered zones of porefilling ferroan dolomite/ ankerite (FDA) cement is most prevalent, closely followed by ferroan- and non-ferroan calcite. The calcite cement is distinguishable from the FDA cement in plane light by its transparent appearance, whereas the FDA cement often appears to be somewhat dirty. The carbonate cement is seen to post-date the quartz cement formation as it partly engulfs quartz cement, as well as envelopes euhedral quartz crystals (Figure 52).

There is a negative correlation between the stratigraphic elevation above the base of the Todalen Member and volume of carbonate cement in the samples (Figure 83) which may be explained by the samples obtained stratigraphically above 20 m were deposited with an environment with less marine influence.

Pyrite and pyrite nodules are present in trace amounts in the samples from Core 18-2009, Core 15-2010 and the Grumantbyen outcrop. The pyrite tends to clusters in and around organic debris which verifies an authigenic origin (Berner 1970, 1981). The initial phase of pyrite formation is

induced by microbiological sulphate reduction close to the sediment surface in marine waters, whereas the actual pyrite forms during early diagenetic processes (Berner 1970, 1981).

Porefilling glauconite cement is present in small volumes between 0.3%-0.7%. The term “glauconite” is applied in its morphologic sense due to the greenish color and internal mottled texture (McRae 1972). The glauconite cement is smoothly filling the pore space between quartz grains with quartz overgrowths, which means that it formed by precipitation post-dating the quartz cementation.

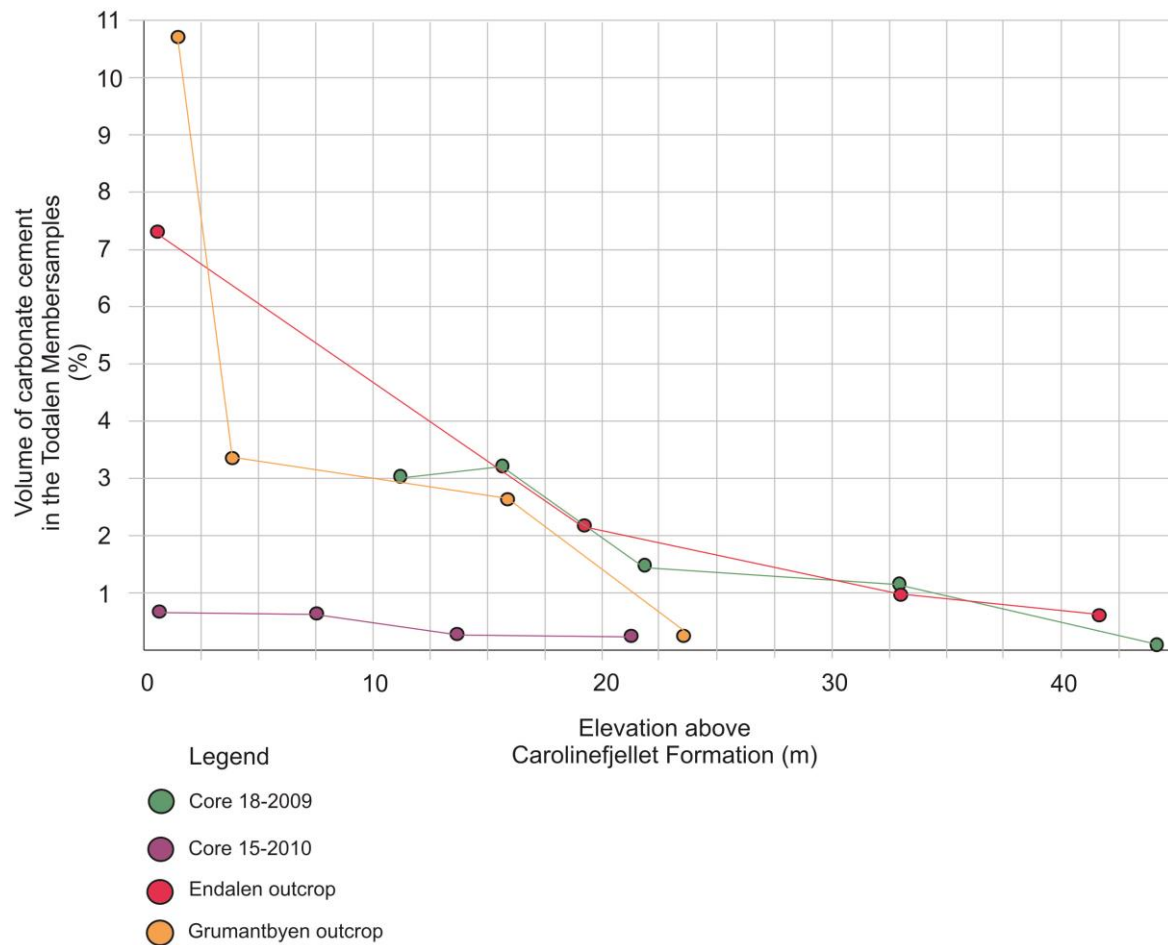


Figure 83: Total point counted volume of carbonate cement in the Todalen Member samples plotted against the height above the Carolinefjellet Formation boundary. Note the overall decreasing volume with increasing distance from the Carolinefjellet Formation.

The diagenetic clay fraction in the Todalen Member thin sections are constituted by illite and kaolinite. A reaction between potassium and kaolinite, as well as temperatures above 70°C, are important for diagenetic illite to form (Hurst and Irwin 1981; Bjørkum and Gjelsvik 1988; Worden and Burley 2003). Possible potassium sources are the mudrock beds (Worden and Burley) within the Todalen Member and K-feldspar grains within the Todalen Member sandstones. The K-feldspar grains with microcline twinning are seen to hold significant intragranular porosity voids (Figure 53a), and have thus clearly provided the pore water with potassium. K-feldspar dissolution occurs primarily at temperatures between 50-150°C, and thus at depth ranges between 1.5-4.5 kilometers (Wilkinson et al. 2001; Worden and Burley 2003).

Trace amounts of microscopic siderite nodules are present in all the Todalen Member samples, the abundances were however too small to be point counted. Nevertheless, by comparison of micrographs of every thin section, the (small) qualitative abundances were found to be 2 times higher for the samples obtained from the upper half of the Todalen Member, and approximately 3 times higher for the Endalen Member samples, than those of the lower half of the Todalen Member. The microscopic siderite nodules are situated on the edges of detrital grains, and are enveloped by quartz cement. This suggests that they formed before the quartz cement, and that they are of an early diagenetic origin. Siderite in sandstones is often regarded as an indicator of brackish waters (Boggs 2006), but it is also reported in sandstones deposited in fresh water lakes (Choi 2003; Lim 2004). Therefore, the implication of this observation in regards to depositional environment alone remains indecisive.

The lower Endalen Member Sandstones

The volume of quartz cement is marginally lower in the Endalen Member samples than the Todalen Member samples. It is primarily seen as thin, in parts syntaxial overgrowths on detrital grains. Ferroan dolomite/ ankerite (FDA) cement is seen patch-wise in the samples from Core 18-2009, the Endalen outcrop and the Grumantbyen outcrop, whereas *poikilitic* calcite cement is sporadically present in the Core 15-2009 samples.

The volume of FDA and calcite cement is between 0.3%-0.7% in most samples, the Grumantbyen samples are an exception with a content of 1.3%-4.7% FDA. These high volumes

are comparable with the volume of FDA and calcite cement in the upper part of the Todalen Member in Grumantbyen.

Scattered pyrite ranging from trace occurrences to 0.7% is present in the matrix in the samples from Core 18-2009, Core 15-2010, the Endalen outcrop and the Grumantbyen outcrop. The Grumantbyen outcrop samples, however, displayed higher abundance of pyrite, between 0.3%-2.7%, largely due to pyritized fragments of organic material (Figure 75). Smooth, porefilling glauconite cement is present on similar terms as in the Todalen Member samples.

Summary of Diagenetic Processes

The similarities in both volume and type of quartz and carbonate cement, pyrite, and siderite between the lower Endalen Member and the upper part of the Todalen Member indicates that the same diagenetic conditions were prevalent for both members in regards to pore water chemistry, pressure and temperature.

The presence of pyrite and siderite in both the Todalen Member and the Endalen Member indicates that the pore water was reducing during the early diagenetic phase (Berner 1970, 1981; Choi et al. 2003; Lim et al. 2004). The quartz cementation process was initiated after this as it is seen to enclose both minerals, and probably at temperatures above 70° (Bjørlykke et al. 1986; Walderhaug 1994; Worden and Burley 2003). There is reason to believe that the quartz cement formed before the diagenetic illite as illite often is seen to coat detrital grains and prevent quartz overgrowths, even though illite may start to form at lower temperatures around 50°C (Wilkinson et al. 2001; Worden and Burley 2003). The mechanisms behind quartz cementation in the thin sections appears to be from 1) the respective grains which the cement is precipitated on, as it most commonly is seen to be in optical continuity with the grain under crossed-nichols, and 2) from pressure solution at grain – to – grain contacts (Figure 52).

The carbonate cement, both calcite and ferroan-dolomite/ ankerite, also post-dates the quartz cement formation in both members as it is seen to enclose the quartz cement (Figure 52).

7. Conclusion

- The Todalen Member on the northeastern flank of the Central Basin represents a delta plain unit deposited on top of the regional Cretaceous Unconformity and the Carolinefjellet Formation.

- More distal delta plain deposits are present on the western reaches of the eastern flank, which together with a north northwest-south southeast trending facies consistency of intertidal- and supratidal flat deposits on the eastern reaches, indicate an overall west-wards orientation of the delta.

- The lower Endalen Member strata display delta front (shoreface) deposits in Grumantbyen, manifested by alternating beds of hummocky cross-stratified sandstones and *Ophiomorpha* burrowed sandstone. Whereas the lower Endalen Member strata in the Endalen outcrop display incised fluvial channels.

- Point counted thin sections from the Todalen Member sandstones reflect primarily a first cycle deposits with a minor influence of a secondary cycle. The source rock assembly is suggested to consist of:

- Intrusive granites north of the Central Basin.
- Spiculite shales of the Tempelfjorden Group, north of the Central Basin.
- Metamorphic basement rocks, north of the Central Basin.
- Sedimentary rocks.

- Thin sections obtained stratigraphically above the lowermost conglomerate of Endalen Member lack evidence of the Tempelfjorden Group, which may imply an alteration in the source rock assembly across the Todalen Member-Endalen Member boundary.

- The Todalen Member sandstones and lower Endalen Member sandstones were subjected to the same diagenetic conditions. Reducing pore waters were present during the early diagenetic stage, which led to the creation of pyrite and siderite. With progressive burial and temperatures reaching above 70°C, quartz cement formed by nucleation of grains and by pressure solution at grain – to – grain contacts. During the late diagenetic stage, an illitization of kaolinite took place in addition to a precipitation of ferroan-dolomite/ ankerite and calcite cement in the remaining pore space.

References

- Adams, A.E., MacKenzie W.S. and Guilford, G.** 1975: Terrigenous clastic rocks. In: Crook, P. (Ed.), first edition, Halsted Press, p.2-31.
- Allen, J.R.L.** 1965: A review of the origin and characteristics of recent alluvial sediments. *Sedimentology*, vol. 5 (2), p. 89–191.
- Basu, A., Young, S.W. and Suttner, L.J.** 1975: Re-evaluation of the use of undulatory extinction and polycrystallinity in detrital quartz for provenance interpretation. *Journal of Sedimentary Petrology*, vol. 45 (4), p. 873-882.
- Bergh, S.G., Braathen, A. and Andersen A.** 1997: Interaction of basement-involved and thin-skinned tectonism in the tertiary fold-thrust belt of Central Spitsbergen, Svalbard. *American Association of Petroleum Geologists, bulletin*, vol. 81, p. 637–661.
- Berner, R. A.** 1970: Sedimentary pyrite formation. *American Journal of Science*, vol. 268, p. 1-23.
- Berner, R. A.** 1981: A new geochemical classification of sedimentary environments. *Journal of Sedimentary Petrology*, vol. 51, p. 359-365.
- Bhattacharya, J.P.** 2006: Deltas. In Posamentier, H.W. and Walker, R.G. (Eds.), *Facies Models Revisited*, Society for Sedimentary Geology, Special Publication, vol. 84, p.237-289.
- Bjørlykke, K. and Egeberg, P.K.** 1993: Quartz cementation in sedimentary basins. *The American Association of Petroleum Geologists, bulletin*, vol. 77 (9), p. 1538-1548.
- Bjørlykke, K., Aagaard, P., Dypvik, H., Hastings, D.S. and Harper, A.S.** 1986: Diagenesis and reservoir properties of Jurassic sandstones from the Haltenbanken area, offshore mid Norway. In: A.T. Spencer, E. Holter, C.J. Campell, S.H. Hanslien, P.H.H. Nelson, E. Nysæther and E. Ormaasen (Eds.), *Habitat of hydrocarbons on the Norwegian continental shelf*, Graham and Trotman, London, p. 275-286.
- Blatt, H.** 1967: Original characteristics of clastic quartz grains. *Journal of Sedimentary Petrology*, vol. 37 (2), p. 401-424.
- Blatt, H. and Christie, J.M.** 1963: Undulatory extinction in quartz of igneous and metamorphic rocks and its significance in provenance studies of sedimentary rocks. *Journal of Sedimentary Petrology*, vol. 33 (3), p. 559-579.
- Blythe, A.E. and Kleinspehn, K.L.** 1998: Tectonically versus climatically driven Cenozoic exhumation of the Eurasian plate margin, Svalbard: Fission track analysis. *Tectonics*, vol. 17 (4), p. 621-639.

- Boggs, S. Jr.** 2006: Principles of Sedimentology and Stratigraphy. In: Lynch, P. (Ed.), fourth edition, Pearson Prentice Hall, p. 74-230.
- Braathen, A., Bergh, S.G. and Maher, H.D.** 1999: Application of a critical taper wedge model to the Tertiary transpressional fold-thrust belt on Spitsbergen, Svalbard. Geological Society of America, bulletin, vol. 111, p. 1468–1485.
- Bruhn, R. and Steel, R.** 2003: High-resolution sequence stratigraphy of a clastic foredeep succession (Paleocene, Spitsbergen): An example of peripheral-bulge-controlled depositional architecture. Journal of Sedimentary Research, vol. 73, p. 745-755.
- Ceppek, P.** 2001: Paleogene calcareous nannofossils from the Firkanten and Sarsbukta Formations on Spitsbergen. Geologisches Jahrbuch Reihe Bulletin, vol. 91, p. 535–547.
- Choi, K.S., Khim, B.K. and Woo, K.S.** 2003: Spherulitic siderites in the Holocene coastal deposits of Korea (eastern Yellow Sea): elemental and isotopic composition and depositional environment. Marine Geology, vol. 202, p. 17-31.
- Clifton, H.E.** 2006: A reexamination of facies models for clastic shorelines. In: Posamentier, H.W. and Walker, R.G. (Eds.). Facies Models Revisited. Society for Sedimentary Geology Special Publication, vol. 84, p. 293-338.
- Dallmann, W.K., Kjærnet, T. and Nøttvedt, A.** 2001: Geomorphological and Quaternary geological map of Svalbard 1:100,000. Adventdalen (sheet C9G). Norwegian Polar Institute.
- Dallmann, W.K., Midbø, P.S., Nøttvedt, A. and Steel, R.J.** 1999: Tertiary lithostratigraphy. In: Dallmann, W.K. (Ed.), Lithostratigraphic Lexicon of Svalbard. Norsk Polarinstitutt, Tromsø, p. 215–263.
- Dallmann, W.K., Ohta, Y., Elvevold, S. and Blomeier, D.** 2002: Bedrock map of Svalbard and Jan Mayen. Norsk Polarinstitutt Temakart no. 33.
- Dypvik, H. and Nagy, J.** 1979: Early Tertiary bentonites from Svalbard. Geological Magazine, vol. 116 (06), p. 457-468.
- Elliot, T.** 1974: Abandonment Facies of High-Constructive Lobate Deltas, with an example from the Yorderdale Series. Proceedings of the Geological Association, vol. 85 (3), p. 359-365.
- Elvevold, S., Dallmann, W. and Blomeier, D.** 2007: Geology of Svalbard. In: Elvevold, S. (Ed.), Norwegian Polar Institute, Tromsø, p. 10-18.
- Gerard, J.R.F. and Bromley, R.G.** 2008: Identifications of the most common trace fossils in cores. In: J.R.F. (Ed.), Ichnofabrics in clastic sediments: Applications to sedimentological core studies, pp. 13-40.

- Gradstein, F., Ogg, J.G. and Smith, A.** 2004: A geologic timescale. In: Gradstein, F., Ogg, J.G. and Smith, A. (Eds.), The concise geologic time scale, Cambridge University Press, p. 5.
- Grenard, S.** 2002: Building a 3D-picture of the Svea Nord mine (Spitsbergen), unpublished diploma thesis, Norwegian University of Science and Technology, p. 40-65.
- Harland, W.B. and Kelly, S.R.A.** 1997: Jurassic-Cretaceous History. In: Harland (Ed.), Geological History of Svalbard, Geological Society of London, memoirs, vol.17, p. 382-383.
- Harrell, J.** 1984: A visual comparator for degree of sorting in thin and plane sections: research method paper. Journal of Sedimentary Petrology, vol. 54 (2), p. 646-650.
- Helland-Hansen, W.** 1990: Sedimentation in Paleogene Foreland Basin, Spitsbergen. The American Association of Petroleum Geologists, bulletin, vol. 74 (3), p. 260-272.
- Hurst, A.R. and Irwin, H.** 1981: A scale of dissolution for quartz and its implications for diagenetic processes in sandstones. Sedimentology, vol. 28, p. 451-459.
- Jochmann, M.** 2004: The geology of the Ispallen area, Svalbard, with emphasis on the coal bearing Firkanten Formation. Diploma thesis at LMU, UNIS, NTNU and SNSG, p. 64.
- Johnson, M.R.**1994: Thin section grain size analysis revisited. Sedimentology, vol. 41, p. 985-999.
- Kalgraff, K.**1978: Aspects of sedimentation in Firkanten Formation, Tertiary, Svalbard. Cand.real. thesis, University of Bergen, p.178.
- Kellogg, H.E.** 1975: Tertiary stratigraphy and tectonism in Svalbard and continental drift. American Association of Petroleum Geologists, bulletin, vol. 59, p. 465– 485.
- Lawver, L.A., Dalziel, I.W.D. and Gahagan, L.M** 2009: Atlas of Plate Reconstructions, 750 Ma to Present Day. Powerpoint Animation, The University of Texas at Austin.
- Leever, K., Faleide, J.I. and Gabrielsen R.I.** 2009: Cenozoic transtensional to transpressional basin development at the sheared Western Barents Sea-Svalbard Margin. EGU General Assembly Conference Abstracts, vol. 12, p. 11929.
- Lim, D.I., Jung, H.S., Yang, S.Y. and Yoo, H.S** 2004: Sequential growth of early diagenetic fresh water siderites in the Holocene coastal deposits, Korea. Sedimentary Geology, bulletin, v. 169, p.107-120.
- Longhitano, S.G., Mellere, D., Steel, R.J. and Ainsworth, R.B.** 2012: Tidal depositional systems in the rock record: A review and new insights. Sedimentary Geology, vol. 279, p. 2–22.

- Maher, H. D., Braathen, A. Jr., Bergh S.G., Dallmann, W. K. and Harland, W. B.** 1995: Tertiary or Cretaceous age for Spitsbergen's fold-thrust belt on the Barents Shelf? *Tectonics*, vol. 14, p. 1321–1326.
- Manum, S. B. and Throndsen, T.** 1986: Age of Tertiary formations on Spitsbergen. *Polar Research*, vol. 4 (2), p. 103-131.
- Martinsen, O. and Nøttvedt, A.** 2008: Norway rises from the sea. In: Rambert, I.B., Bryhni, I., Nøttvedt, A. and Rangnes, K.(Eds.), *The making of a land*. The Norwegian Geology Association, p. 442-478.
- McBride, E.F.** 1989: Quartz cement in sandstones: A review. *Earth Science Reviews*, vol. 26, p. 69-112.
- McCabe, P.J. and Parrish, J.T.** 1992: Tectonic and climatic controls on the distribution and quality of Cretaceous Coals. In: McCabe, P.J. and Parrish, J.T. (Eds.), *Distribution and quality of Cretaceous coals*, Geological Society of America, special papers, vol. 267, p. 1-11.
- McRae, S.G.** 1972: Glauconite. *Earth-Science Reviews*, vol. 8, p. 397-440.
- Middleton, G.V.** 1978: Facies. In: Fairbridge, R.W. and Bourgeois, J. (Eds.), *Encyclopedia of sedimentology*, Dowden and Ross, p.323-325.
- Müller, R. D. and Spielhagen, R. F.** 1990: Evolution of the Central Tertiary basin of Spitsbergen: towards a synthesis of sediment and plate tectonic history. *Paleogeography, Paleoclimatology, Paleoecology*, vol. 80, p. 153–172.
- Nagy, J.** 2005: Delta-influenced foraminiferal facies and sequence stratigraphy of Paleocene deposits in Spitsbergen. *Palaeogeography, Palaeoclimatology, Palaeoecology*, vol. 222, p.161–179.
- Nagy, J., Kaminski, M.A., Kuhnt, W. and Bremer, M.** 2000: Agglutinated foraminifera from neritic to bathyal facies in the Paleogene of Spitsbergen and the Barents Sea. In: Hart, M.B., Kaminski, M.A. and Smart, C.W. (Eds.), *Proceedings of the Fifth International Workshop on Agglutinated Foraminifera*, Grzybowski. Foundation special publication, vol. 7, p. 333– 361.
- Nichols, G.** 1999: *Sedimentology and Stratigraphy*. In: Nichols, G. (Ed.), second edition, Wiley-Blackwell Publishing Company, p. 38-40, 44-68, 79, 179-186, 342-343.
- Nøttvedt, A.** 1985: Askeladden delta sequence (Paleocene) on Spitsbergen sedimentation and controls on delta formation. *Polar Research*, vol. 3, p. 21–48.
- NPI/stadnavn 2013:** Norwegian Polar Institute website, <http://www.npolar.no/en/the-arctic/place-names>, visited on 03.02.2013.

- Orheim, A.**, Bieg, G., Brekke, T., Horseide, V. and Stenvold, J. 2007: Petrography and geochemical affinities of Spitsbergen Paleocene coals, Norway. *International Journal of Coal Geology*, vol. 70, p.116-136.
- Paech, H.J.** 2001: The Tertiary and Cretaceous of Spitsbergen and North Greenland: Its Alpine Signature. *Polarforschung*, vol. 69, p. 107-115.
- Pettijohn, F.J.**, Potter, P.E. and Siever, R. 1972: Sand and Sandstone. Springer-Verlag, p. 618-625.
- Reading, H.G.** and Collinson 2006a: Clastic coasts. In: Reading, H.G (Ed.), *Sedimentary environments, processes, facies and stratigraphy*. Third edition, Blackwell publishing, p.181-210.
- Reading, H.G.** and Collinson, J.D. 2006b: Alluvial sediments. In: Reading H.G. (Ed.), *Sedimentary environments: processes, facies and stratigraphy*. Third edition, Blackwell publishing, p. 37-81.
- Reading, H.G.** and Levell, J. 2006: Controls on the sedimentary rock record. In: Reading, H.G (Ed.), *Sedimentary environments, processes, facies and stratigraphy*. Third edition, Blackwell publishing, p.5-36.
- Reidenouer, D.**, Williams, E.G. and Dutcher, R.R. 1979: The relationship between palaeotopography and sulphur distribution in some coals of western Pennsylvania. In: Ferm, J.G. and Horne, J.C (Eds.), *Carboniferous depositional environments in the Appalachian region*. University of South Carolina, p. 88-101.
- Ritzmann, O.** 2003: Architecture and geodynamic evolution of the Svalbard Archipelago, the Yermak Plateau and the Fram Strait oceanic province from deep seismic experiments. *Berichte zur Polar- und Meeresforschung*, vol. 439, p. 136-143.
- Ryer, T.A** and Langer, A.W. 1989: Thickness change involved in peat-to-coal transformation for a bituminous coal of Cretaceous age in central Utah. *Journal of Sedimentary Petrology*, vol. 50, p. 987-992.
- Selley, R.C.** 2000: Applied sedimentology. In: Selley, R.C (Ed.), second edition, Elsevier, p. 1-124.
- Spielhagen, R.F.** and Tripathi, A. 2009: Evidence from Svalbard for near-freezing temperatures and climate oscillations in the Arctic during the Paleocene and Eocene. *Palaeogeography, Palaeoclimatology, Palaeoecology*, vol. 278, p. 48–56.
- Steel, R.J.**, Dalland, A., Kalgraf, K. and Larsen, V. 1981: The central Tertiary basin of Spitsbergen-sedimentary development in a sheared margin basin. In: Kerr, J.W. and Fergusson, A.J. (Eds.). *Geology of the North Atlantic Borderlands*, Memoir Canadian, Society of Petroleum Geologists, vol. 7, p. 647– 664.

- Steel, R.J., Gjelberg, J., Helland-Hansen, W., Kleinsphen, K., Nøttvedt, A. and Rye-Larsen, M.** 1985: The Tertiary strike-slip basins and orogenic belt of Spitsbergen. In: Biddle, K.T. and Christie-Blick, N. (Eds.), *Strike-Slip Deformation, Basin Formation and Sedimentation*, Special Publication Society of Economic Paleontologists and Mineralogists, vol. 37, p. 339–359.
- Steel, R.J., Winsnes, T.S. and Salvigsen, O.** 1989: Geological map of Svalbard 1:100,000, Braganzavågen (sheet C10G). Norwegian Polar Institute.
- Steel, R.J. and Worsley, D.** 1984: Svalbard's post-Caledonian strata. An atlas of sedimentation patterns and paleogeographic evolution. In: Spencer, A.M (Ed.), *Petroleum Geology of the North European Margin*. Norwegian Petroleum Society, Graham and Trotman Ltd., p. 109–135.
- Thomas, L.** 2002: Coal geology. In: Thomas, L. (Ed.), second edition, Wiley-Blackwell Publishing, p. 3-33.
- Tucker, M.** 2003: Sedimentary rocks in the field. In: Tucker, M. (Ed.), third edition, Wiley, p. 83-158.
- Tønseth, D.** 1981: The sedimentary history of Firkanten Formation (Paleocene) in the Adventdalen area. Cand. real. Thesis, University of Bergen, p.181.
- Von Gosen, W.** 2003: Thrust tectonics in the North Patagonian Massif (Argentina): Implications for a Patagonia plate. *Tectonics*, vol. 22, p. 3-15.
- Vonderbank, K.** 1970: Geologie und Fauna der Tertiären Ablagerungen Zentral Spitsbergens. *Norsk Polarinstitutt Skrifter nr. 153*, p. 156.
- Walderhaug, O.** 1994: Precipitation rates for quartz cement in sandstones determined by fluid-inclusion microthermometry and temperature-history modeling. *Journal of Sedimentary Research*, vol. 64, p. 324-333.
- Walker, R.G. and James, N.P.** 1994: Facies models. In: Walker, R.G. and James, N.P. (Eds.), second edition, *Geological Association of Canada Publications*, p. 1-15.
- Wilkinson, M., Milliken, K.L. and Haszeldine, R.S.** 2001: Systematic destruction of K-feldspars in deeply buried marine sandstones. *Journal of the Geological Society, London*, vol. 158, p. 675-683.
- Wilson, M.D. and Pittman, E.D** 1977: Authigenic clays in sandstones: recognition and influence on reservoir properties and paleoenvironmental analysis. *Journal of Sedimentary Petrology*, vol. 47 (1), p. 401-424.
- Worden, R.H. and Burley, S.D.** 2003: Sandstone Diagenesis: The evolution of sand to stone, in sandstone diagenesis: Recent and ancient. In: Burley, S.D. and Worden, R.H. (Eds.), *Blackwell Publishing*, p. 231-261.

Worsley, D. 2008: The post-Caledonian development of Svalbard and the western Barents Sea. *Polar Research*, vol. 27, p.298-317.

Young, S.W. 1976: Petrographic textures of detrital polycrystalline quartz as an aid to interpreting crystalline source rocks. *Journal of sedimentary petrology*, vol. 46 (3), p. 595-603.

Ytreland, G.K. 1980: Sedimentation along the Western Margin of the Central Tertiary Basin (Firkanten Formation), Spitsbergen. Cand. real. Thesis, University of Bergen, p. 183.

Appendix

Appendix 1.1 Description of Facies

Facies (F)	Facies Name	Description	Flow Regime Interpretation
A	Coal	Shiny and brittle coal seams.	Very low flow regime (Nichols 2009).
B	Mudrock	Fissile mudrock with thin silt laminas and occasional burrows.	A sufficiently low flow regime for clay to settle out of suspension. (Longhitano et al. 2012).
C	Rippled mud rich sandstone	Mud rich very fine to fine grained sandstone with bi-directional/ unidirectional ripples. Mud drapes on ripple crests and foresets. Flaser bedding and wavy bedding with increasing clay content.	Subaqueous and alternating low- and very low flow regime. Deposited by bidirectional/ unidirectional currents. Clay settled out of suspension during periods of very low flow, ripples during periods of low flow (Selley 2000).
D	Planar bedded sandstone	Includes very fine-fine grained sandstone with planar laminas or beds, and siltstones interbedded by small scale cross-laminated very fine-fine sand.	Upper or lower flow regime (Nichols 2009), siltstone with small scale cross-lamination indicates the lower flow regime (Tucker 2003).
E	Asymmetrically rippled sandstone	Clean sandstone of very fine to fine grain size. Asymmetric ripples with one preferred orientation.	Unidirectional currents within the lower flow regime (Boggs 2006).
F	Symmetrically rippled sandstone	Very fine to fine grained sandstone with symmetrical ripples forming sinusoid crests.	Oscillatory motion within a standing body of water. Lower flow regime (Nichols 2009).
G	Tabular- and trough- cross-bedded sandstone	Very fine to fine grain size, normal or none-graded. Tabular: high angle cross-beds with tabular foresets. Planar upper and lower bed-set surface. Trough: curved upper/lower bed set surface. Tangential foresets towards the lower bedding surface.	Tabular: straight crested dunes with 2D bed form, moderate flow regime (Nichols 2009). Trough: curved crested dunes with 3D bed form. Formed within the upper part of the moderate flow regime (Nichols 2009).
H	Hummocky cross-stratified sandstone	Undulating low angle, cross-stratified beds. Very fine-fine grain size. Includes concave-up bedding style (swales) and convex-up bedding style (hummocks).	Diagnostic of re-worked and subsequently deposited sands between fair-weather wave base and the storm-wave base (Nichols 2009).
I	Burrowed sandstone	Very fine-fine grained sandstone with burrows. <i>Ophiomorpha</i> : vertical tubes, pellet-lined surface. Up to 30 cm long, 1 cm in diameter. <i>Skolithos</i> : smooth, vertical tubes. Max 0.5 cm diameter, variable length of 2-10 cm.	<i>Ophiomorpha</i> : lagoon-upper shoreface (Gerard and Bromley 2008). <i>Skolithos</i> : lagoon-offshore basin, most common in a beach environment (Gerard and Bromley 2008).
J	Carbonate cemented sandstones and concretions	Carbonate cemented sandstones: massive appearance. Fine-coarse grained. Carbonate concretions: in a silty to fine grained matrix. Brick like structures coated by a reddish brown layer.	Does not apply
K	Rooted sandstone	Dark, vertical and down-wards branching thread-like streaks in a silty to fine grained sandstone. 2-15 cm long, thicker diameter in the top (~3 mm) than in the base (~1 mm).	Lower flow regime as the roots were able to fasten in the sediments.
L	Conglomerate	Orthoconglomerate: bimodal, polymict and clast supported. Sub- to well-rounded granule-cobble size clasts. Very fine-fine grained matrix. Paraconglomerate: thin or discontinuous conglomerate beds or lenses. Bimodal (max pebble size), polymict and matrix supported. Very fine-medium grained matrix.	High flow regime, subaqueous environment. Orthoconglomerates deposited under higher flow velocities than the Paraconglomerates due to larger and better rounded clasts as well as little matrix.

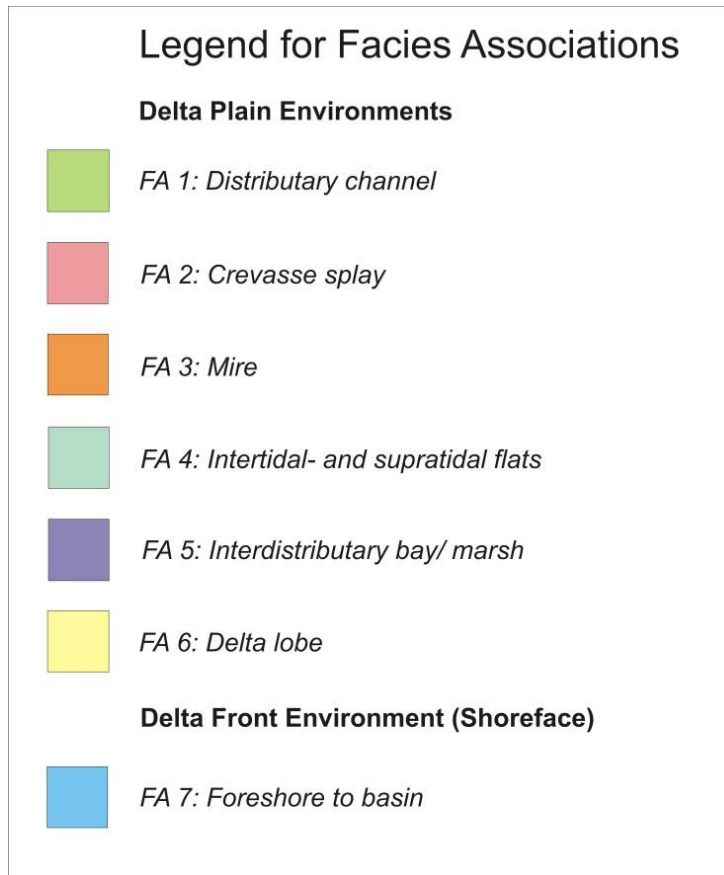
Appendix 1.2 Overview of Facies Associations

Facies Association (FA)	Interpretation	Depositional Environment	Facies
1	Distributary channels	Delta plain	C, D, E, G, G, J and L
2	Crevasse splays	Delta plain	B, E, G, J and K
3	Mire	Delta plain	A
4	Intertidal- and supratidal flat	Delta plain	B and C
5	Interdistributary bay/ marsh	Delta plain	A, B, I and J
6	Abandoned delta lobe	Delta plain	J and E
7	Foreshore to basin deposits	Delta front (shoreface)	B, E, F, H, I, J and L

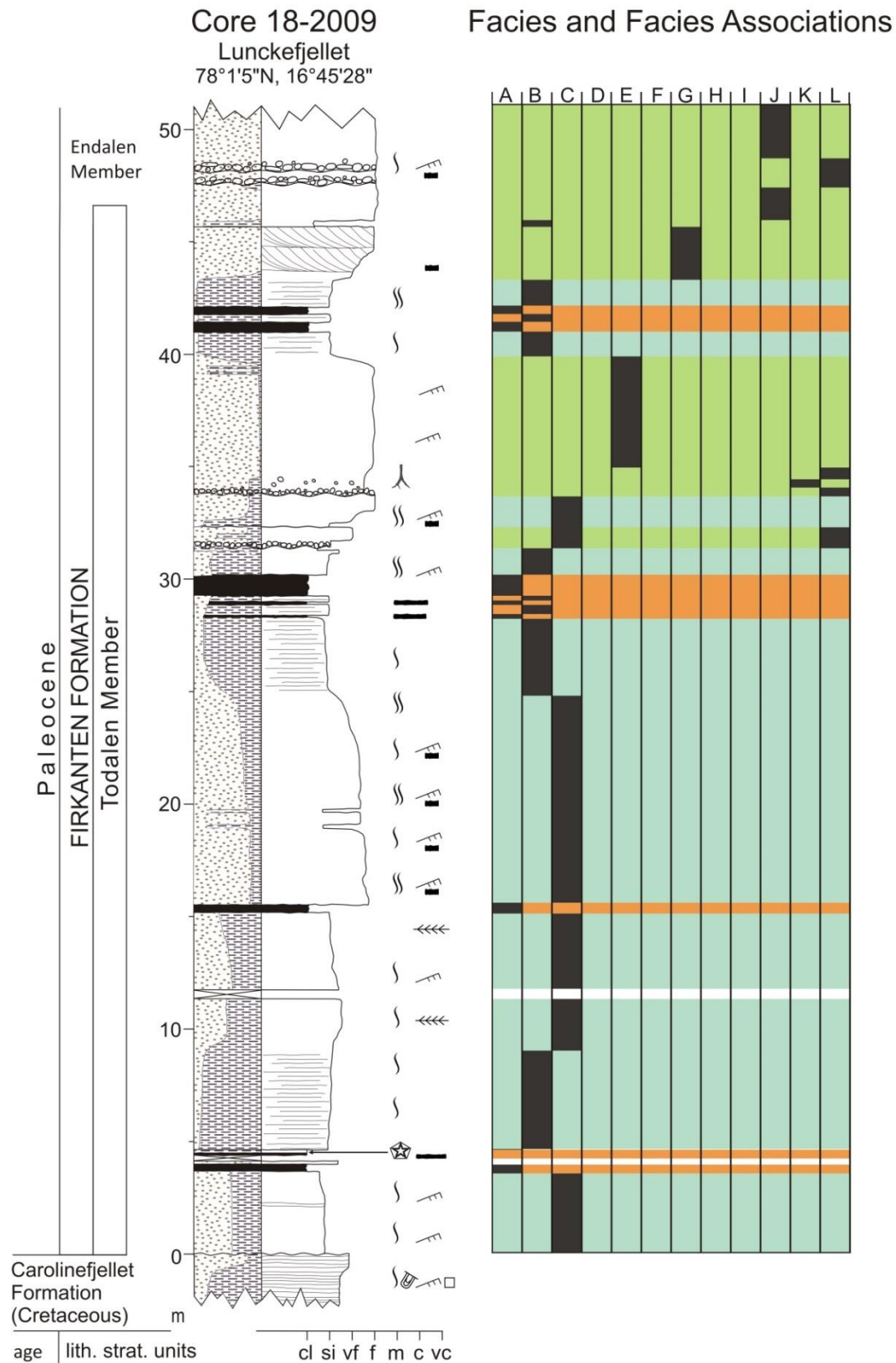
Appendix 2.1 Legend for Logs

Legend for Logs			
Sedimentary Structures			
	Erosional surface		Lenticular bedding
	Planar bedding		Flaser bedding
	Planar lamination		Current ripples (asymmetrical)
	Wave-ripple lamination		Unspecified ripples
	Large scale angular cross-stratification		Herringbone lamination
	Large scale tangential cross-stratification		Wave ripples (symmetrical)
	1-5 cm thick sand beds		Hummocky cross-stratification
Features			
	Thin coal seam		Dropstone
	Coal fragment		Lense
	Roots		Siderite cemented
	Pyrite		Concretion
	Pebbels		Siderite cemented concretion
	Bentonite bed		Ball concretion
			Degree of bioturbation (increasing)
			Skolithos type burrows
			Ophiomorpha type burrows
			Zoophycos type burrows
Lithology			
	Sandstone		Coal
	Mudrock		Missing core
			Scree covered

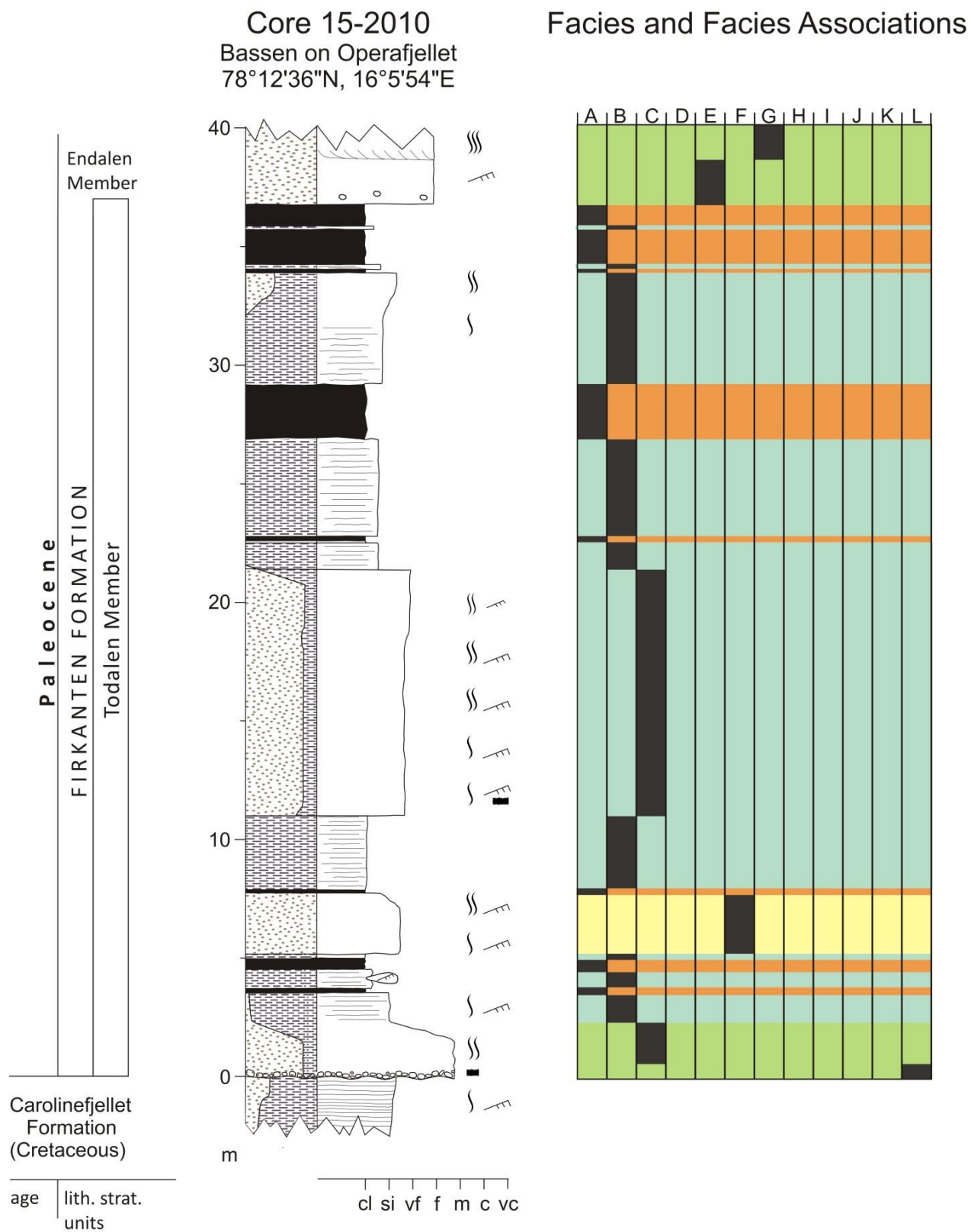
Appendix 2.2 Legend for Facies Associations



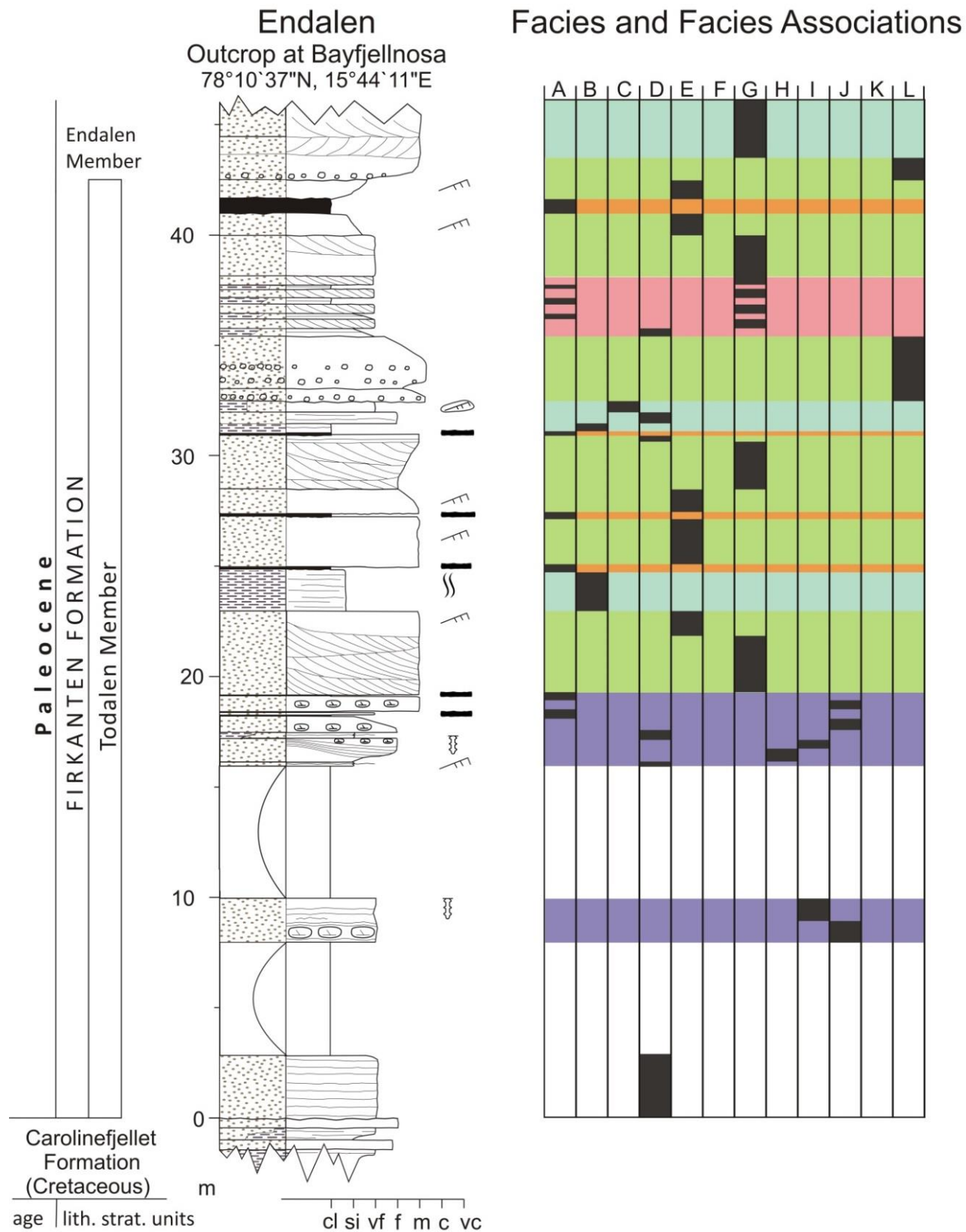
Appendix 2.3 Core 18-2009 Sedimentological Log, Facies and Facies Associations.



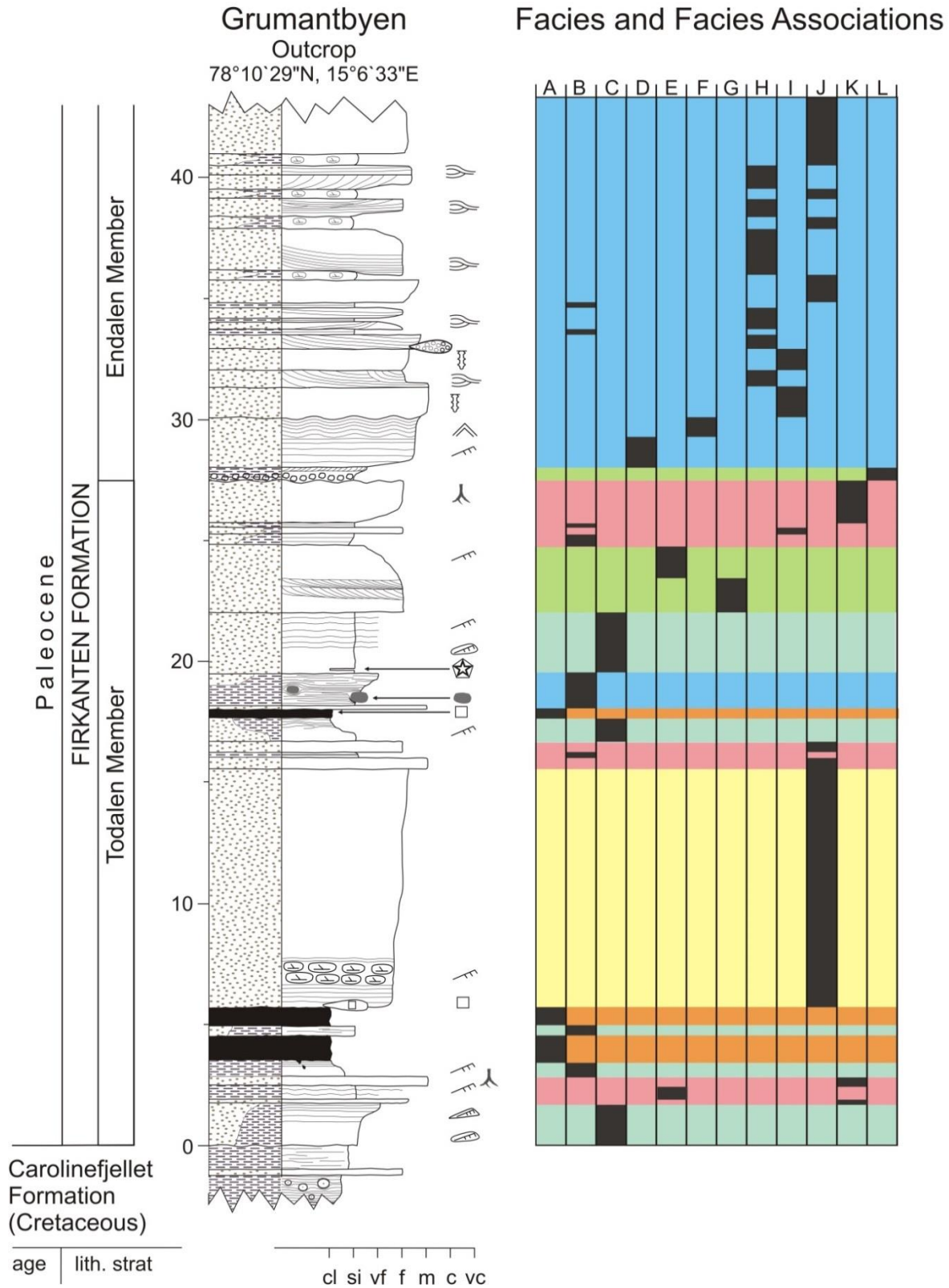
Appendix 2.4 Core 15-2010 Sedimentological Log, Facies and Facies Associations



Appendix 2.5 Endalen Outcrop Sedimentological Log, Facies and Facies Associations.



Appendix 2.6 Grumantbyen Outcrop Sedimentological Log, Facies and Facies Associations



Appendix 3.1 Sandstone classifications of the point counted samples

Core/ Outcrop	Thin Section #	Elevation a.C.Fm. (m)	Member	Classification (Pettijohn 1972)
Core 18-2009, Lunckefjellet				
Core 18-2009	18-3	11,00	Todalen	Subarkose
Core 18-2009	18-6	15,60	Todalen	Subarkose
Core 18-2009	18-8	22,20	Todalen	Lithic wacke
Core 18-2009	18-10	33,80	Todalen	Subarkose
Core 18-2009	18-13	43,73	Todalen	Subarkose
Core 18-2009	18-16	47,10	Endalen	Lithic arenite
Core 18-2009	18-17	50,45	Endalen	Lithic wacke
Core 15-2010, Bassen				
Core 15-2010	15-2	0,72	Todalen	Sublitharenite
Core 15-2010	15-5	7,30	Todalen	Quartz arenite
Core 15-2010	15-6	14,29	Todalen	Quartz arenite
Core 15-2010	15-8	21,05	Todalen	Subarkose
Core 15-2010	15-9	33,50	Endalen	Subarkose
Core 15-2010	15-10	37,75	Endalen	Subarkose
Core 15-2010	15-11	38,92	Endalen	Subarkose
Endalen Outcrop				
Endalen	EN 1-2	1,00	Todalen	Subarkose
Endalen	EN 1-3	9,70	Todalen	Subarkose
Endalen	EN 1-5	22,90	Todalen	Subarkose
Endalen	EN 1-6	31,70	Todalen	Subarkose
Endalen	EN 1-7	43,05	Endalen	Subarkose
Grumantbyen Outcrop				
Grumantbyen	GR 1-2	1,80	Todalen	Subarkose
Grumantbyen	GR 1-3	2,87	Todalen	Quartz arenite
Grumantbyen	GR 1-4	16,67	Todalen	Quartz arenite
Grumantbyen	GR 1-7	23,13	Todalen	Quartz arenite
Grumantbyen	GR 1-9A	27,87	Endalen	Lithic arenite
Grumantbyen	GR 1-9	28,45	Endalen	Quartz arenite
Grumantbyen	GR 1-10	32,42	Endalen	Subarkose

Appendix 3.2 Abbreviations for tables

Abbreviations	
a.C. Fm.	Above Caroliefjellet Formation (Cretaceous Hiatus)
-	None observed
Cryst.	Crystalline
Frag.	Fragments
Ca	Calcite
Qtz	Quartz
gr.	Granular
Org. Mat	Organic material
Lith.	Lithic